PB94-145661

NISTIR 5338

A System for Calibration of the Marshall Compaction Hammer

Harry W. Shenton III
Building and Fire Research Laboratory
National Institute of Standards and Technology
Gaithersburg, Maryland 20899

Michael M. Cassidy
Peter A. Spellerberg
David A. Savage
AASHTO Materials Reference Laboratory
Gaithersburg, Maryland 20899

Prepared for the Federal Highway Administration under Interagency Agreement DTFH61-92-Y-30052. Also published as Federal Highway Research Report FHWA-RD-94-002.

January 1994

U.S. Department of Commerce
Ronald H. Brown, *Secretary*
Technology Administration
Mary L. Good, *Under Secretary for Technology*
National Institute of Standards and Technology
Arati A. Prabhakar, *Director*

ABSTRACT

The Marshall method is used by many state and local highway agencies for the design of hot-mix asphalt pavement. Although the procedure is specified by several industry standards, round-robin programs have confirmed wide variability in Marshall test results. Much of the scatter in the data is attributed to compaction hammer variables, such as: variation in drop weight, drop height, friction, hammer alignment, pedestal support and foundation. With the objective of reducing the variability of Marshall test results, a robust, easy to use and relatively inexpensive test apparatus has been developed for calibration of mechanical Marshall compaction hammers. The system consists of a spring-mass device with force transducer, power supply and data acquisition system. The device replaces the standard specimen mold during calibration. Force time histories from multiple hammer blows are recorded and analyzed to determine average peak force, energy and cumulative impulse. The proposed calibration procedure requires adjusting the number of blows to achieve a "standard" cumulative impulse. A limited laboratory evaluation program has been undertaken to demonstrate the system. The variability of test results for specimens prepared in calibrated machines was reduced by as much as 60%, as measured by the reduction in standard deviation and range of data for 15 specimens. A draft calibration standard has been developed and formatted according to AASHTO standards.

Acknowledgements

The authors would like to gratefully acknowledge Tracy McInturff, Steve Vaclavik and Tim Maust of the AASHTO Materials Reference Laboratory, for preparing and testing numerous Marshall specimens, and assisting in other areas during the course of the study. The authors would also like to acknowledge Jim Pielert of NIST for input and guidance during various stages of the study. Finally, the authors would like to acknowledge the contract technical representatives from the Federal Highway Administration, Doug Brown and Mike Rafalowski for their constructive input and comments.

Disclaimer

Certain trade names and company products are mentioned in the text or identified in an illustration in order to adequately specify the equipment, experimental procedure, and fabricated device. In no case does such identification imply recommendation or endorsement by the National Institute of Standards and Technology, nor does it imply that the products are necessarily the best available for the purpose.

TABLE OF CONTENTS

LIST OF FIGURES

LIST OF TABLES

LIST OF ABBREVIATIONS AND SYMBOLS

The following symbols and notation are used in the report:

E	=	elastic energy of the calibration device
E_{50}	=	standard 50-blow cumulative energy
$(F_{ave})_{min}$	=	minimum average peak force
F_m	=	force in the device at maximum compression
g	=	acceleration due to gravity
h	=	hammer drop height
I_{50}	=	standard 50-blow cumulative impulse
k	=	stiffness of the device spring assembly
k_p	=	stiffness of the pedestal
k_s	=	stiffness of the foundation/support
M	=	designation for Manual Standard machine setup in laboratory evaluation program
m_f	=	mass of the hammer foot, top plate, and contributory mass of the hammer shaft
m_p	=	mass of the pedestal and contributory mass of the machine
m_s	=	mass of the foundation/support
m_t	=	combined mass of the drop weight, hammer foot, top plate, and contributory mass of the hammer shaft
m_w	=	mass of the drop weight
N_E	=	blow count from calibration based on cumulative energy
N_E^i	=	individual set blow count from calibration based on cumulative energy
N_I	=	blow count from calibration based on cumulative impulse
N_I^i	=	individual set blow count from calibration based on cumulative impulse
PS	=	designation for Pine Standard machine setup in laboratory evaluation program

PW	=	designation for Pine with Weight machine setup in laboratory evaluation program
RS	=	designation for Rainhart Standard machine setup in laboratory evaluation program
RP	=	designation for Rainhart with Pad machine setup in laboratory evaluation program
x_f , $\dot{x}_f$, $\ddot{x}_f$	=	displacement, velocity, and acceleration of the foundation/support
x_p , $\dot{x}_p$, $\ddot{x}_p$	=	displacement, velocity, and acceleration of the pedestal/machine
x_t , $\dot{x}_t$, $\ddot{x}_t$	=	displacement, velocity, and acceleration of the device top plate

CHAPTER 1. INTRODUCTION

Background

Asphalt concrete consists of graded aggregate, mineral fillers, and asphalt cement. The concrete is usually mixed hot at the plant, delivered to the job site, laid, and compacted, to form what is commonly referred to as asphalt pavement. When properly designed, the pavement will be stable under load, durable, and skid resistant.

Most State and local highway agencies use the Marshall method for the design of asphalt paving mixtures. The Marshall method is described in several industry standards, including ASTM D-1559, AASHTO T-245, and Military MIL-STD-620A. The procedure requires compacting a small sample of hot-mix asphalt in a 102-mm (4-in) diameter cylindrical mold, using a manual or mechanically operated Marshall compaction hammer. The standard procedure requires 35, 50, or 75 blows (according to traffic category) from the hammer on one side of the specimen, then the same number of blows from the hammer on the opposite side of the specimen. The sample is then extruded from the mold and tested to determine the density, percentage of air voids, stability, and flow. The composition of the mixture is varied and the procedure is repeated until the desired mix characteristics are achieved.

The Marshall compaction hammer (referred to from here on as simply "the hammer") consists of a tamping foot, shaft, drop weight, and pedestal, as illustrated in figure 1. The diameter of the foot (98.4 mm [3.875 in]), the drop height (457 mm [18 in]), weight of the drop weight (44.5 N [10 lb]), and pedestal (dimension, materials, and anchorage to a concrete slab) are all specified by the industry standards. Years ago, only manually operated hammers were used. However, it was not long before mechanically operated hammers were developed. The mechanical hammers automatically raise and release the drop weight at the specified height, and most include automatic counters that turn the machine off after a pre-selected number of blows. Mechanically operated hammers are most prevalent today. Multi-hammer systems are also in use and consist of two or three hammers in line that run in tandem. The industry standards do not prohibit the use of mechanical hammers, but normally require that the test results should be consistent with those obtained when using a manual hammer.

The results of several round-robin mix exchange programs have shown wide variability in Marshall test data. Much of the variability has been attributed to the compaction process and, in particular, the Marshall compaction hammer. A number of hammer-related variables have been suggested that might influence the Marshall test results; these include variations in the drop weight, drop height, friction, type of pedestal, hammer alignment, and base support (foundation).

In order to reduce the variability of the Marshall test results it was recognized that a method for quantifying the effect of key equipment-related variables was needed, i.e., a calibration procedure. In this way, a "standard" compactive effort could be delivered to specimens regardless of slight variations in the hammer. The system would ideally include a simple-to-use, robust calibration device, suitable for a laboratory or field environment, and a calibration

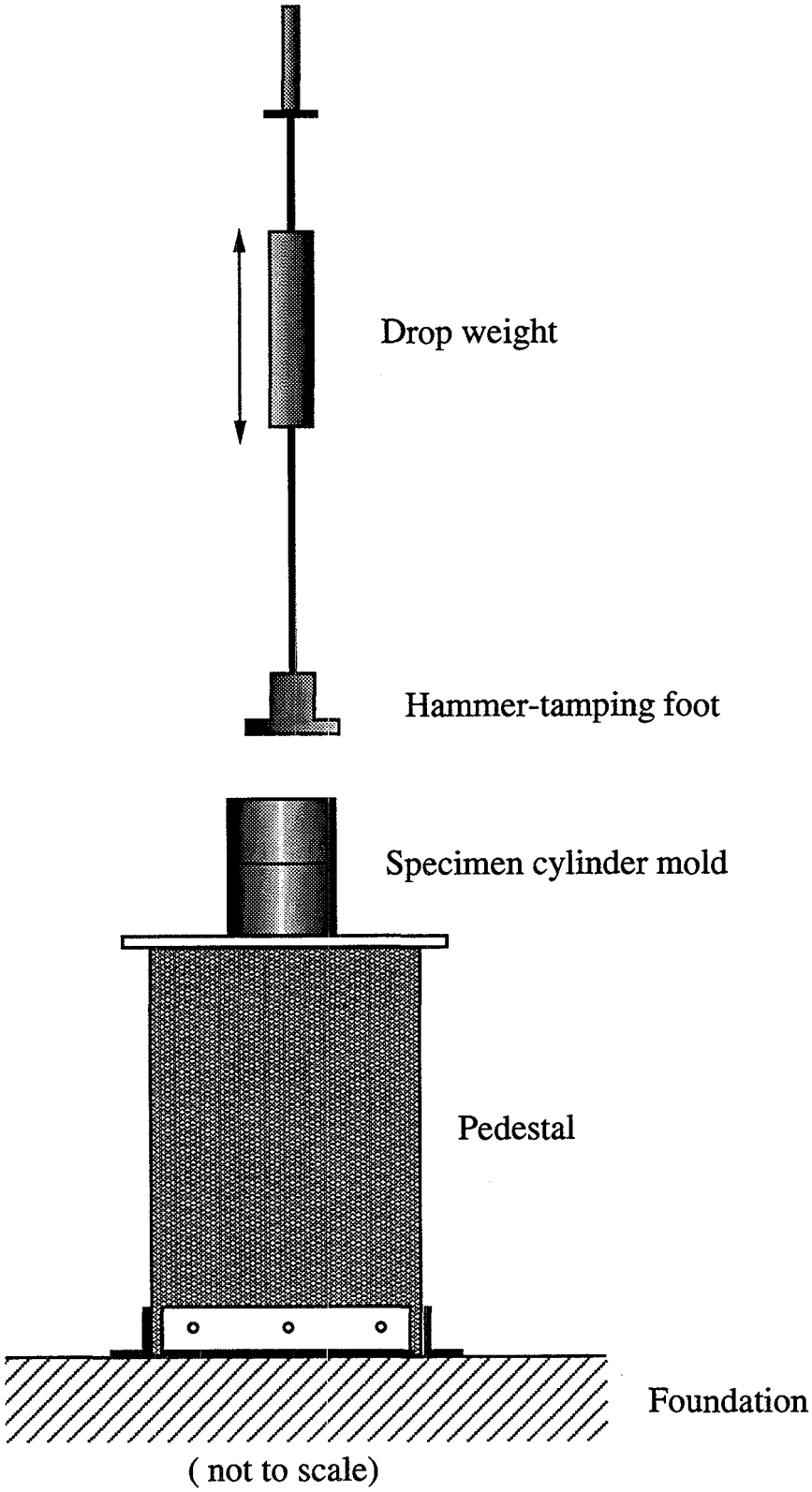

Figure 1. Marshall compaction hammer.

procedure. This report summarizes the results of a study to develop and test a calibration system for mechanical Marshall compaction hammers.

Objective and Scope

The objective of the study was to develop a practical testing apparatus or device that can be used to calibrate mechanical Marshall compaction hammers. A calibration procedure would be established for adjusting the number of blows so that a "standard" compactive effort can be supplied to a specimen, regardless of slight variations in the Marshall equipment. The device and procedure are to be used in the field and laboratory, by technicians with limited training in sophisticated electronic and computer equipment; therefore, the device should be simple to use, robust, and capable of withstanding a field/site environment.

Scope has been limited to compaction hammers with the following characteristics: mechanically operated, 102-mm (4-in) diameter mold cylinder, fixed base (i.e., non-rotating), and flat tamping foot. Excluded are certain variations of compaction hammers that are in use, or under development today, such as those that use a 152-mm (6-in) diameter mold and mechanical hammers with a tapered foot and rotating base. Manually operated hammers were specifically excluded from this initial development study because, (1) the manual hammer is rarely used today for "production" work, and (2) the additional variability inherent with using the manual hammer because of the operator.

The study was divided into six tasks that are briefly discussed below:

Task A: Literature Survey

Review the literature for studies dealing with test result inconsistencies in the Marshall design procedure and related compaction hammer variables. Review the literature for studies on the load-deformation and energy-absorption characteristics of asphalt samples during Marshall specimen compaction.

Task B: Experimental Investigation

Conduct a limited experimental investigation to determine the load-deformation and energy absorption characteristics of four typical asphalt mix designs. The four mix designs are to have a range of characteristics that encompass those of many of the designs currently used in the field today. Data to be collected from the experiments is to include specimen load-time and compression-time histories for selected blows during a standard 50-blow Marshall test.

Task C: Prototype Design Concept

Based on the results of tasks A and B, develop one or more design concepts for the calibration device. Describe the concepts and provide a recommendation on the most promising concept in writing to the contract sponsor in the form of a 6-month interim report.

Task D: Fabricate, Test, and Redesign Prototype

Proceed with development of the design concept selected by the contract sponsor in task C. Obtain the instrumentation and other materials necessary to fabricate the device. Assemble the prototype calibration device. Conduct limited laboratory tests to demonstrate the performance of the device; redesign or modify as needed to bring the calibration device to final prototype form.

Task E: Inhouse Evaluation

Using the equipment and procedure developed in task D, establish a calibration procedure for adjusting the number of blows for a given set of Marshall equipment so that a "standard" compactive effort can be applied to test specimens. Conduct an "inhouse" laboratory evaluation of the calibration procedure. Simulate in the "inhouse" evaluation some of the varying conditions that result in inconsistencies in the Marshall test procedure (i.e., variation in drop weight, friction, foundation compliance, etc).

Task F: Final Report

Document the results of the study in a final report and technical summary. Describe in detail the work accomplished in the study. Provide a complete description of the development and evaluation of the testing equipment that measures the compactive effort delivered to Marshall specimens during the compaction process. The component parts of the testing equipment, the steps involved in assembling these parts, and the procedure for using the testing equipment should also be prepared in a format used by the American Association of State Highway and Transportation Officials (AASHTO) Subcommittee on Materials.

Outline of the Report

The report is divided principally according to the tasks listed above. Chapter 2 describes the computer-based literature review and summarizes the references that were found to be relevant to the study. The experimental investigation is described in chapter 3. This includes a description of the test setup, procedure, results, and a discussion of the findings. Chapter 4 provides details on the design, fabrication, testing, and evaluation of the prototype calibration system (task D). The calibration procedure developed for the "inhouse" laboratory evaluation program is outlined in chapter 5. The laboratory evaluation is reported in chapter 6. Conclusions are presented in chapter 7.

There are five appendixes to the report. Detailed information on fabrication and assembly of the calibration device is presented in appendix A. A listing of computer programs developed as part of the calibration system for processing data are presented in appendix B. Calibration reports and raw Marshall test data from the laboratory evaluation program are presented in appendixes C and D, respectively. The final, recommended calibration procedure is presented in appendix E (in AASHTO standard format).

CHAPTER 2. LITERATURE SURVEY

Introduction

A literature survey was conducted using the online computer data bases available through the Research Information Center of the National Institute of Standards and Technology. Searches were conducted for references dealing with the variability of Marshall test results, factors affecting the results of the Marshall test, calibration of the Marshall hammer, and the load-deformation and energy absorption characteristics of asphalt specimens during Marshall compaction. Three data bases were surveyed:

- Engineering Index (COMPENDEX) covering the period 1970 - March 1992;
- National Technical Information Service (NTIS) covering the period 1964 - April 1992;
- Transportation Research Information Services (TRIS) covering the period 1970-December 1991

The data bases were searched for citations using the keywords ASPHALT, BITUMINOUS, CALIBRATE, MATERIAL, and MARSHALL. This produced a large number of potential citations from the three data bases. The list was then narrowed by searching within the group for the two keywords MARSHALL and COMPACT. The list obtained from TRIS was narrowed again by searching for the additional keyword LABORATORY.

A total of 172 citations remained after the final online screening. After reviewing the citation titles, the list was narrowed to 26 by eliminating those that were clearly not relevant. Of the 26, only 2 references addressed issues specifically related to the project.

ASTM standards were also surveyed for calibration or test procedures that are related or could be adapted to meet the objectives of the project. A few were found that are worth noting and are discussed below.

Review of Pertinent Literature from the Survey

The first comprehensive study to address variables affecting Marshall test results was reported by Siddiqui, Tretheway, and Anderson in 1987 (Siddiqui et al., 1987; also, Siddiqui, et al., 1988). The study was conducted under contract to the Arizona Department of Transportation, and in cooperation with the Federal Highway Administration. The purpose of their study was to identify key equipment-related variables associated with test result inconsistencies, and to recommend calibration equipment and techniques to be used with the Marshall hammer. The work of Siddiqui, et al., is most relevant to the investigation reported herein. Some of their significant findings are summarized below.

Siddiqui, et al., identified eight equipment variables that may influence Marshall test results (i.e., height, density, stability, percent air voids). The team then surveyed 11 experienced individuals from the asphalt industry and had them rank the variables in order of significance. The factors that ranked highest among the group were: alignment of the hammer, pedestal

support, variation in drop height, variation in drop weight, pedestal construction, and friction. The results of round-robin mix-exchange programs in Georgia, Utah, and Canada were also summarized. The programs demonstrated the inconsistency in test results due to variations in equipment. Next, the authors reviewed the current methods for "calibrating" the Marshall hammer. The two methods described include, direct comparison of bulk density obtained with 50-blows per side of a manual hammer, to the density obtained with a mechanical hammer and a varied number of blows; and the purely empirical "penny test," where a penny is placed in the specimen mold and subjected to 35 blows of the hammer. Machine performance is gauged by the diameter of the flattened penny.

Siddiqui, et al., also conducted experiments to determine the feasibility of measuring accelerations on parts of the machine and foundation during specimen compaction. The test setup included a shock accelerometer mounted on the drop weight, one on the top plate of the pedestal, and one on the floor in the vicinity of the machine. Acceleration data was recorded for 15 specimens of similar mix composition for 35 blows on each side. Results indicated that the process is repeatable, and slight variations in hammer alignment, friction, etc., did not significantly affect the acceleration time histories. Interaction between the machine and foundation was considered significant, noting an order of magnitude difference in the peak accelerations. Owing to this finding, the authors suggested that the pedestal be supported on a 0.9- by 0.9- by 0.9-m (3- by 3- by 3-ft) block of concrete, instead of simply a concrete slab. The authors concluded that reliable data can be extracted using relatively simple instrumentation; however, the impact signal tended to be swamped by high frequency vibration induced in the machine as a result of the hammer blow (i.e., structural ringing).

In their original report, Siddiqui, et al. (Siddiqui et al., 1987) also suggest a potential calibration test apparatus. Recognizing the problem of structural ringing with accelerometers, the proposed system would utilize a force transducer placed between the specimen and the hammer foot. A calibration procedure was proposed that would use a "standard" specimen in conjunction with the load transducer. Noting the variability inherent in the preparation, mixing, and placement of asphalt concrete, the authors recommended a homogeneous, easily reproducible material for the "standard" specimen that would provide impact load and compaction characteristics similar to asphalt. The system would require a data acquisition system and development of processing software.

Review of Pertinent Standards

There are numerous ASTM standards that involve some sort of impact or drop testing. Many of these are geared toward determining the energy needed to fail an object or specimen. These are usually simple "pass-fail" tests, where the failure energy is equal to the potential energy of the drop weight. These standards are of limited use here; however, there are three standards worth noting that are relevant. These include:

ASTM D 2168-66 Standard Method for Calibration of Mechanical Laboratory Compactors.

ASTM D 4633-86 Standard Test Method for Stress Wave Energy Measurement for Dynamic Penetrometer Testing Systems.

ASTM D 4945-89 Standard Test Method for High-Strain Dynamic Testing of Piles.

ASTM D 2168-66 uses the single-blow deformation of a 38-caliber lead alloy cylinder to compare the compactive effort of a mechanical soil compaction hammer with that of a manual compaction hammer. Originally adopted in 1966, the purpose of the standard is similar to that being considered here. It is meant to serve as a calibration procedure for mechanically operated hammers used in compaction of soil samples, and to ensure that the results obtained with a mechanical hammer are consistent with those of a manual hammer at a particular field/laboratory site. However, the procedure is only a comparative test and does not provide a means of measuring the actual energy that can be delivered to a soil specimen, nor does it allow for a comparison of the compactive effort between different hammers at different sites. In a way, this standard is a sophisticated "penny test," described previously for the Marshall hammer.

ASTM D 4633-86 uses a sophisticated instrumentation package and test procedure to determine the percentage of available drop weight energy that enters the connecting rod of a penetrometer in the Standard Penetration Test (SPT). This is very similar to the objective of the Marshall calibration device. The test setup uses a load cell placed in the connecting rod to measure stress waves in the rod during the test. Recorded force time histories are squared, integrated, and multiplied by various factors to determine the energy transferred to the rod. The calculations involve a number of correction factors that must be determined and applied to account for limitations in the setup and other assumptions. Sy and Campanella (Sy and Campanella, 1991) have proposed a modification to the setup that utilizes an accelerometer mounted to the connecting rod in addition to the load cell. The technique utilizes a more fundamental approach to calculate energy transfer and eliminates the need for the correction factors required in ASTM D 4633-86. The technique proposed by Sy and Campanella (Sy and Campanella, 1991) was actually adapted from ASTM D 4945-89, as described next.

ASTM D 4945-89 outlines a procedure for measuring the force and velocity response of a pile during the pile-driving operation. The test setup utilizes strain gauges and accelerometers mounted to the pile near the driving head. The force time history in the pile is computed from the measured strains, pile cross-sectional area, and dynamic modulus; velocity is obtained by integrating the acceleration time history. Rather than strain gauges, a force transducer may be used between the driving head and pile. The strain and acceleration of the pile are recorded during the pile-driving operation and subsequently processed. The energy transferred to the pile is computed by integrating the force times the velocity.

Summary

Although it is widely recognized as a problem, aside from the work of Siddiqui, Tretheway, and Anderson (Siddiqui et al., 1987; Siddiqui et al., 1988), there has been little effort to establish the cause of inconsistencies in Marshall test results, or to develop a robust calibra-

tion system for the equipment. A system was proposed by Siddiqui, et al., but it apparently was never pursued. There are a few ASTM standards that do involve tests, the object of which is similar to that being considered for the Marshall system, and could possibly be adapted for use here.

CHAPTER 3. EXPERIMENTAL INVESTIGATION

Introduction

A limited number of experiments were conducted to establish the load, deformation, and energy absorption characteristics of an asphalt specimen during compaction. Of particular interest was the variation in apparent stiffness of the specimen with blow count. The information derived from the experiments was needed for the design of the calibration device. In particular, to establish the stiffness of the device, such that the loads imposed on the machine and its support during calibration would be similar in magnitude to the loads imposed during normal operation.

Experimental Program

Test Setup

The experimental setup consisted of a force transducer, two shock accelerometers, and an LVDT (figure 2). The instrumentation was selected and installed with the objective of measuring the force and deformation of the top surface of the specimen during compaction. All tests were conducted using a Rainhart Testing Equipment mechanical Marshall compaction hammer. The machine is approximately 20 years old and shows considerable wear.

To measure load, a PCB Piezotronics piezoelectric force ring (model 216M05) was placed inline between a modified hammer foot and new base plate. An inline amplifier (model 402M144) was used which provided a range of 89 kN (20 kip) and a nominal sensitivity of 0.9 V/kN (0.4 V/kip). The force ring was bolted between the base plate and modified foot using a 12.7-mm (1/2-in) flat head cap screw, and tightened to provide a preload on the transducer of approximately 18 kN (4 kip). After assembly, the force transducer was calibrated statically in a universal test machine as prescribed in the manufacturers instructions. The calibration factor of the force transducer was within 5 percent of the factory value.

To measure acceleration, two PCB Piezotronics shock accelerometers (model 305A04) were mounted diametrically opposed to each other on the new base plate. The accelerometers have a range of 5000 g, an overrange of 10,000 g, and a nominal sensitivity of 1 mV/g. Power to the two accelerometers and the force transducer was supplied by a PCB Piezotronics, 4-channel power supply (model 482A05).

An LVDT was used to measure the incremental compaction of the specimen. The limited frequency response of the instrument prohibited measuring the actual deformation during compaction; however, with instrument readings taken prior to each blow it was possible to measure the net deformation resulting from each blow. The LVDT was mounted to a rigid stand with a magnetic base that could be attached to the pedestal support of the machine. After the specimen, mold, and hammer were installed, the LVDT was lowered into the mold and secured to the pedestal. A small aluminum angle attached to the end of the LVDT rested

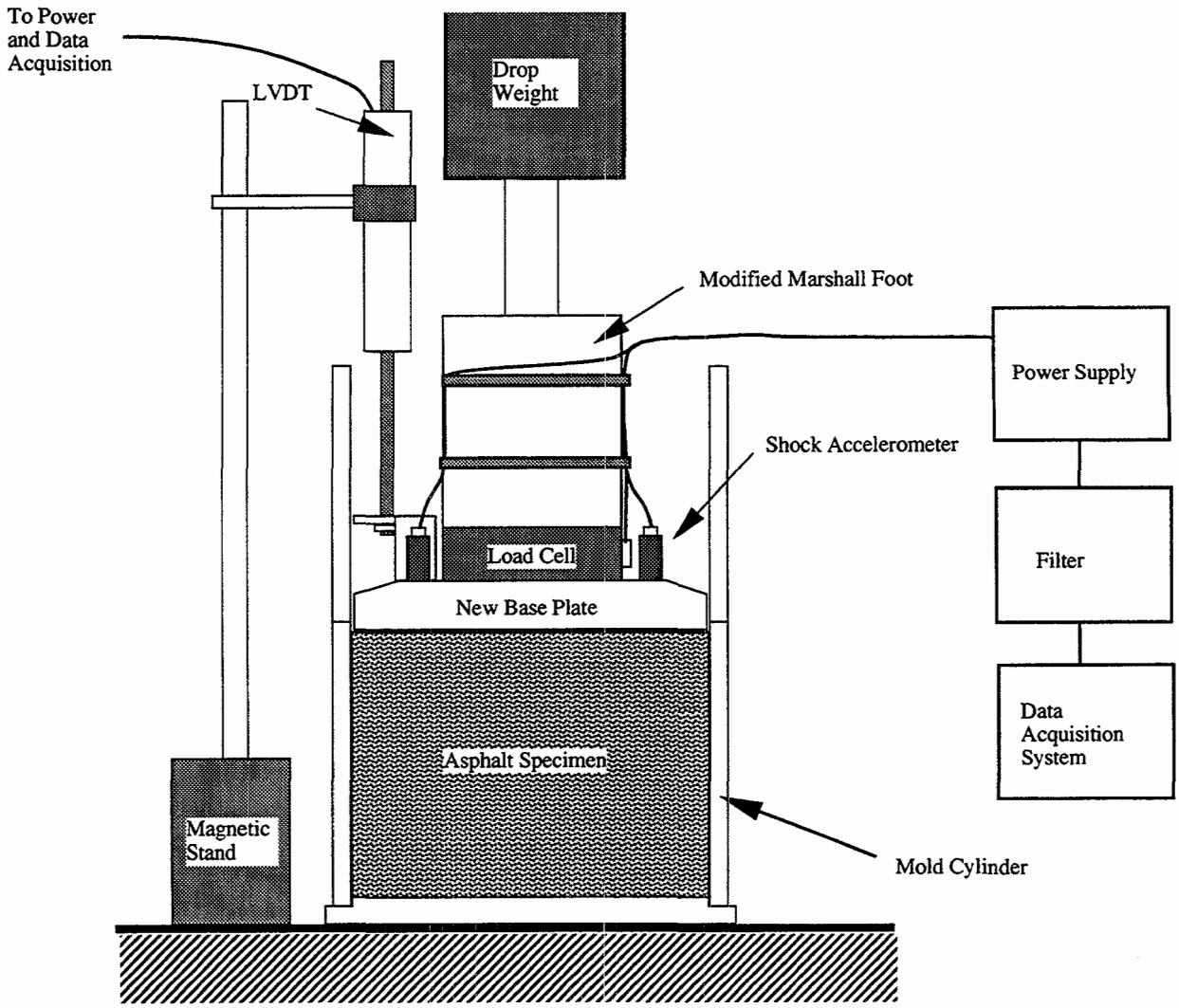

Figure 2. Experimental setup.

on the base plate during testing - the LVDT shaft was not mechanically connected to the base plate.

Data was recorded using an Optim Electronics Megadac 5717 high-speed digital data acquisition system. The 4 channels were sampled at the maximum possible rate of 45,500 samples/s, yielding a resolution in time of 22 μs. The Megadac uses a 12-bit A/D converter and simultaneous sample-hold for all data input. Programmable gains were selected to provide a full-scale range of ±10V and resolution of ±2.5 mV. This yielded a resolution of approximately ±29N (±6.5 lb) for the force measurement. The system was automatically triggered to record data when the load in the force transducer went above 4.5 kN (1.0 kip), and automatically stop recording when the load went below 0.9 kN (0.2 kip). With appropriate pre- and post-trigger values, this resulted in data sets ranging in duration from 4 ms to 14 ms. Data sets were automatically stored to a mass storage device for later retrieval and analysis.

Mix Design

Three replicates of four different mix designs were tested. The mix-design parameters were chosen to encompass many of the designs currently used, or likely to be encountered in the field. This included two designs with what would be considered a very low percentage of air voids (3 percent), and two designs with what would be considered a very high percentage of air voids (seven percent). The four mix designs are presented in table 1.

Table 1. Asphalt mix designs.

Mix Design	Maximum Aggregate Size [mm (in)]	Asphalt Content (% by weight)	Percent Air Voids
1	9.53 (3/8)	5.1	3
2	9.53 (3/8)	4.5	7
3	19.1 (3/4)	4.9	3
4	19.1 (3/4)	5.8	7

Procedure

Specimens were compacted using the instrumented hammer as they would normally for a standard Marshall test. The asphalt mix was prepared and placed in the cylinder mold. The mold was then placed in the Marshall machine and secured using the hold-down device. The instrumented hammer was placed in the mold and connections were made to the machine as usual. The LVDT was then lowered into the mold and anchored to the pedestal using the magnetic clamp. Next, the data acquisition system was armed to trigger and the compaction machine was started. After the first 50 blows, the LVDT was removed, the specimen was rotated, and the LVDT reinstalled. An additional 50 blows were supplied to the opposite side of the specimen.

Data Analysis

For each specimen, a total of 100 data sets were generated, one for each blow recorded. Data sets were converted to ASCII format and saved on the host computer disk. After some initial interrogation of sample time histories, the data files were processed using a FORTRAN program to extract pertinent information. This included determining the maximum and minimum force and the corresponding times, maximum and minimum acceleration and the corresponding times, and the average LVDT reading for the first 20 points of the data set.

Further detailed analysis of the acceleration data was undertaken in an attempt to generate a displacement time history of the top surface for each blow. This involved first averaging the two acceleration time histories, then double integrating the resulting signal. The commercial software package, DADISP, was used for the signal processing. The results, however, proved to be of little use. Integration yielded unrealistic displacements due to slight DC offsets and high-frequency noise in the recorded accelerations. Attempts at digital filtering and smoothing were also unreliable, in that any result could be generated with the appropriate selection of filter parameters. The results of this effort are not reported in the following. Without displacement data, a detailed analysis of apparent specimen stiffness and energy absorption, as originally intended, was not possible. Nevertheless, important load and deformation data was obtained from the investigation and is described in the following.

Results

Sample time histories are presented in figures 3 through 5 for mix design 2 (table 1). These are typical of the results observed for all mix designs.

Presented in figure 3 are five force time histories corresponding to blows 1, 2, 10, 25, and 50. The characteristics of the force time histories clearly change with blow count. The first time history is characterized by multiple pulses that occur in a time interval of approximately 4 ms - the repeated pulses are attributed to bouncing of the drop weight. The peak force for the first blow is approximately 36 kN (8 kip) and occurs on the first pulse. As blow count increases, the peak force increases, bouncing appears to diminish, and the duration of the total event decreases to approximately 1 ms.

The time history average of the two recorded accelerations are presented in figure 4 for blows 1, 2, 10, 25, and 50. The difficulty in integrating for displacement, as described previously, is apparent from the figure. The acceleration time history is characterized by a large initial pulse, corresponding to the initial force pulse, followed by a signal that is predominately of high frequency with some large pulses intermixed. The complex acceleration behavior could be due to a number of factors, including multiple blows (i.e., bouncing) from the drop weight, the foot lifting-off of the specimen surface, and simultaneous foot lift-off and rotation (the foot can swivel on the hammer shaft).

Presented in figure 5 are time histories of the LVDT reading for blows 1, 2, 10, 25, and 50. The time histories are relatively flat within the interval plotted, the only change noted is the

average reading from one blow to the next. The flat response is a result of the LVDT not being physically connected to the base plate. As a result, the transducer did not move instantaneously with the base plate, but instead, dropped under its own weight until it regained contact with the base plate. A time history of longer duration would illustrate the slow drop relative to the blow and change in reading. To evaluate incremental compaction, the LVDT reading at the beginning of the time history for blow i+1 was subtracted from the reading at the beginning of blow i. For example, the compaction due to blow 1 is 10.4 - 7.3 = 3.1 mm (0.409 - 0.285 = 0.124 in).

Peak load versus blow count is plotted in figures 6 through 9 for the four mix designs. Presented in each figure are the results of the three replicates and the average peak load. The average peak load versus blow count for the four mix designs are plotted together in figure 10.

The variation in peak load with blow count is fairly typical, regardless of the mix design. The peak load for the first blow ranges from approximately 26 to 36 kN (6 to 8 kip), then increases and levels to a maximum of between 58 and 67 kN (13 and 15 kip) near the end of the first 50 blows. This trend would be expected as the specimen is compacted and becomes stiffer during the test. A similar trend is observed for the second series of 50 blows. It is noted from figure 10 that average peak load varies only slightly with mix design.

The scatter in some of the data, as noted by points that fall well away from the average, is attributed to the drop weight not hitting squarely on the hammer foot. Miss-hits could be picked out easily during testing by the distinct sound of the blow, and were likely due to the age and wear of the compaction hammer. The scatter is most pronounced for the 19.11-mm (3/4-in) - 7 percent design (figure 9).

Plotted in figures 11 through 14 is the incremental compaction versus blow count for the four mix designs. Again, shown in each figure are the results of the three replicates and the average. As would be expected, the greatest compaction occurs in the early blows of the test. The incremental compaction is minimal after about 20 blows in the first set of 50, and after about 10 blows in the second set of 50. The large compaction in the first few blows of the second series is a result of the gap between the specimen and mold base that results when the specimen is flipped for the second set of 50. The results tend to indicate that the majority of the compactive effort is supplied during the first 20 to 30 blows of the Marshall test. The significance of the remaining blows, however, should not be discounted, as these blows most likely have other beneficial effects that were not born out by this instrumentation setup.

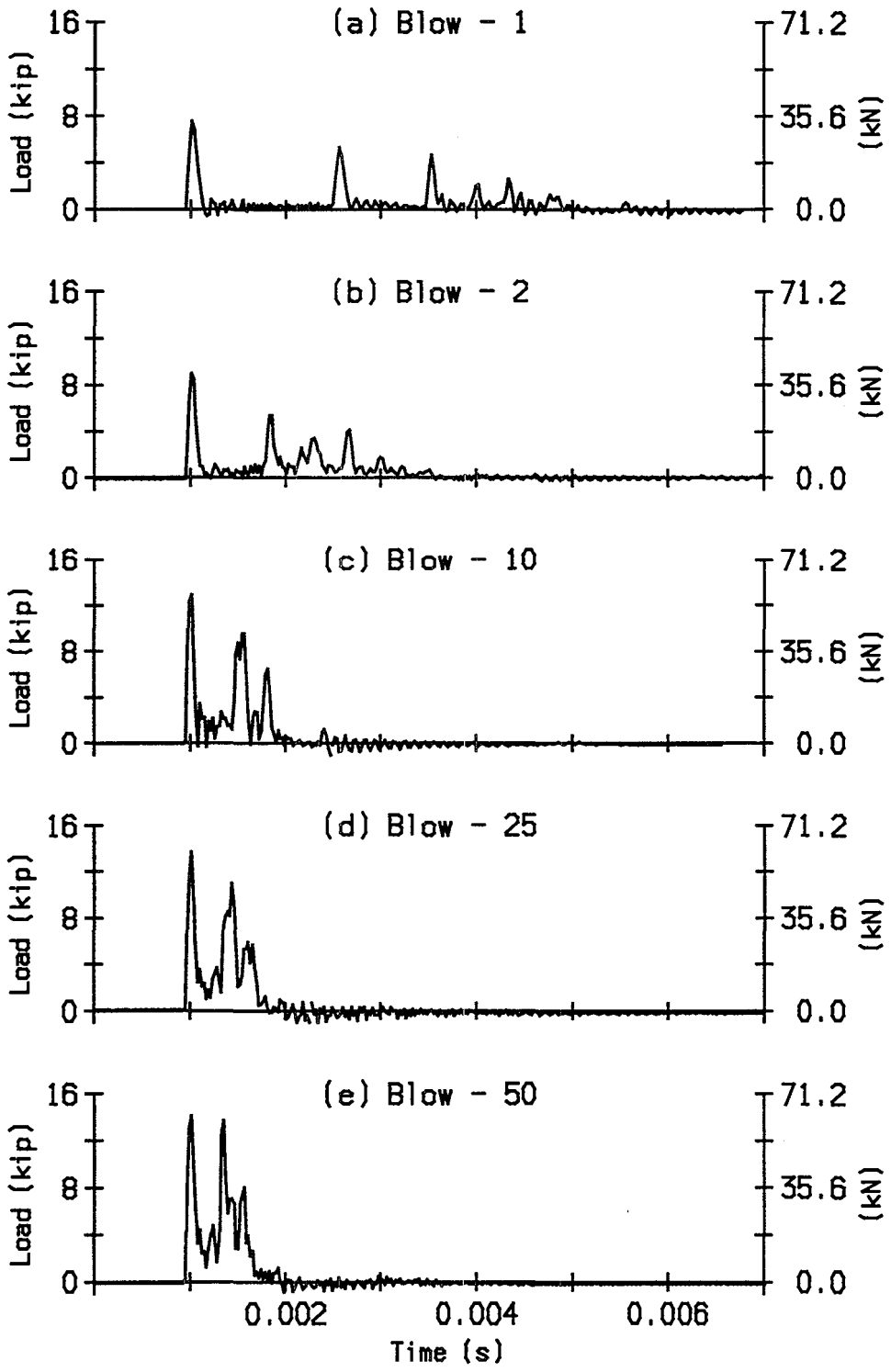

Figure 3. Typical force time histories (mix design 2).

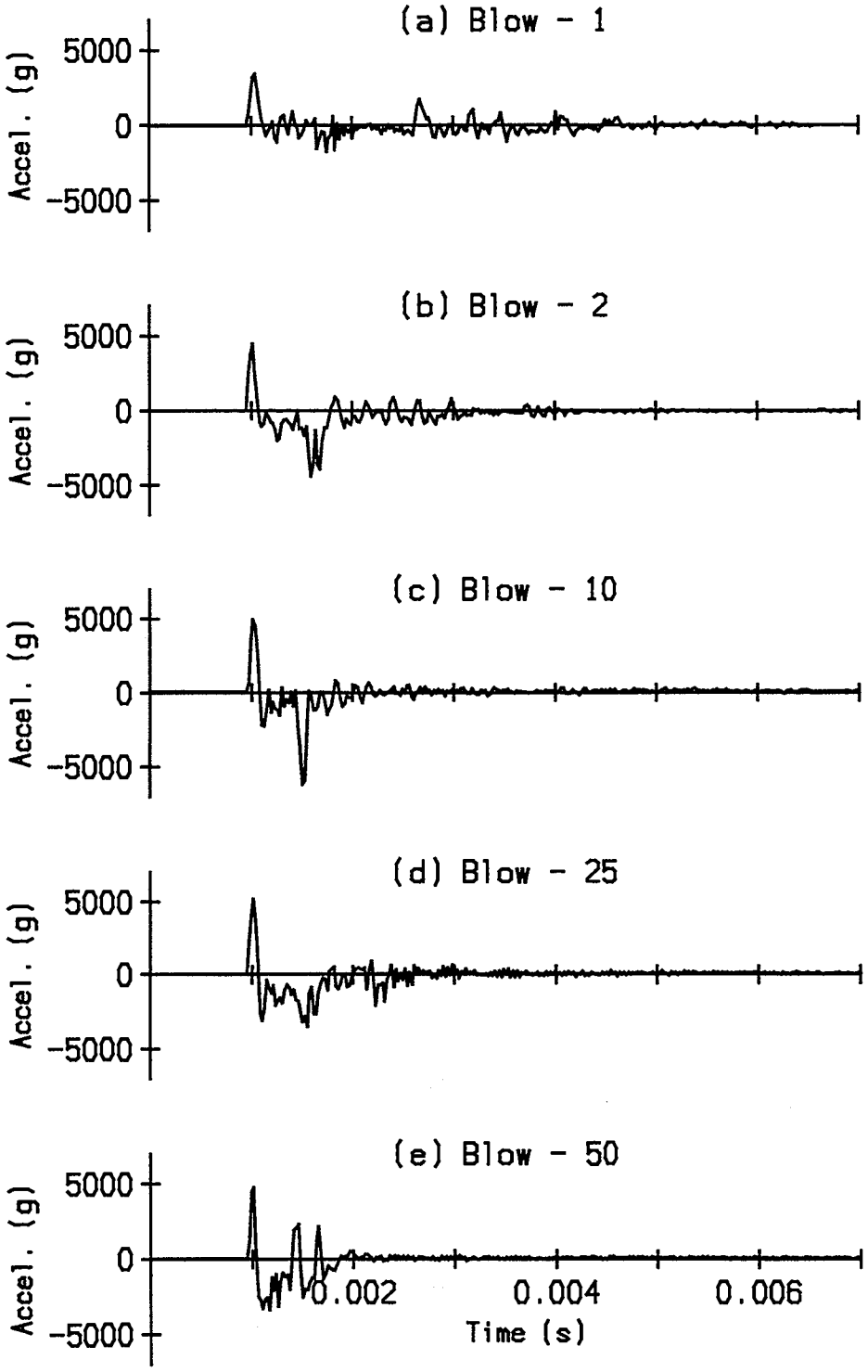

Figure 4. Typical acceleration time histories (mix design 2).

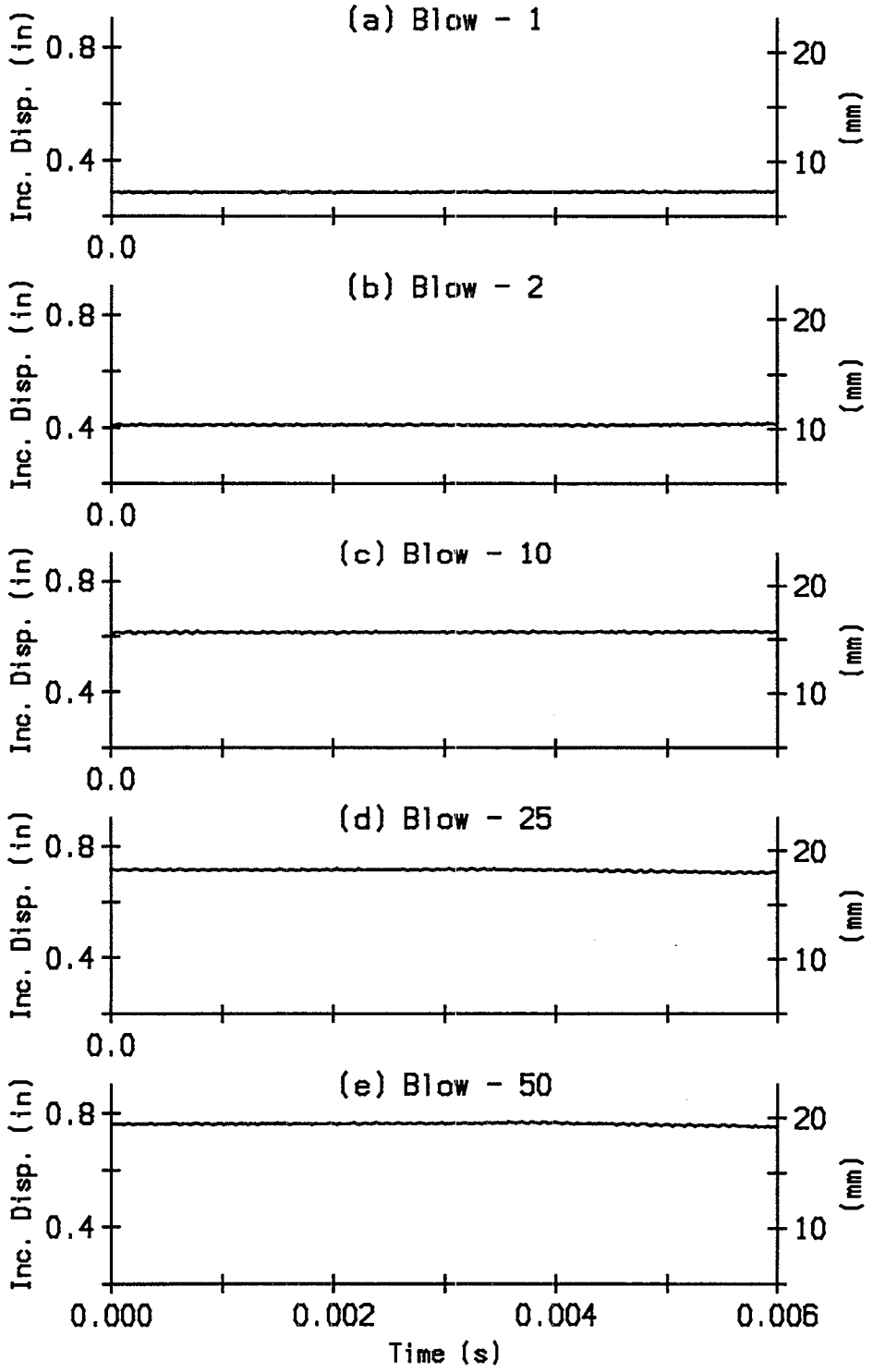

Figure 5. Typical LVDT time histories (mix design 2).

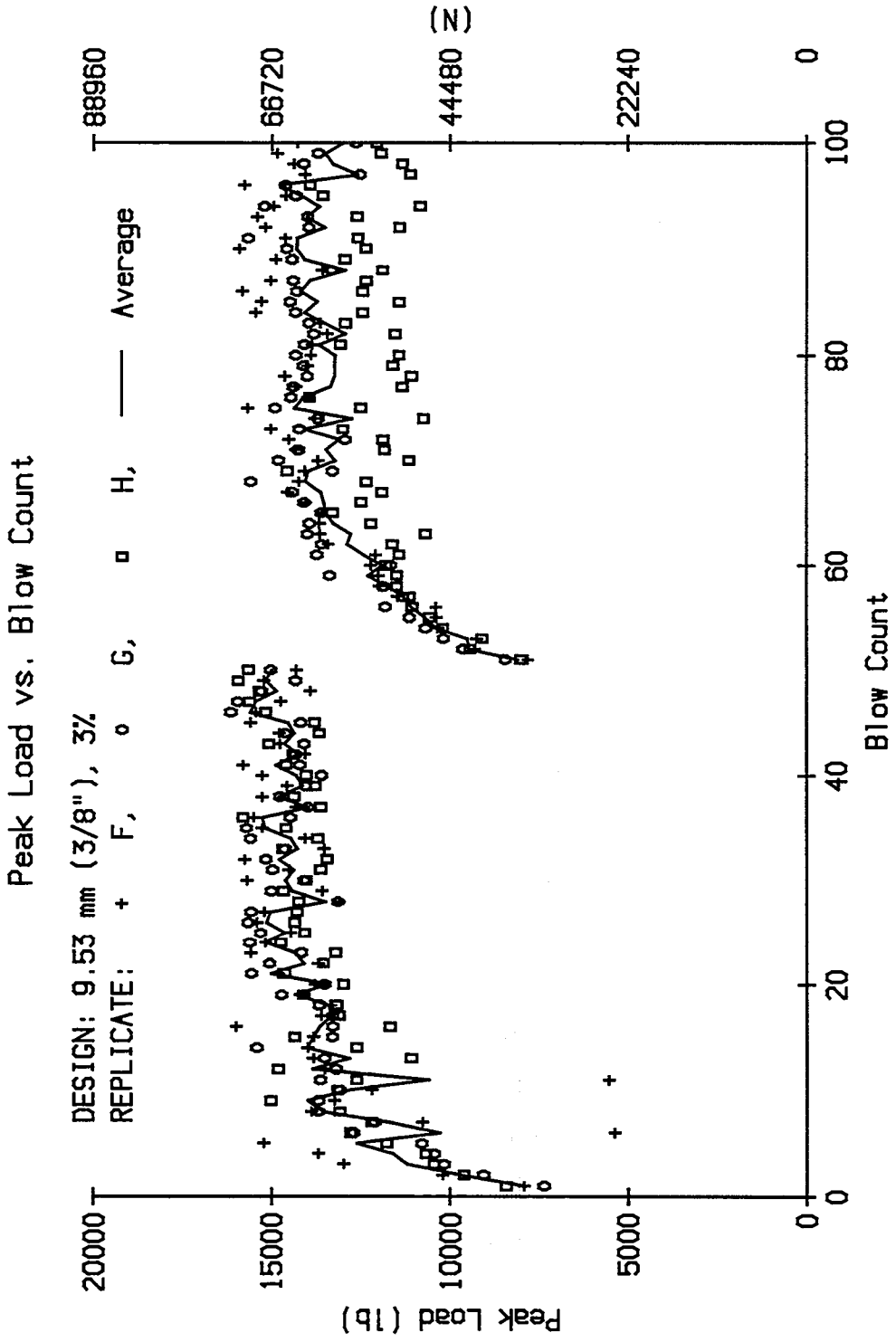

Figure 6. Peak force versus blow count (mix design 1).

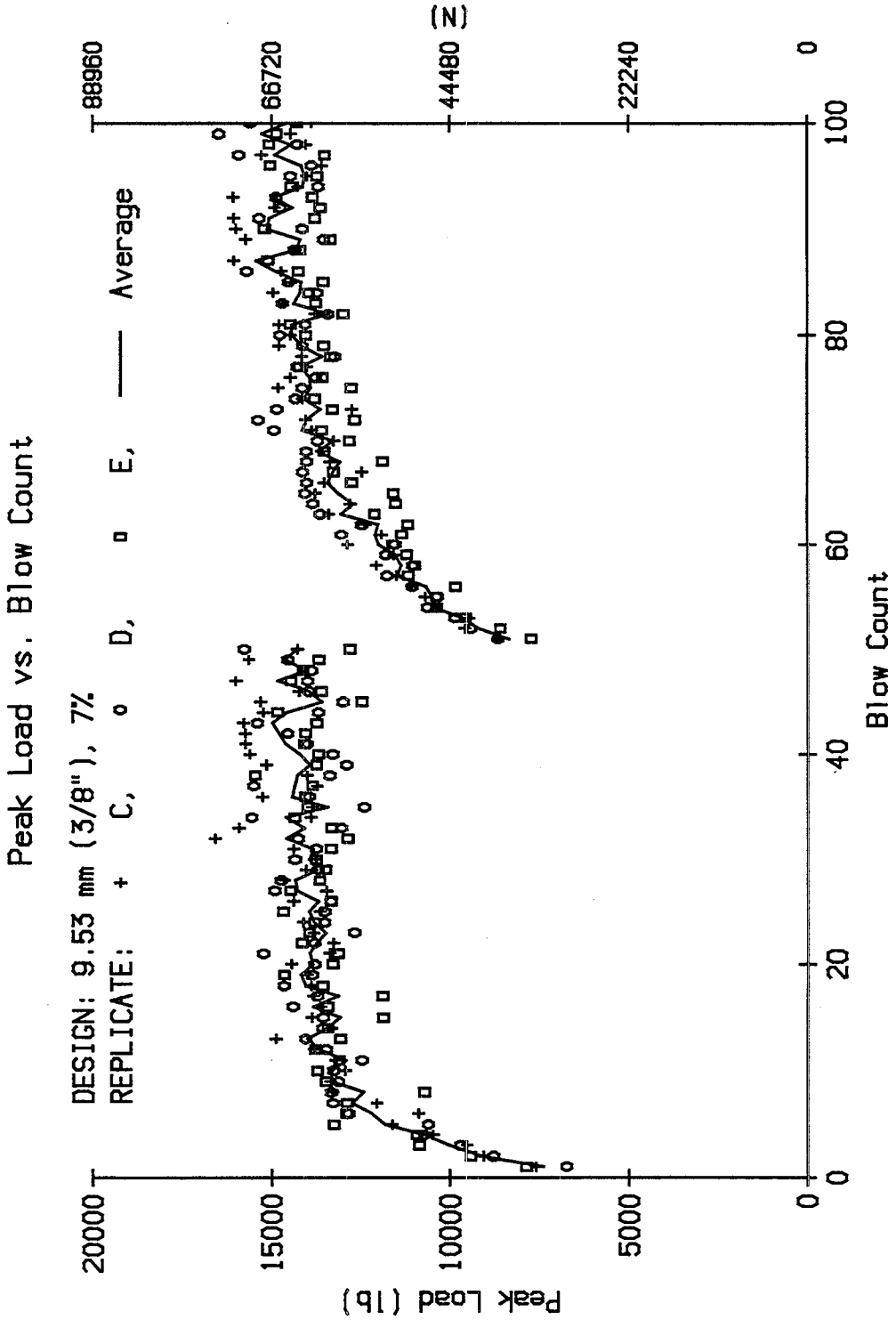

Figure 7. Peak force versus blow count (mix design 2).

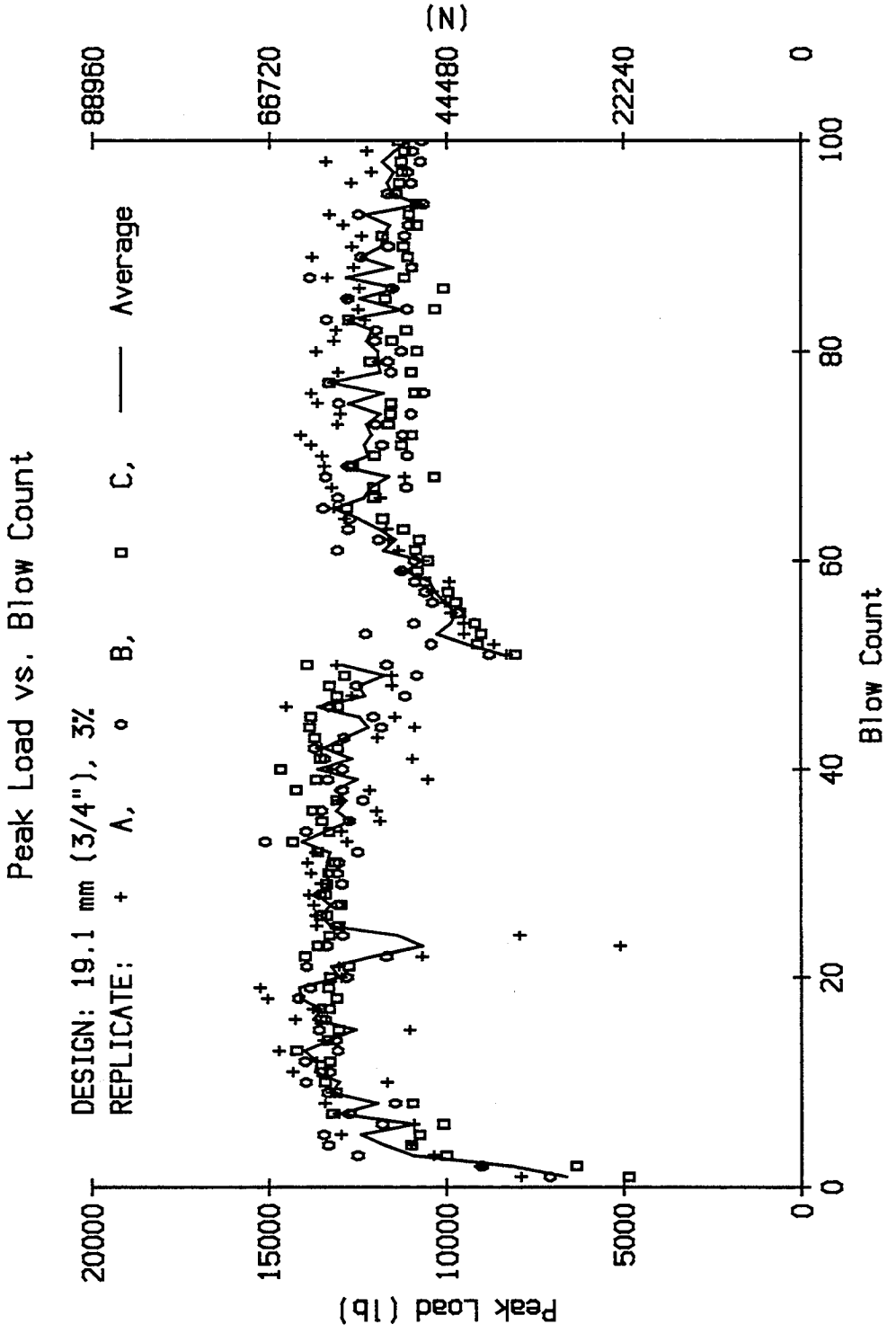

Figure 8. Peak force versus blow count (mix design 3).

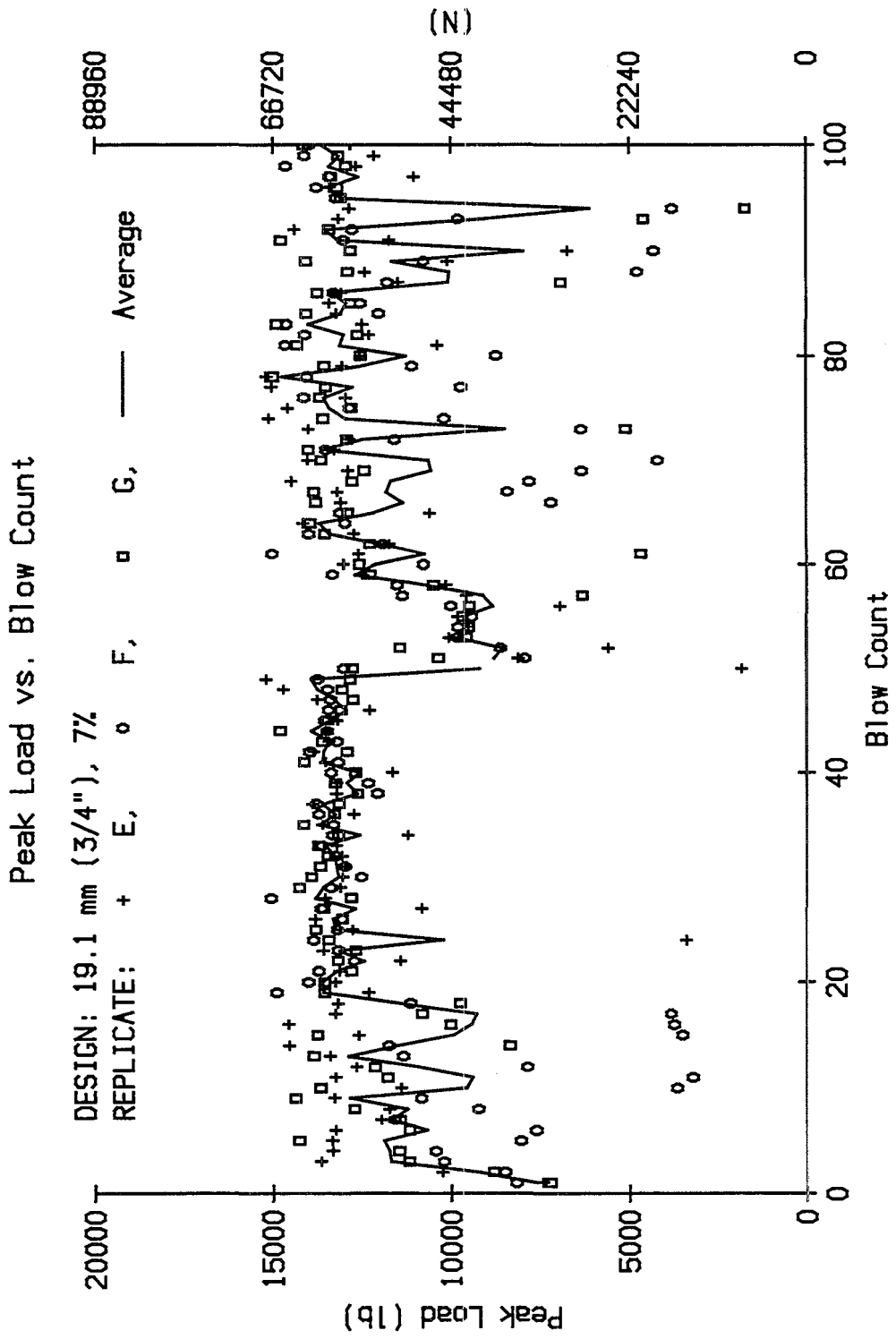

Figure 9. Peak force versus blow count (mix design 4).

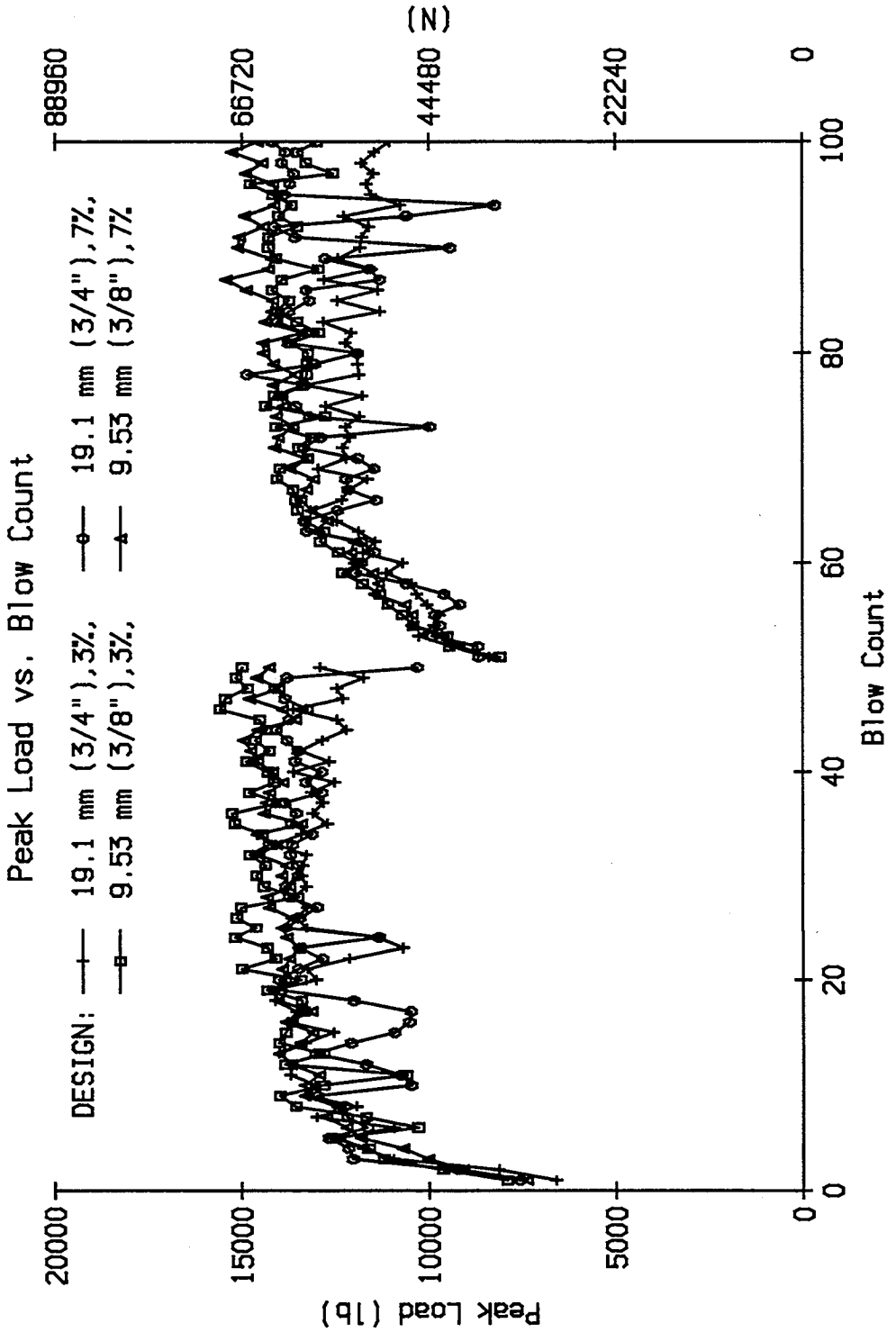

Figure 10. Average peak force versus blow count (all mix designs).

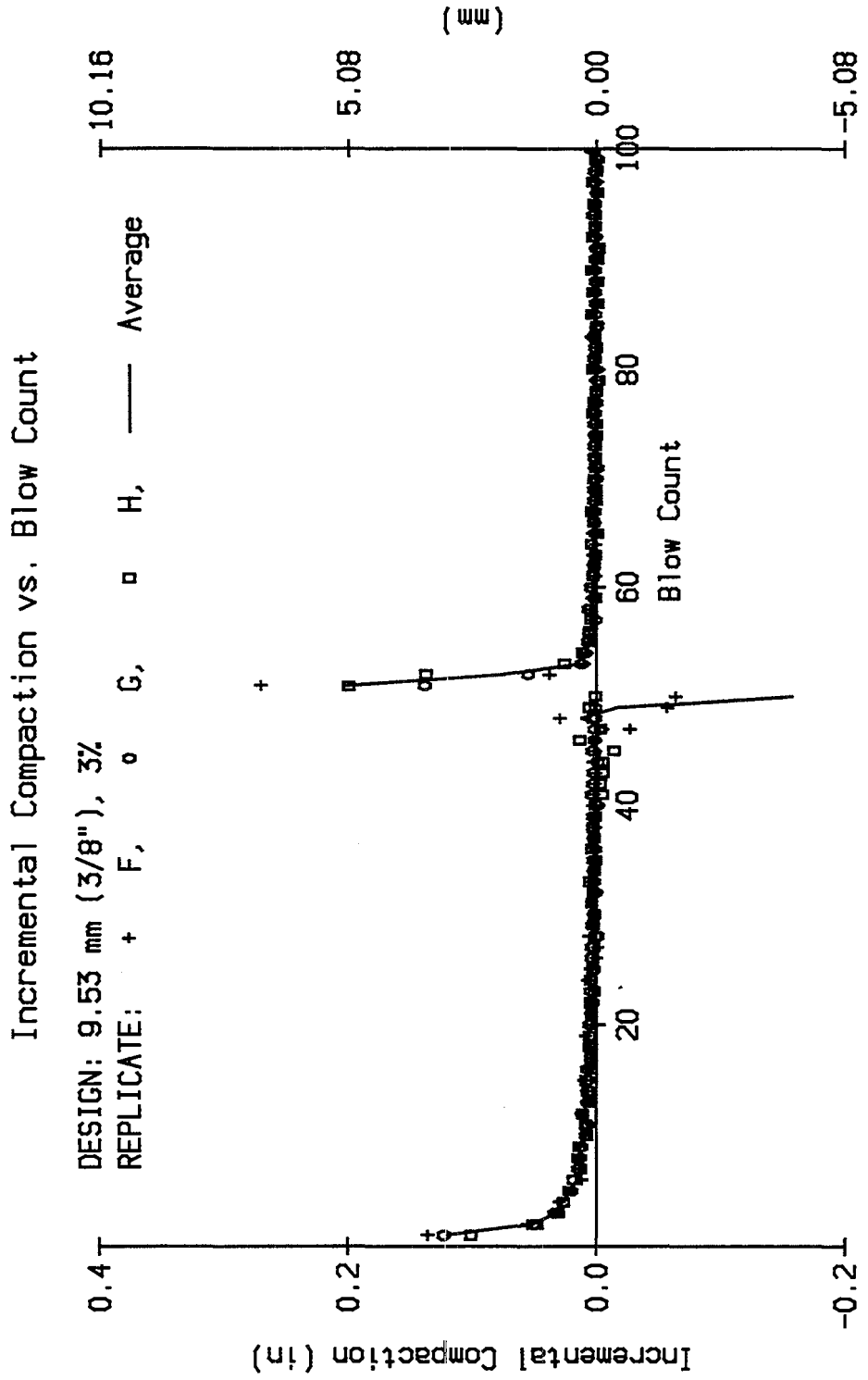

Figure 11. Incremental compaction versus blow count (mix design 1).

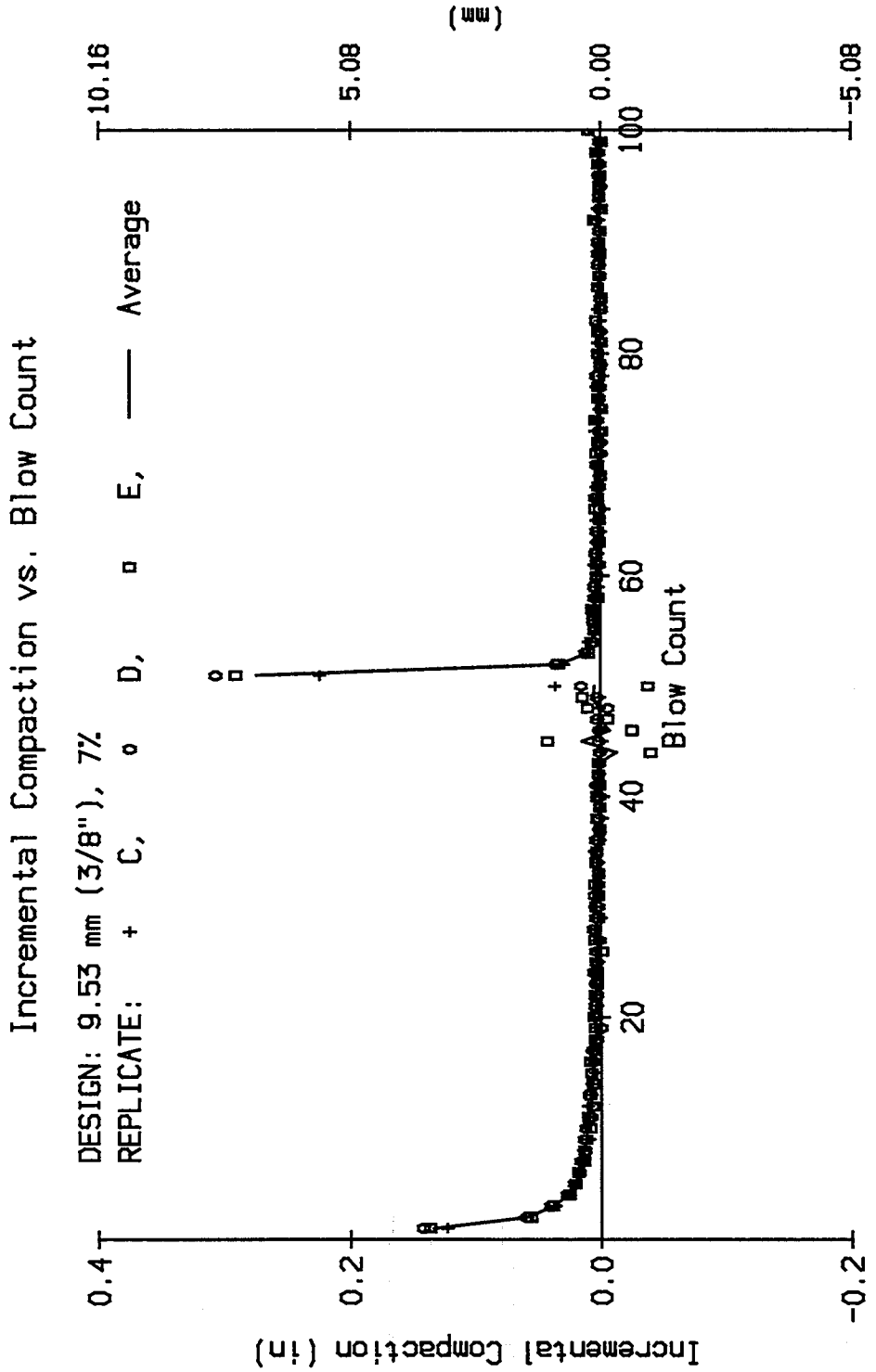

Figure 12. Incremental compaction versus blow count (mix design 2).

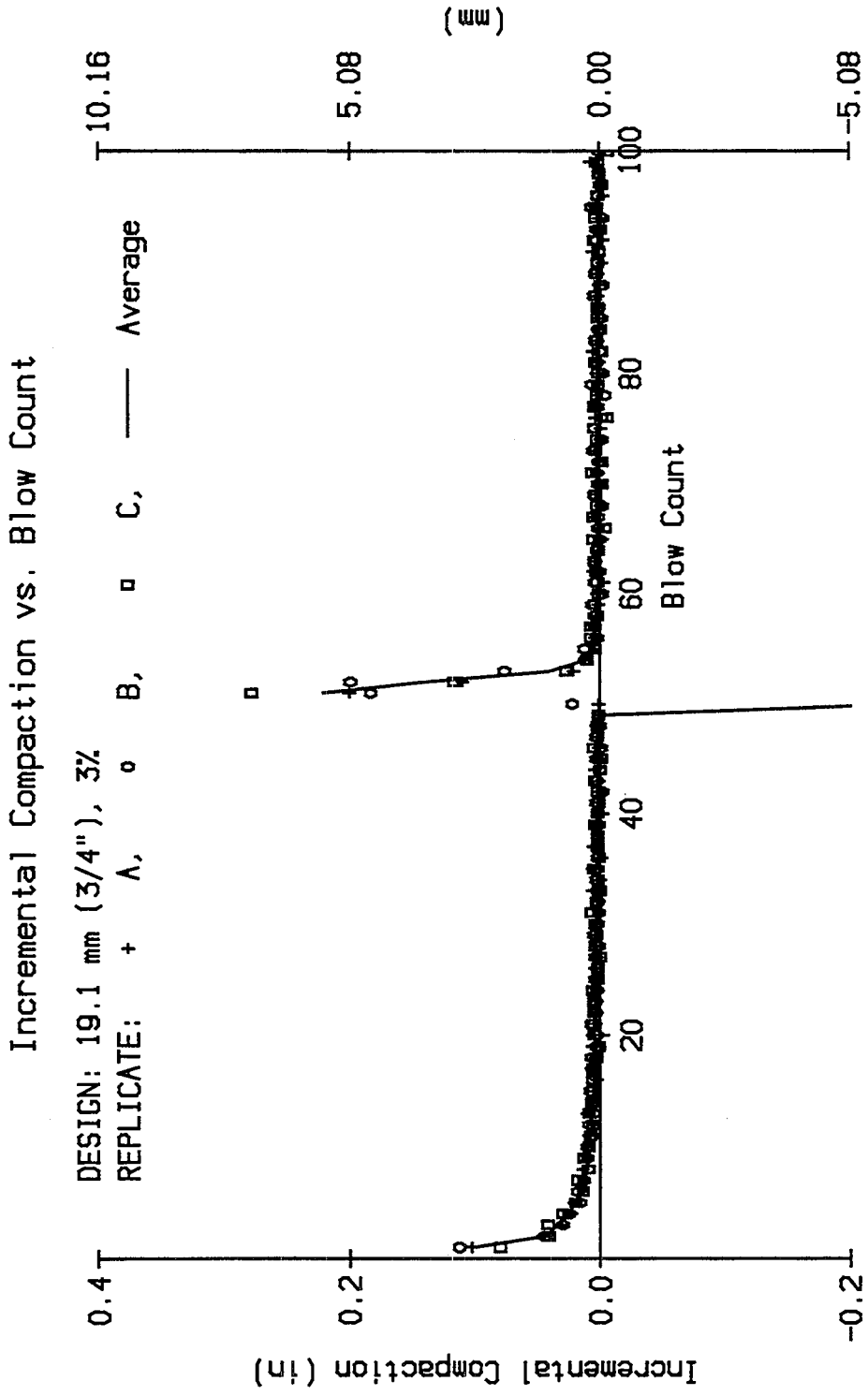

Figure 13. Incremental compaction versus blow count (mix design 3).

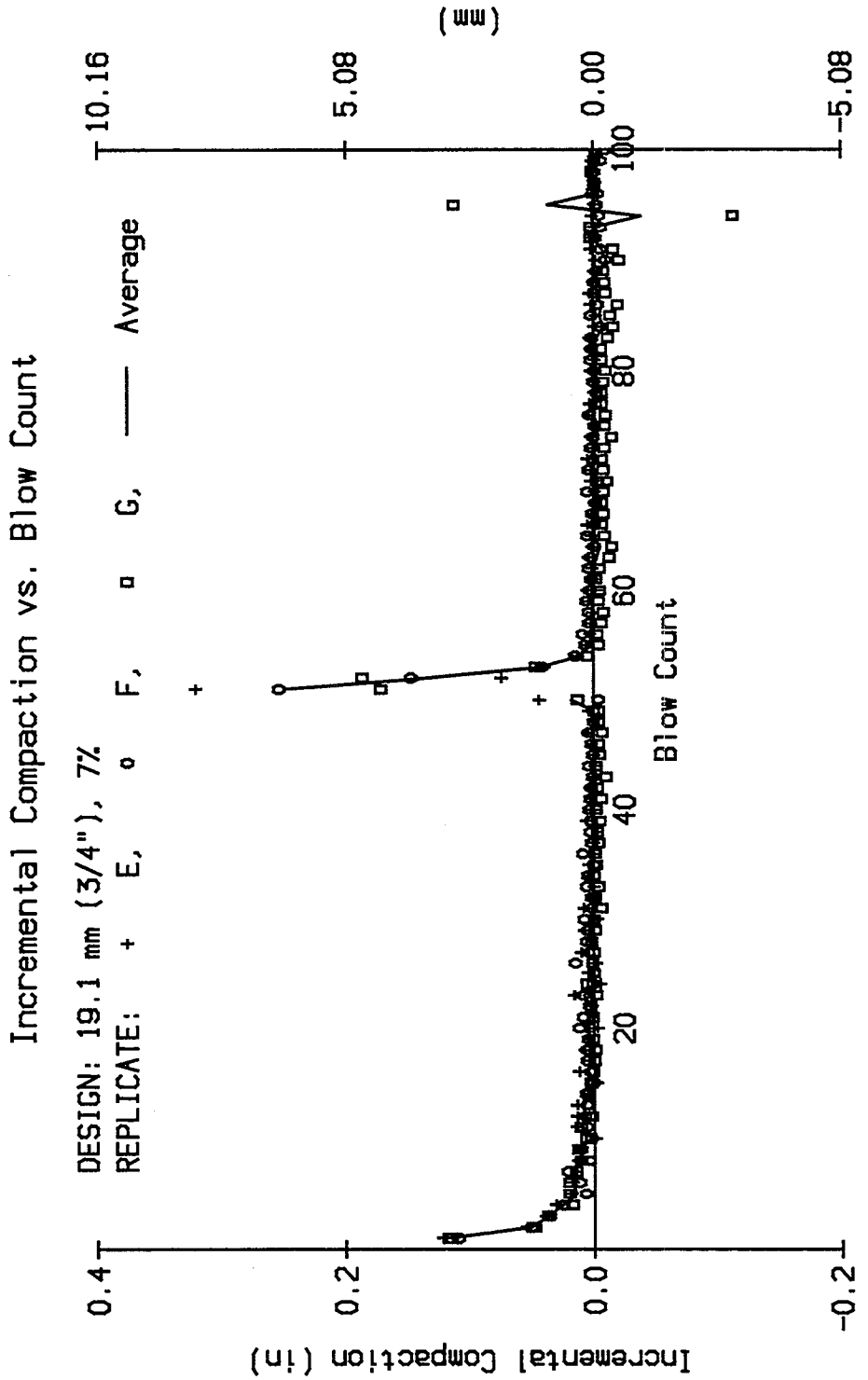

Figure 14. Incremental compaction versus blow count (mix design 4).

Summary

The experimental investigation yielded a number of important results that are summarized below:

- The maximum peak load imposed on a specimen is approximately 67 kN (15 kip). The duration of the corresponding force pulse is approximately 1 ms.
- The minimum peak load imposed on a specimen is approximately 36 kN (8 kip). The duration of the corresponding force pulse train is approximately 4 ms.
- Peak load increases and duration of the pulse decreases with blow count.
- The majority of the compactive effort is supplied in the first 20 to 30 blows.
- Results are generally insensitive to the mix-design composition.

CHAPTER 4. DESIGN AND TESTING OF THE CALIBRATION DEVICE

Introduction

Several prototype design concepts for the calibration system were developed and studied under task C (chapter 1) of the study. The two concepts considered to be the most viable--Probe Penetration Method and Elastic Spring Measuring Force Method-- were described in the 6-month interim letter report to the contract sponsor. Briefly, the Probe Penetration Method would relate the depth of penetration of probes into a "standard specimen" (e.g., synthetic disk), to the energy delivered by the machine. The method would be simple to use and the cost to assemble the package would be nominal; however, the expendable specimen would increase the cost per calibration. The Elastic Spring Measuring Force Method uses springs, a force transducer, and a data acquisition system to measure the force, impulse, and energy of an individual blow. The cost to fabricate the calibration device is moderate, but the cost per calibration is negligible. The Elastic Spring Measuring Force Method was selected by the contract sponsor for further development.

The general design requirements of the calibration system included robustness, ease of use, capability of withstanding a field environment, good repeatability, and adequate sensitivity. The results of the experimental investigation provided detailed requirements for the calibration device, i.e., stiffness such that the average peak force for a single blow in a typical machine is approximately 67 kN (15 kip) and the pulse duration is between 1 and 4 ms. Many mechanical hammers limit the height above the pedestal that the hammer can be installed and properly operated; therefore, a practical constraint was imposed on the maximum height of the device at 110 mm (4.5 in). Other design considerations included overstress and fatigue resistance of components of the device, and the cost to fabricate and operate the calibration system. Details of the design, assembly, and testing of the prototype calibration system developed under task D (chapter 1) are described in the remainder of this chapter.

General Description

A schematic drawing of the final prototype calibration system is presented in figure 15. The system consists of: (1) the elastic spring-mass device with integral force transducer (referred to from here on as "the calibration device" or simply, "the device"), (2) power supply, and (3) data acquisition system. The calibration device is fabricated from "off-the-shelf" and custom-manufactured parts. The principal components of the device include the base, assembly bolt, force transducer, sleeve, two Belleville springs (sometimes referred to as disk springs or disk washers), and top plate. The data acquisition system consists of a portable microcomputer with a high-speed analog-to-digital input card.

Presented in figure 16 (a) is a photograph of the complete calibration system. On the left in the photograph is the data acquisition system and power supply, and on the right is the assembled calibration device. Presented in figure 16 (b) is a photograph of the calibration device with the top and bottom collars removed. Shown on the right in the photograph is the calibration device, in which can be seen the base, force transducer and cable, sleeve,

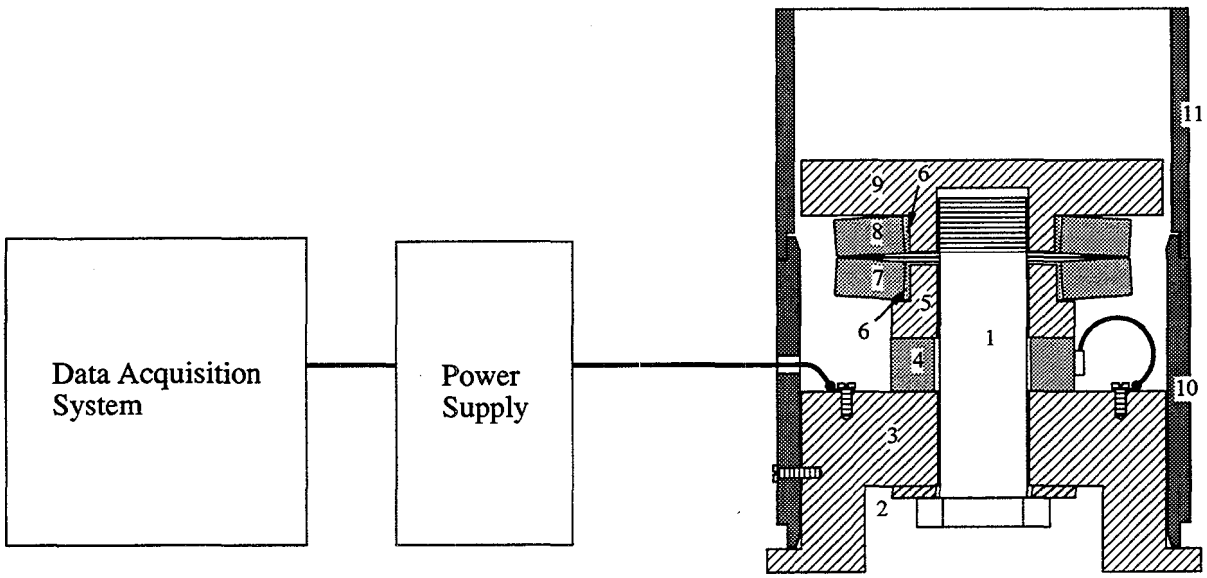

Parts:

1 -	Bolt	5 -	Sleeve	9 -	Top Plate
2 -	Washer	6 -	Elastic Band	10 -	Bottom Collar
3 -	Base	7 -	Bottom Belleville Spring	11 -	Top Collar
4 -	Force Transducer	8 -	Top Belleville Spring		

Figure 15. Calibration system.

(a) Data acquisition system, power supply and device.

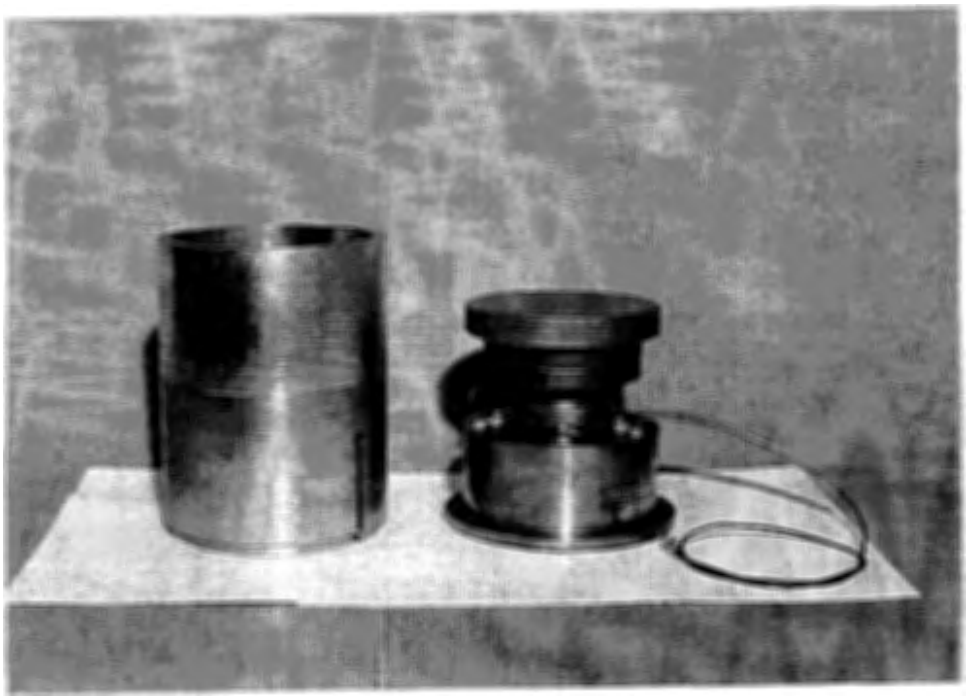

(b) Device with collars removed.

Figure 16. Photograph of calibration system.

Belleville springs and top plate. Presented in figure 17 is a photograph of the calibration system with the device installed in the compaction hammer.

The principal of operation of the calibration device is simple. The device is installed in the machine and secured with the mold hold-down device (the outside dimensions of the device are exactly equal to that of a standard Marshall specimen mold). The Marshall hammer is placed in the device such that the foot of the hammer rests on the top plate. When the hammer is in operation the impact of the drop weight with the hammer foot causes the Belleville springs to compress. Load is transferred through the force transducer, to the base, and into the pedestal. The force of the blow is recorded and stored by the data acquisition system for subsequent analysis. Each force time history is analyzed to establish the peak force, stored energy and impulse.

The information needed to fabricate and assemble the calibration system is presented in appendix A. This includes a parts list, engineering drawings, and assembly instructions. The parts list includes the part number; part name; specification; and, where applicable, the vendor and vendor model number of the part used in the prototype system for the study. Vendors are listed for reference only. This should not be construed as an endorsement of a particular manufacturer or product. The system can be assembled from any parts that meet the design specifications.

Design and Assembly of the Calibration Device

Design of the Spring Assembly

The characteristics of the load transferred to the pedestal, e.g., peak force, duration, impulse, etc., is a function of the stiffness of the device spring assembly (all other factors being equal). Thus, the design of the spring assembly proved to be the most critical development issue. Elements of the design included establishing the correct stiffness of the spring assembly to achieve the desired pulse characteristics, selecting the springs based on stiffness, stress analysis and fatigue life, and a number of other issues. These are described in the following.

Establishing the Design Spring Stiffness

The stiffness of the spring assembly was determined based on the target peak force (67 kN [15 kip]) and pulse duration (1 to 4 ms), established during the experimental program. The stiffness was determined using a simple analytical model of an elastic spring-mass system that is intended to represent the drop weight and calibration device. The model is illustrated in figure 18. The model consists of two masses and an elastic spring -- mass m_w represents the mass of the drop weight (4.53 kg [10 lb]); mass m_f represents the mass of the hammer foot, top plate, and contributing mass of the hammer shaft; the spring of stiffness k represents the spring assembly of the calibration device. In this analysis the pedestal and machine foundation are assumed to be infinitely rigid.

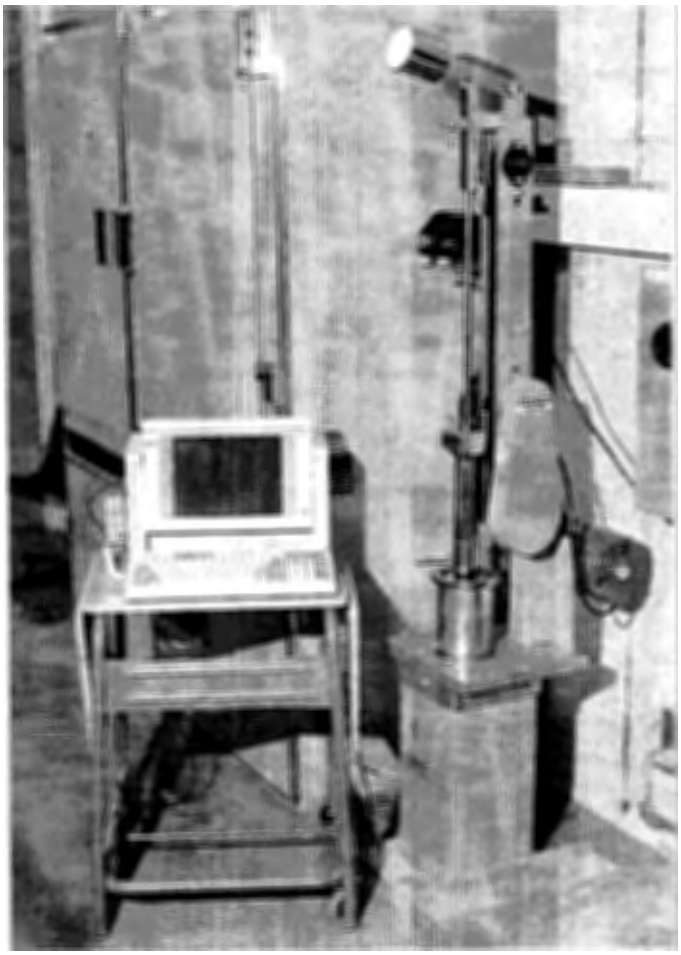

Figure 17. Photograph of system installed in compaction hammer.

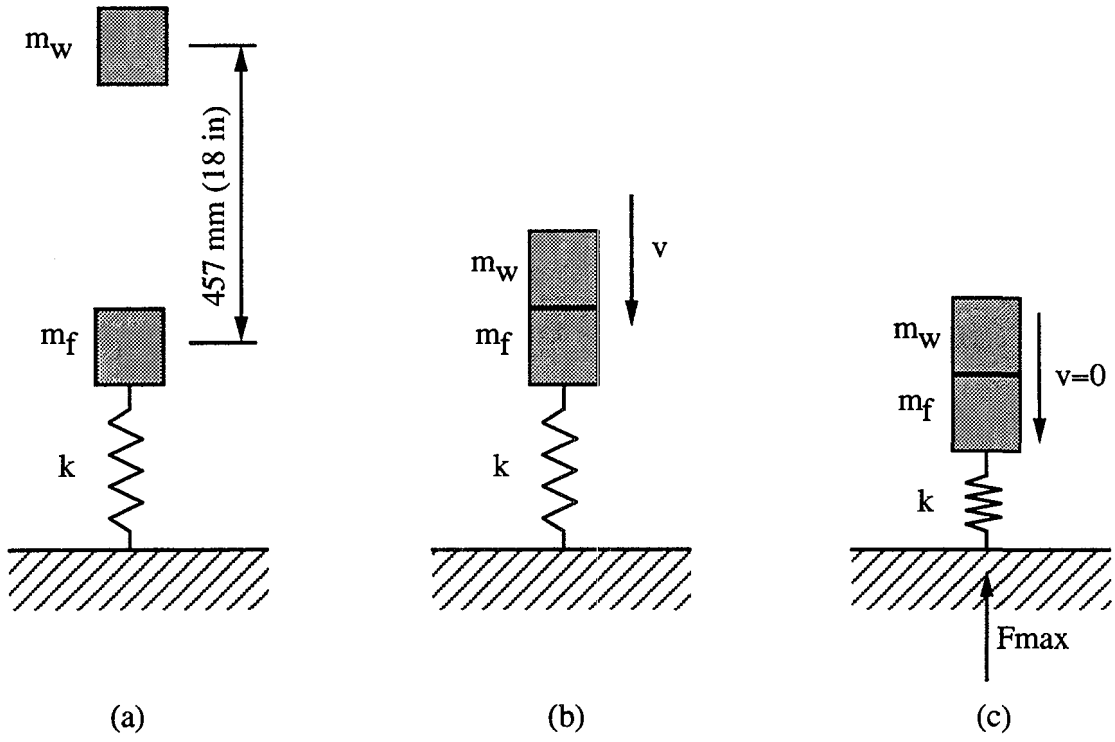

Figure 18. Single-degree-of-freedom model of drop weight and device.

Mass m_w is assumed to be released from rest a distance of 457 mm (18 in) above mass m_f, as shown in figure 18 (a). Mass m_w falls and impacts with mass m_f. By conservation of energy, the velocity of mass m_w just prior to impact is given by

$$v = \sqrt{2gh} \tag{1}$$

in which h is the drop height (457 mm [18 in]) and g is the acceleration due to gravity. Based on the observed behavior of the drop weight during actual compaction, the impact is assumed to be perfectly plastic, i.e., mass m_w does not bounce, but becomes permanently attached to mass m_f. Following the impact, the combined mass is $m_t = m_w + m_f$. By conservation of momentum, the velocity of the combined mass just after impact is given by

$$v' = \frac{m_w}{m_w + m_f} v = \frac{m_w}{m_t} v \tag{2}$$

Expressing conservation of energy for the instant just following impact and the instant of maximum force in the spring (i.e., maximum compression of the spring), yields

$$\frac{1}{2} m_t v'^2 = \frac{1}{2} \frac{F_m^2}{k} - m_t g \frac{F_m}{k} \tag{3}$$

in which F_m is the maximum force in the spring. Solving for the spring stiffness yields

$$k = \frac{2}{m_t v'^2}\left(\frac{F_m^2}{2} - m_t g F_m\right) \tag{4}$$

All of the parameters in equation (4) are known with confidence except mass m_f. Recall, this represents the mass of the tamping foot, top plate, and contributing mass of the hammer shaft. Mass m_f is bounded, however, by a mass equal to that of the tamping foot and a mass equal to that of the top plate plus the entire hammer assembly, excluding the drop weight. To establish these bounds a typical hammer was disassembled and the component parts were weighted. The mass of the particular tamping foot measured was found to be approximately 1.4 kg (3 lb), and that of the entire hammer, excluding drop weight, was approximately 4.1 kg (9 lb). Therefore, the parameter values used in evaluating equation (4) are m_w = 4.53 kg; m_f = 1.36, 2.72, and 4.08 kg; h = 457 mm; F_m = 66720 N; and g = 9.81 m/s^2. The resulting stiffness is summarized in table 2 for the three values of mass m_f.

Table 2. Calculated spring stiffness for varying total mass.

Mass m_f (kg) [lb]	Mass m_t (kg) [lb]	Stiffness k (kN/mm) [kip/in]
1.36 [3]	5.89 [13]	142.3 [811]
2.72 [6]	7.25 [16]	175.0 [998]
4.08 [9]	8.61 [19]	207.8 [1185]

The target stiffness for the spring assembly was established to be in the range of 140 to 210 kN/mm (800 to 1200 kip/in).

It can be shown, using the equations of motion for an undamped single-degree-of-freedom oscillator with prescribed initial velocity that the resulting pulse duration for the three combinations of mass and stiffness shown in table 2 are all on the order of 1 ms.

Spring Stiffness and Stress Evaluation

The load-deflection characteristics (i.e., stiffness) and state of stress of a Belleville spring is calculated using linear elastic theories that were established many years ago (e.g., Wahl, 1944). The theory and equations are not presented here. The interested reader may refer to the referenced text for more details. The load-deflection and stress equations were entered into a computer spreadsheet such that potential springs and combinations of springs could be easily evaluated for the device.

A number of options were considered in the design of the spring assembly. This included a single spring, identical dual springs in series, and two different dual springs in series (figure 19). Each option presented advantages and disadvantages to be considered. Several different springs were purchased and tested to determine the optimal configuration and actual stiffness

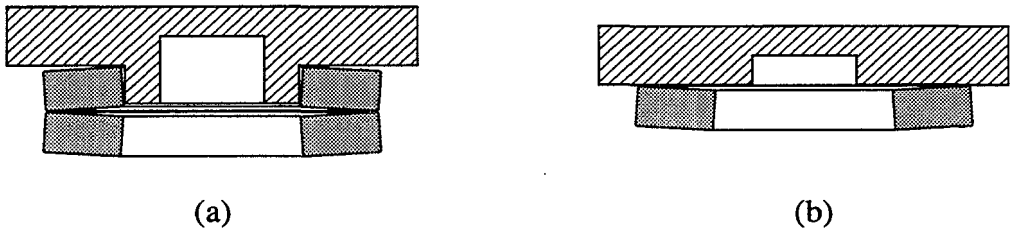

Figure 19. Single- and dual-spring design options.

of the assembly.

Stiffness of the assembly was measured in a universal test machine using a dial gauge with a resolution of 0.0025 mm (0.0001 in). Displacement of the top plate was measured for increments of load, ranging from 0 to 67 kN (15 kip). Readings were taken for increasing and decreasing load to determine the extent of hysteresis in the assembly. Stiffness was determined by the slope of the best fit line to the load-displacement data. All of the spring assemblies demonstrated some hysteresis. The slope of the best fit line yields an estimate of stiffness that is between the loading and unloading stiffness, i.e., is an average stiffness for the assembly.

The single spring configuration has the advantage of lower total height, greater selection of available stock springs to meet the stiffness requirement, and generally smaller inner diameter for a given stiffness. The latter was a consideration because it affects the design of the sleeve (part 5, figure 15) and dimensions of the force transducer. The single spring configuration was ruled out, however, after initial testing showed greater hysteresis in the load-deflection curve when compared to the dual configuration. An example of this is shown in figure 20. Measured results for a single spring are shown in the left of the figure, and for a dual configuration in the right of the figure (the same size spring was used in both configurations). The greater hysteresis is evident by the wider loop for the single spring and is attributed to friction between the spring and top plate. The long-term stability of the device was an additional concern for this configuration due to wearing between the spring and top plate.

Dual springs, arranged as shown in figure 19 (a), act in series. In this case, the effective stiffness of two identical springs in series is equal to half the stiffness of one spring. This is evident in the measured results shown in figure 20. The stiffness reduction is a disadvantage of the dual-spring configuration, since thicker springs are needed to achieve the same target stiffness. This is offset, however, by better linearity of the spring assembly (figure 20) and by what should be greater long-term stability.

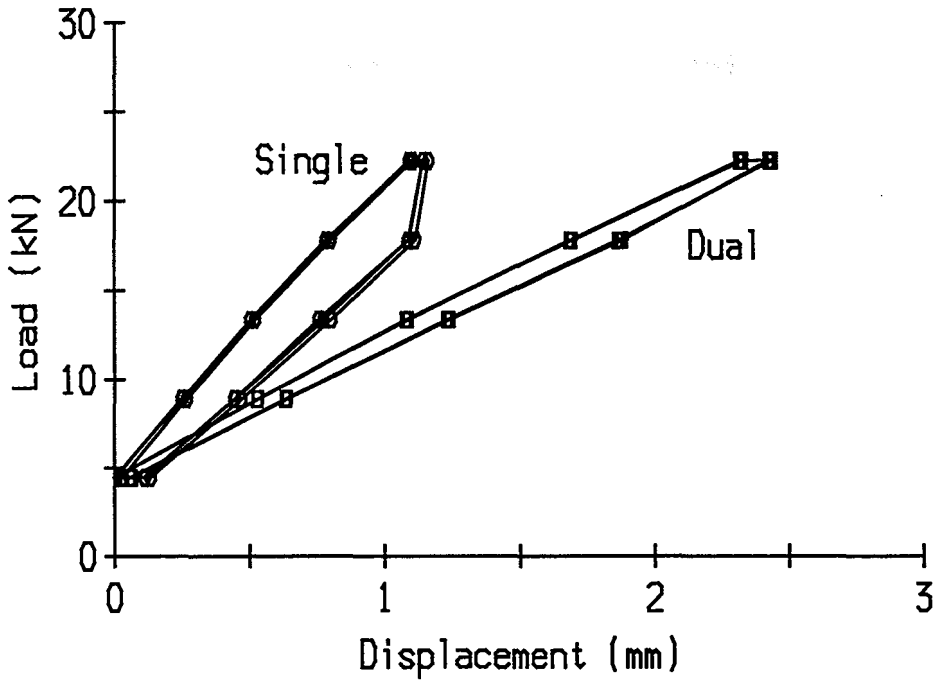

Figure 20. Load-deflection behavior of single- and dual-spring assemblies.

Belleville springs were located that satisfy the design requirements in a dual configuration. The dimensions of the spring are:

outer diameter:	82.6 mm (3.25 in)
inner diameter:	43.2 mm (1.7 in)
thickness:	10.7 mm (0.420 in)
dish:	0.76 mm (0.03 in).

The spring is made of high-carbon steel with a Young's modulus of 207 GPa (30,000 kip/in^2) and a yield strength of between 1378 and 1584 MPa (200 to 230 kip/in^2). The measured load-deflection behavior of the final spring assembly is shown in figure 21. The stiffness of the dual-spring assembly, as given by a best fit line to the data is 154 kN/mm (879 kip/in).

The spring selected for the prototype device happened to come from the manufacturer's overstock of a custom design spring. In the future, it may be necessary to special order springs of the correct dimension. Otherwise, the springs can be fabricated by milling the inner and/or outer diameters of larger stock springs to the correct dimension, provided the thickness of the stock spring is the same and the resulting measured stiffness is within the design-specified range.

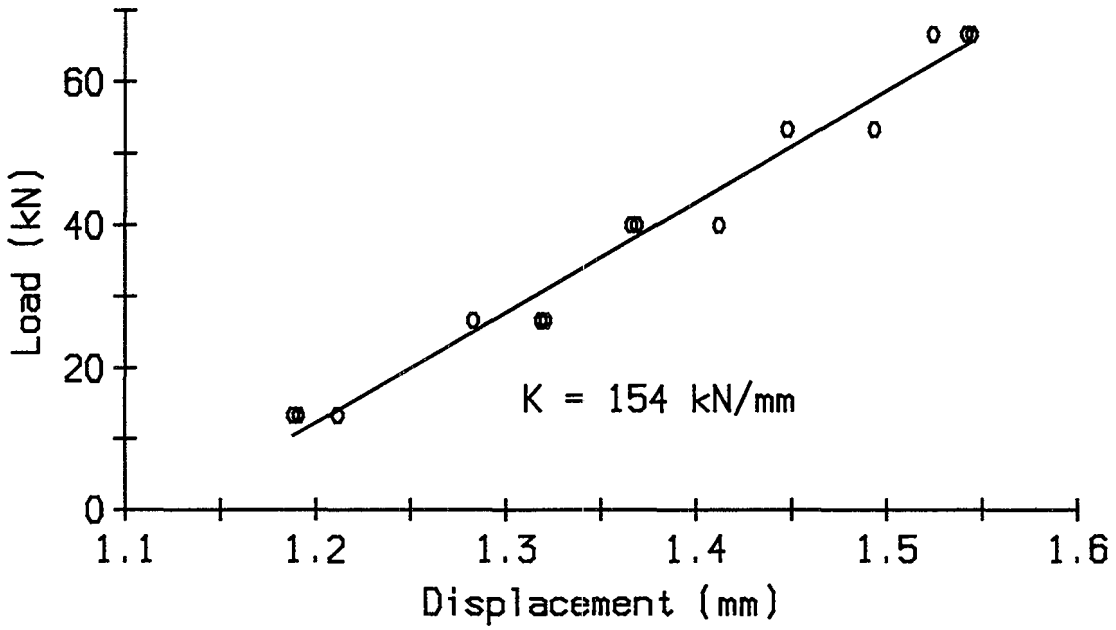

Figure 21. Stiffness measurement of prototype device dual-spring assembly.

Presented in figure 22 is a section of a Belleville spring with the points of critical stress indicated. The stress calculation for the prototype device spring yields a peak stress on the section under static or quasi-static load of 827 MPa (120 kip/in^2) for a load of 67 kN (15 kip). The maximum stress occurs at point S_I on the section and is 40 percent less than the yield stress of the material.

Based on the stress calculation and the manufacturer's data, the fatigue life of the spring assembly is estimated at 100,000 cycles. The estimate is most likely conservative, since the manufacturer's data is for continuous, repeated cycles, not intermittent cycling of relatively short duration. Assuming a typical calibration requires 3 sets x 70 blows/set = 210 blows or cycles (appendix E), the estimated fatigue life of the device is 476 calibration procedures. Therefore, the calibration device springs should be replaced approximately every 500 procedures.

Base Design

A finite element stress analysis of the base (part 3, figure 15) was conducted to determine the stress distribution and deformation of the base during operation. A schematic of the axisymmetric model analyzed is presented in figure 23. The model analyzed is of an earlier base design that is similar, but not identical, to the final prototype base design. An analysis of the final design was felt to be unnecessary based on the favorable results of the first analysis and because the final design is more conservative in critical stress areas.

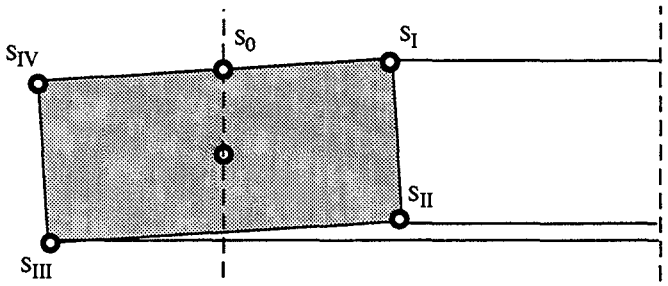

Figure 22. Section of Belleville spring indicating points of peak stress.

The analysis was conducted assuming linear elastic behavior, nominal properties for mild steel, rigid fixity to the foundation, and a load of twice the maximum expected peak load (133.2 kN = 2 x 66.7 kN). The load was applied as a distributed pressure from the inner radius of the assembly bolt hole to the outer radius of the force transducer (25.4 mm).

The maximum Von Mises stress on the section occurs at corner A with a magnitude of 290 MPa (42 kip/in^2). This is approximately 17 percent greater than the yield stress of low-carbon steel (248 MPa [36 kip/in^2]). The stress reduces to 248 MPa (36 kip/in^2) a distance of 2.5 mm from the corner. The second largest stress occurs at point B with a magnitude of 269 MPa (39 kip/in^2). The maximum overall deformation occurs at point B: 0.019 mm (7.41 x 10^{-4} in) radially toward the center and 0.054 mm (2.12 x 10^{-3} in) vertically down. The corresponding stresses and deformations are half that computed, assuming elastic behavior, for the expected peak load of 67 kN (15 kip). In that case, the stress at point A is less than 60 percent of the yield stress, which is quite satisfactory.

Force Transducer

Although there are perhaps other transducers that would be better suited for the device, e.g., because of lower profile and larger outer diameter, the transducer used in the prototype device is the same one that was used in the experimental program, as described in Experimental Program, Test Setup. The transducer has the desired load capacity (89 kN [20 kip]) and dynamic range.

A critical consideration in selection of the force transducer is the cable connection detail. There must be sufficient clearance between the connection and the bottom collar (part 10, figure 15) so that the cable is free to run out the port hole in the collar. This may be a problem with larger diameter transducers. The instrument used in the prototype device was specially modified for the experimental program to have an integral, low-profile connection, so clearance was not a problem.

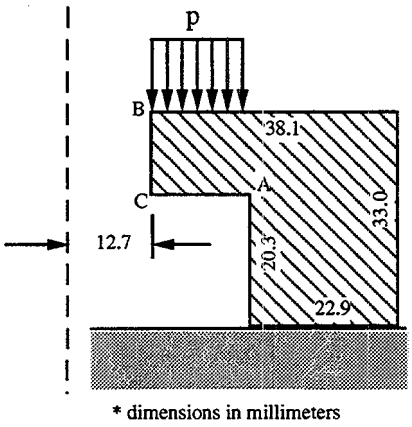

Figure 23. Diagram of model used in finite element analysis of the device base.

Effect of Assembly Pre-Load

The calibration device is assembled with a small pre-load, such that a tensile force exists in the assembly bolt, and the springs, sleeve, and force transducer are in compression. In assembling the device, the pre-load is established via a specified torque on the bolt (41 N-m [30 ft-lb]). The pre-load is necessary for several reasons: (1) to minimize the occurrence of superficial cracks in the Belleville springs, (2) to maintain a small pre-load on the force transducer, as suggested in the manufacturers instructions, and (3) to keep the device together. The pre-load, however, affects the sensitivity of the force transducer and the load-deflection behavior of the device.

The design of the device is such that for small loads, the effective stiffness of the device is equal to the stiffness of the spring assembly plus the stiffness of the bolt. This is illustrated in figure 24. Presented in the figure are load-deflection curves for the device assembled without pre-load (figure 24 (a)) and with pre-load (figure 24 (b)). To exaggerate the effect, the device in the pre-load case was assembled with a torque equal to more than three times the design-specified torque (i.e., with a pre-load more than three times the design specified). Under low loads, the stiffness of the device assembled with pre-load is dominated by the stiffness of the assembly bolt, which is much greater than that of the two springs in series. This is evident in the figure from the initial high stiffness in the pre-load case. For loads greater than the pre-load (estimated at about 40 kN in this case), the stiffness is equal to that of the spring assembly. This is clear as the slope of the curves in figure 24 (a) and (b) are nearly identical for loads greater than the pre-load. The stiffness that is specified for fabrication of the calibration device is that of the two Belleville springs in series only. This stiffness should be evaluated from the load-deflection data corresponding to loads greater than the pre-load.

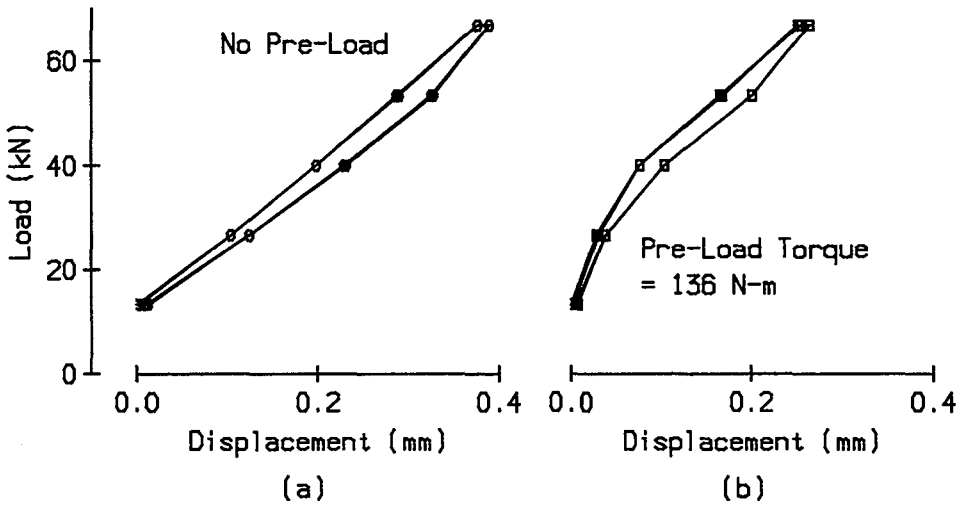

Figure 24. Stiffness of spring assembly with and without pre-load.

A similar effect is observed in the force transducer and produces a bilinear readout under increasing load. This is illustrated in figure 25. Presented in the figure are calibration curves for the transducer in the assembled device for three different torques, corresponding to three different pre-loads. The solid lines in the figure are best fit lines to the data over a particular range of loads. For low loads up to the pre-load, some of the force is shunted through the assembly bolt and reduces the sensitivity of the force transducer. For loads greater than the pre-load, the entire applied load is transmitted through the transducer and increases the sensitivity of the device. Note, the slope of the curves are nearly identical in all cases for loads greater than the pre-load. The magnitude of the pre-load can be estimated from the intersection of the best fit lines of the calibration curve.

The effect of the pre-load must be considered when calibrating the force transducer in the assembled device. Calibration requires measuring the device readout at several loads below the estimated pre-load, and several loads above the pre-load. The equations of the best fit lines over the two regions are determined by the method of least squares. The equation for low loads is described by slope (m_1), the equation of the line for high loads is described by a slope and y-intercept (m_2, b_2). The calibration data and equations are presented in figure 26 for the final prototype device, assembled according to the specifications.

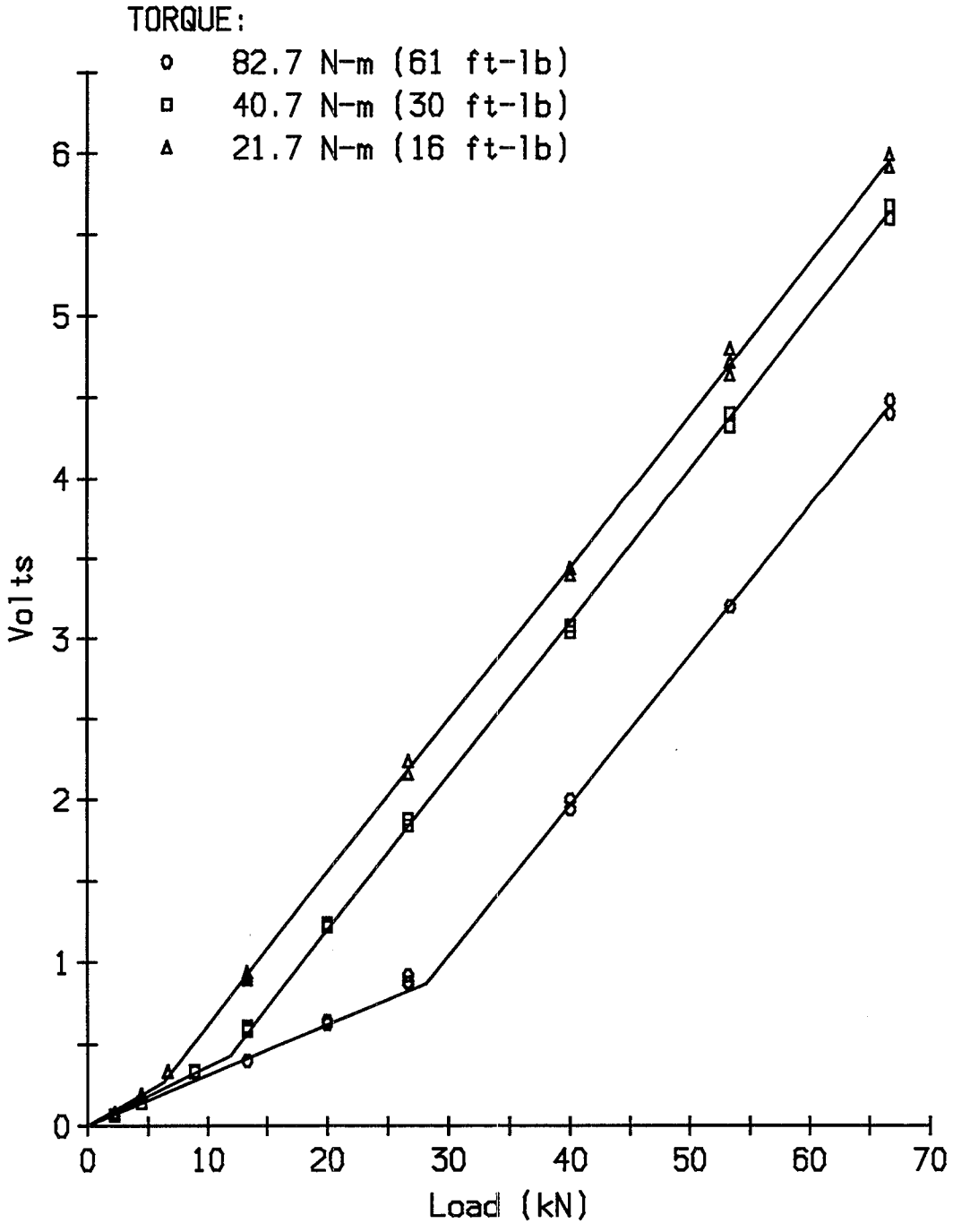

Figure 25. Force transducer calibration curve for varying assembly torques (pre-load).

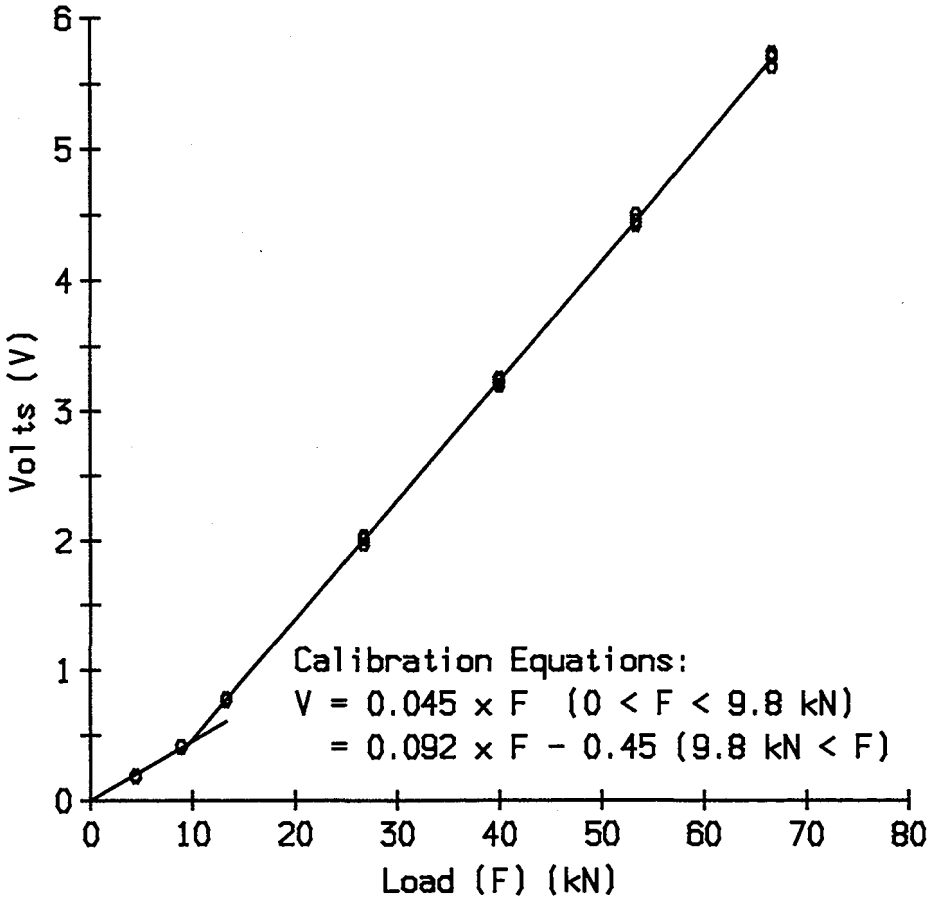

Figure 26. Force transducer calibration curve with design torque of 40.7 N-m (30 ft-lbs).

Data Acquisition and Data Analysis

Data Acquisition System

Selection of the data acquisition system was based on the requirements for triggering, recording, and storing multiple force time histories. The principal requirements are summarized as follows. The data acquisition system should have, at a minimum, an 8-bit A/D converter, otherwise load resolution will be poor. A 12-bit A/D converter is preferable. The system should have a sample rate of at least 100,000 samples/s. At this rate, a pulse duration of 1 ms will be resolved by approximately 100 data points. The system should have trigger and storage capabilities such that multiple force time histories can be automatically captured and stored for subsequent processing. The system should be capable of storing a minimum of

100 force time histories of 500 data points each. Triggering should be such that the start of the pulse is easily and clearly defined for any given time history. Programmable or switch selectable gains are a desirable option.

Data acquisition for the prototype calibration system is provided by a "lunch box" portable 386 computer with a high-speed analog-to-digital input card. The computer was purchased from a local supplier and is equipped with a standard hardware package: 80-megabyte hard disk, one 1.44-megabyte floppy disk drive, and 4 megabytes of memory. An A/D input card was selected that satisfies the requirements previously mentioned. In addition to the general requirements, the choice of the board selected for the prototype system was based on a number of other factors, including price, experience with the particular brand of A/D board, the availability of software drivers for the board, and technical support.

After purchasing the A/D input card, it was discovered that the triggering function of the board is software, and not hardware, controlled. For fast transients, this results in a significant time delay between triggering and actual recording. As a result, pulses of the duration expected could not be captured and consistently recorded. The prototype system, therefore, uses a commercial software package that permits "streaming" of data from the A/D input card directly to the host computer hard disk at the maximum sampling rate. Using this approach, data is recorded continuously during the calibration procedure (e.g., 70 blows) at the maximum sample rate, and stored in a single large buffer data file. A computer program was developed, using Microsoft C5.1, that scans the large data file to locate the force pulses based on input trigger levels. The pulses are extracted and saved for subsequent processing. Approximately 15 megabytes of data are collected in the buffer file for a set of 70 blows. It takes approximately 1 minute to scan and extract the force time histories from the buffer file. Presented in appendix B is a listing of the C program that was developed to scan and extract the force time histories from the buffer file.

To overcome the trigger limitations of the A/D input card, an optical trigger that would sense the passing of the drop weight was also given consideration. Although a viable and relatively inexpensive solution, the optical trigger would expand the hardware and power requirements of the calibration system.

Data Analysis

Subsequent analysis of the recorded force time histories is straightforward. A computer program was developed using Microsoft C5.1 to do the analysis. A listing of the program is presented in appendix B.

Each time history is analyzed to determine the peak force (F_m), impulse (I), and peak energy stored in the springs (E). The peak energy is approximately equal to

$$E = \frac{1}{2}\frac{F_m^2}{k} \tag{5}$$

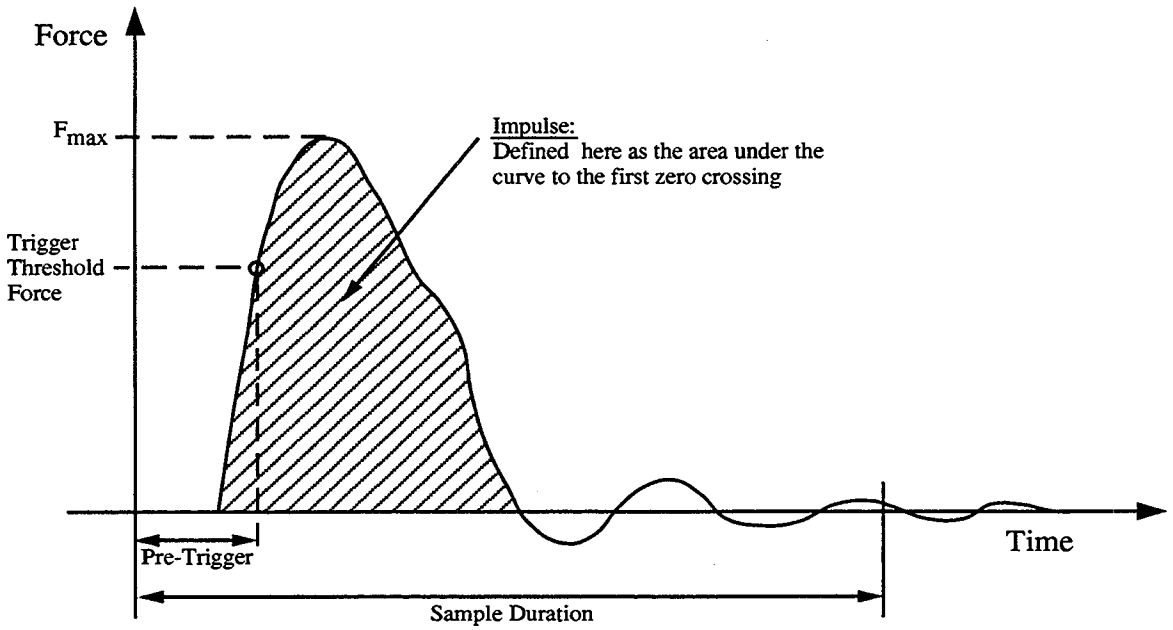

Figure 27. Typical force-time history.

where k is the stiffness of the spring assembly. The impulse is defined here as the area under the force time history curve, from the beginning of the pulse to the first zero crossing. A typical time history is illustrated in figure 27 with the quantities indicated.

The peak force, impulse, and energy are compiled for multiple blows and statistics for the data computed. This includes average, maximum, minimum, and standard deviation of peak force, peak energy, and impulse. In addition, a running total or cumulative impulse is tabulated as a function of blow count. Cumulative energy is also tabulated. Results of the analysis are saved to a file that can be displayed on screen or printed. Sample output from the program is presented in figure 28. Presented at the top of the figure are the statistics for the various quantities. A summary of the results for individual blows, and the cumulative energy and impulse, are listed below the overall statistics. The columns in the figure correspond to, from left to right, blow count, peak force, peak energy, cumulative energy, impulse and cumulative impulse. Note, results in the figure are shown in English units (i.e., kip, in, s).

Testing and Evaluation of the Calibration Device

A variety of tests were conducted under controlled conditions to assess and evaluate the performance of the calibration device. The tests were designed to examine such things as repeatability, sensitivity, and stability after repeated blows. The tests were conducted at different times throughout the development phase. Some tests resulted in design modifica-

Summary of Results: Number of blows: 70

	Peak Force	Peak Energy	Impulse
Average :	16.16	0.146857	5.144556
Standard Deviation :	0.36	0.006396	0.044169
Maximum :	16.73	0.157215	5.246208
Minimum :	15.20	0.129868	5.039124

Summary of Per Blow Results:

Blow	P_max	E_max	E_sum	I_max	I_sum
1	16.7285	0.1572	0.1572	5.1177	5.1177
2	15.8949	0.1419	0.2992	5.1084	10.2260
3	16.3474	0.1501	0.4493	5.2462	15.4722
4	15.8710	0.1415	0.5908	5.1263	20.5985
5	16.4546	0.1521	0.7429	5.1935	25.7920
6	16.2521	0.1484	0.8913	5.1589	30.9509
7	16.0616	0.1449	1.0362	5.1067	36.0576
8	16.2045	0.1475	1.1837	5.1117	41.1693
9	16.2879	0.1490	1.3328	5.1562	46.3255
10	15.9425	0.1428	1.4756	5.1174	51.4430
11	15.3470	0.1323	1.6079	5.0789	56.5218
12	16.3117	0.1495	1.7574	5.1791	61.7009
13	16.3593	0.1504	1.9077	5.2000	66.9010
14	15.7520	0.1394	2.0471	5.1167	72.0177
15	15.9663	0.1432	2.1903	5.1607	77.1784
16	15.8472	0.1411	2.3314	5.0942	82.2726
17	16.1211	0.1460	2.4774	5.1137	87.3863
18	16.1688	0.1469	2.6243	5.1150	92.5012
19	16.4903	0.1528	2.7771	5.1492	97.6504
20	16.4189	0.1514	2.9285	5.1646	102.8150
21	16.3951	0.1510	3.0795	5.1341	107.9490
22	15.2399	0.1305	3.2100	5.0391	112.9882
23	15.2637	0.1309	3.3409	5.1053	118.0934
24	16.3832	0.1508	3.4917	5.2100	123.3035
25	16.4665	0.1523	3.6440	5.2110	128.5145
26	16.5975	0.1548	3.7988	5.0846	133.5991
27	16.2402	0.1482	3.9470	5.1088	138.7079
28	16.0378	0.1445	4.0915	5.0911	143.7990
29	16.1211	0.1460	4.2375	5.1834	148.9823
.					
.					
.					
39	15.6805	0.1381	5.7195	5.0770	200.2773
40	15.2041	0.1299	5.8494	5.1469	205.4241
41	16.5380	0.1537	6.0030	5.2260	210.6501
42	16.2640	0.1486	6.1516	5.1299	215.7799
43	16.6928	0.1565	6.3082	5.1079	220.8878
44	15.6448	0.1375	6.4457	5.1546	226.0424
45	16.4427	0.1519	6.5976	5.2180	231.2604
46	16.4784	0.1525	6.7501	5.1419	236.4023
47	16.2283	0.1480	6.8981	5.1029	241.5053
48	15.9068	0.1421	7.0402	5.1191	246.6243
49	16.0259	0.1443	7.1845	5.1917	251.8160
50	16.2521	0.1484	7.3329	5.1341	256.9501
51	16.6451	0.1557	7.4885	5.2083	262.1584
52	16.5022	0.1530	7.6415	5.1195	267.2779
53	16.5142	0.1532	7.7947	5.2045	272.4824
54	16.2402	0.1482	7.9429	5.1454	277.6277
55	16.3832	0.1508	8.0937	5.1903	282.8180
56	15.9306	0.1426	8.2363	5.1499	287.9679
57	16.2045	0.1475	8.3838	5.1958	293.1637
58	16.0259	0.1443	8.5281	5.1462	298.3099
59	16.3355	0.1499	8.6780	5.2115	303.5214
60	16.0735	0.1451	8.8231	5.1283	308.6497
61	16.4189	0.1514	8.9746	5.1107	313.7604
62	16.1688	0.1469	9.1215	5.0914	318.8518
63	16.0021	0.1439	9.2653	5.1900	324.0418
64	15.6805	0.1381	9.4035	5.1617	329.2035
65	16.2879	0.1490	9.5525	5.1678	334.3713
66	16.0735	0.1451	9.6976	5.1132	339.4845
67	16.5499	0.1539	9.8515	5.1722	344.6567
68	15.3709	0.1327	9.9843	5.1583	349.8150
69	16.4427	0.1519	10.1361	5.2148	355.0298
70	16.0021	0.1439	10.2800	5.0891	360.1189

Figure 28. Sample output from data analysis.

tions and others simply served to verify or confirm the performance of the system. Results of the tests are described in the following.

The tests were conducted using two mechanical compaction hammers: (1) a Pine Instruments machine that was new at the start of the project and (2) the Rainhart compaction hammer that was used in the experimental program. The Rainhart machine is more than 20 years old and shows considerable wear. Certain tests were conducted using a Rainhart Test Equipment manual compaction hammer. Although the calibration system was not developed with manual hammers in mind (chapter 1), certain tests were best conducted, or could only be conducted, using a manual hammer.

In the following, a "set" is defined as a series of blows recorded in sequence and without pause, in a given machine setup.

Typical Output and Blow Repeatability

A set of 50 blows was recorded from the Pine machine, with the hammer operating under normal conditions. The time histories of the device output for blows 1, 2, 5, 10, and 50 are plotted together in figure 29. The time histories are offset slightly in the figure for easier comparison. Blows 1 and 50 are shown separately in figure 30. The force time histories are typical of the recorded output from the device. The duration of the main pulse is approximately 0.6 ms and the shape is approximately that of a triangle or half sine wave. The main pulse is followed by oscillations of a much higher frequency that dampen rapidly. The high-frequency components are likely due to the natural vibration of the device after the blow.

For a compaction hammer in good condition that is operating smoothly, the recorded output from the device should be fairly consistent and repeatable over multiple blows. Slight variations are likely to occur, however, as the machine heats up during operation and the hammer foot shifts slightly between blows. The time histories recorded in the Pine machine are consistent in peak force, characteristic shape of the time history, and duration. The average peak force for 50 blows in the Pine machine was approximately 69.1 kN (15.5 kip), with a standard deviation of approximately 2.9 kN (0.65 kip). This yields a coefficient of variation (defined as the standard deviation divided by the mean) of 4.2 percent. Similarly, the average peak energy for 50 blows was 15.8 kN-mm (0.14 in-kip), with a standard deviation of 1.3 kN-mm (0.012 in-kip) and coefficient of variation of 0.9 percent. The average impulse for 50 blows was 23.2×10^{-3} kN-s (5.22×10^{-3} kip-s), with a standard deviation of 0.44×10^{-3} kN-s (0.099×10^{-3} kip-s) and coefficient of variation of 1.9 percent. The measured quantities indicate good repeatability over multiple blows.

Set Repeatability

The set repeatability of the device was evaluated by recording 3 sets of 10 blows each with the device in the Pine machine. To confirm the repeatability of the device only, i.e., eliminate slight variations that might result because of the machine lift and release mechanism, and the hammer foot shifting between blows, the drop weight was released by hand in this test. Note,

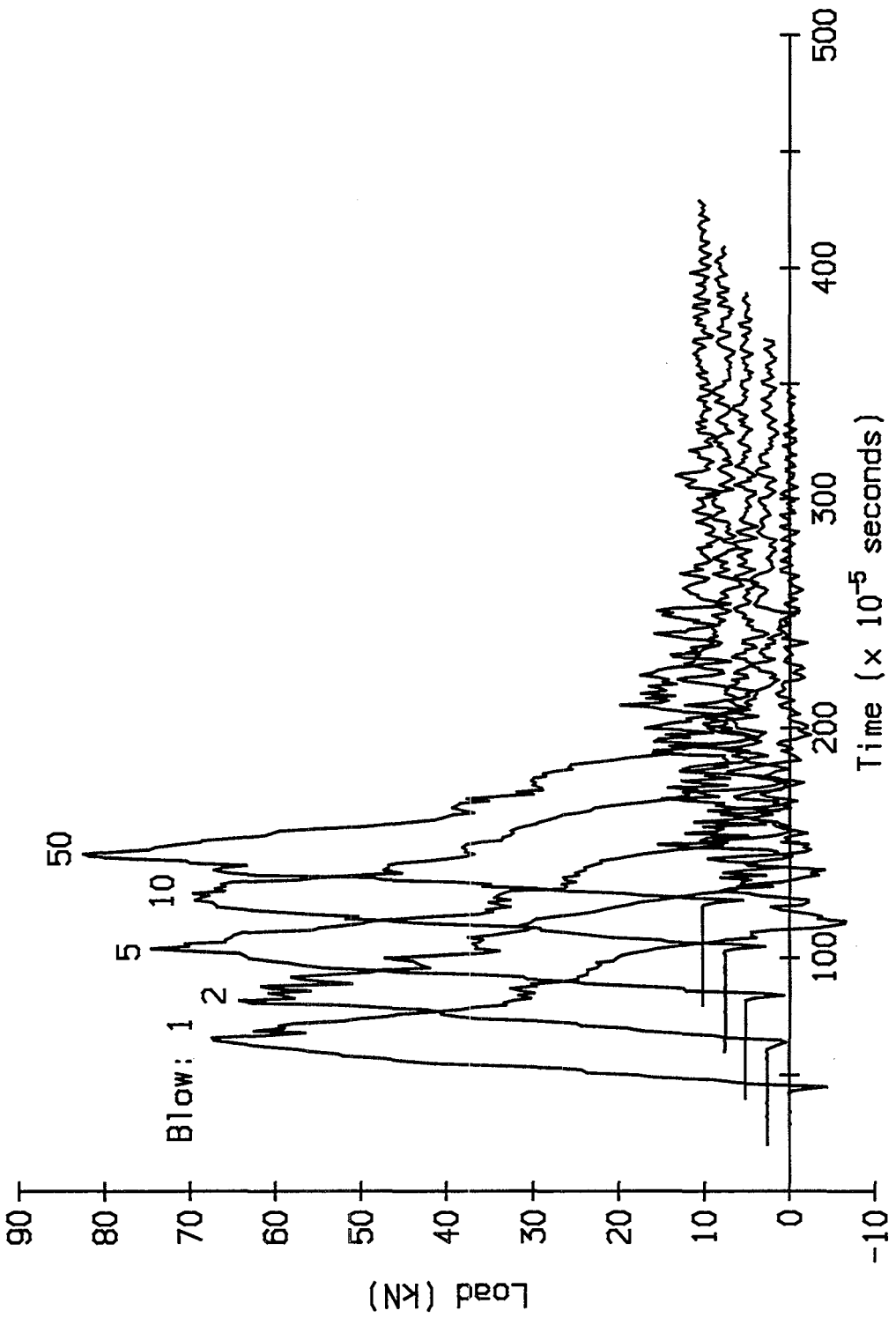

Figure 29. Typical recorded force-time histories.

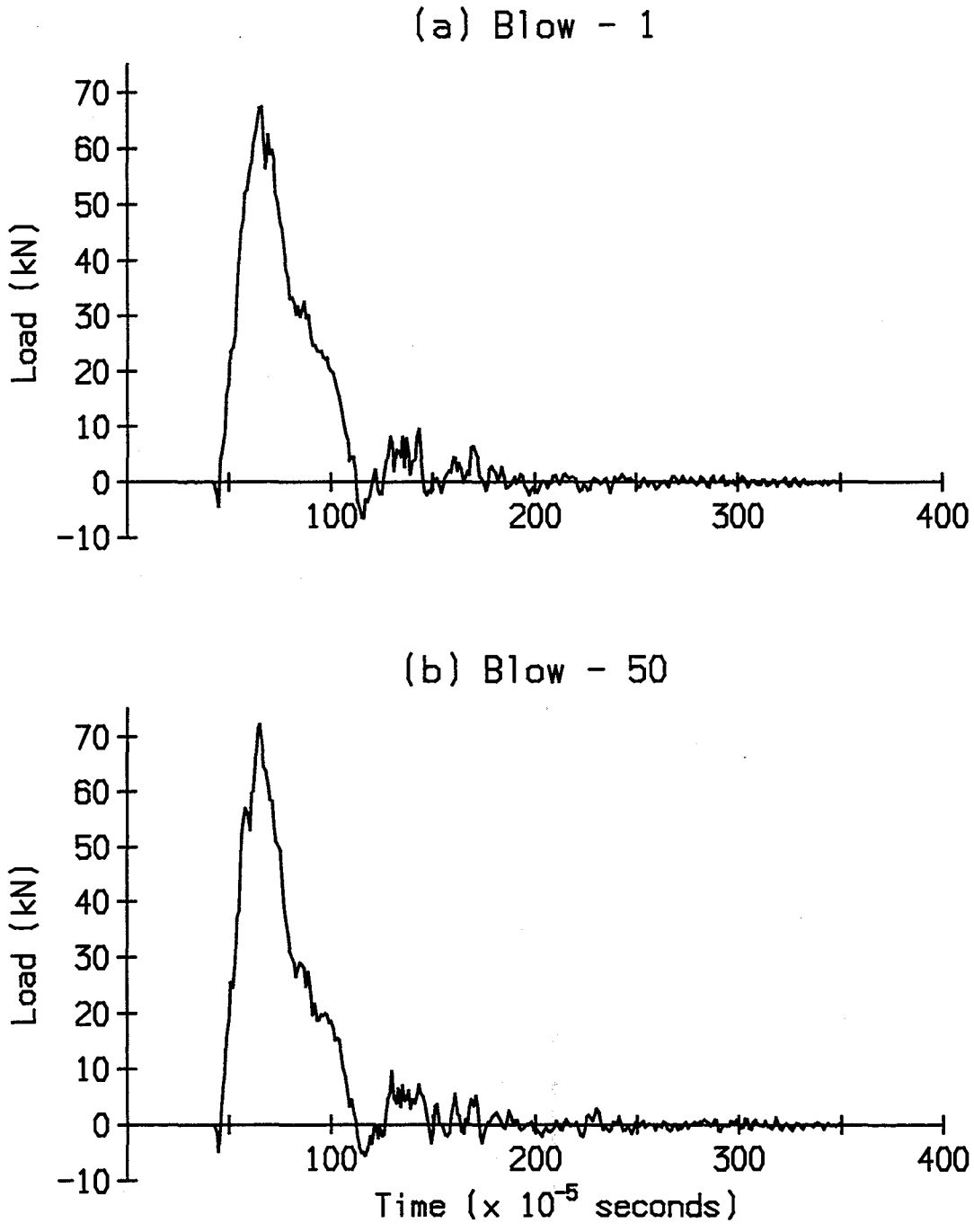

Figure 30. Typical recorded force-time histories - blows 1 and 50.

because of the design of the lift mechanism of the Pine machine, the drop weight could only be released consistently by hand from a height of 429 mm (16.875 in).

The average peak forces for the 3 sets of 10 blows were 69.5, 69.4, and 69.7 kN (15.6, 15.6, and 15.7 kip), respectively; the largest standard deviation in force for any one set was 1.2 kN (0.27 kip). The average peak energies for the 3 sets of 10 were 16.0, 16.0, and 16.1 kN-mm (0.142, 0.142, and 0.143 in-kip), respectively; the largest standard deviation in energy for any one set was 0.56 kN-mm (0.005 in-kip). The average impulse for the 3 sets of 10 blows were 23.4, 22.6, and 22.9 x 10^{-3} kN-s (5.26, 5.08, and 5.15 x 10^{-3} kip-s), respectively; the largest standard deviation in impulse for any one set was 1.47 x 10^{-3} kN-s (0.33 x 10^{-3} kN-s). The results of the test demonstrated very high repeatability within the set and also over the three sets.

Rotational Bias

Tests were conducted to determine if the results were dependent on the orientation of the device in the machine. Tests were conducted in the Pine machine with the device oriented in different positions, for both hand release and mechanical operation. The angular orientation of the device is referenced by the clock position of the bottom collar port hole, as measured when facing the machine (e.g., at 12 o'clock, the port hole faces the rear of the machine).

Two sets of ten blows each were recorded with the device oriented at 3, 6, 9, and 12 o'clock. Tests were conducted by releasing the drop weight by hand from a height of 429 mm (16.875 in). The average peak force and standard deviation for each set is presented in table 3.

Table 3. Average peak force for different orientations
(Pine machine, hand release from 429 mm (16.875 in).

Orientation	Average Peak Force kN (kip)	Standard Deviation kN (kip)
3 o'clock	70.59 (15.87)	1.11 (0.25)
3 o'clock	69.57 (15.64)	2.27 (0.51)
6 o'clock	70.10 (15.76)	2.76 (0.62)
6 o'clock	69.39 (15.60)	2.89 (0.65)
9 o'clock	72.24 (16.24)	2.71 (0.61)
9 o'clock	72.55 (16.31)	2.62 (0.59)
12 o'clock	66.28 (14.90)	0.71 (0.16)
12 o'clock	65.83 (14.80)	0.93 (0.21)
Average	69.57 (15.64)	
Standard Deviation	2.45 (0.55)	

The data shows that results are somewhat dependent on orientation. The average peak force of the two sets in the same position are very consistent, regardless of orientation. The average force varies slightly, however, as the orientation changes. The force ranges from a low of approximately 66 kN at 12 o'clock, to a high of approximately 72 kN at 9 o'clock. The coefficient of variation for the eight sets, however, is still low (3.5 percent).

Another series of tests was conducted in the Pine machine, using full-height automatic drops. One set of 50 blows each was recorded with the device oriented at 4, 8, and 12 o'clock. Results of the test are presented in table 4. Again, a slight dependence on orientation is noted, with the largest average force occurring with the device oriented near the 8 o'clock position. The coefficient of variation for the three sets is 2.6 percent.

Table 4. Average peak force for different orientations (Pine machine, automatic full-height drops).

Orientation	Average Peak Force kN (kip)	Standard Deviation kN (kip)
4 o'clock	63.96 (14.38)	1.33 (0.30)
8 o'clock	67.21 (15.11)	2.71 (0.61)
12 o'clock	66.72 (15.00)	3.56 (0.80)
Average	65.96 (14.83)	
Standard Deviation	1.75 (0.39)	

Tests were subsequently conducted to determine if the dependence existed also in the measurement of stiffness of the device. Stiffness was measured, as described previously, with the device oriented in the universal test machine at 4, 8, and 12 o'clock. The displacement of the top plate was measured in all three cases with a dial gauge located at the 4 o'clock position. For each orientation, the device was subject to three cycles of loading. The displacement of the top plate was measured at loads corresponding to 13.3, 26.7, 40.0, 53.4, and 66.7 kN (3, 6, 9, 12, and 15 kip), during both loading and unloading. The stiffness in each orientation was determined by the slope of the best fit line to the data. Results of the test are shown in figure 31.

The stiffness measurement is also slightly dependent on the orientation of the device. The stiffness ranges from a low of 154 kN/mm (880 kip/in) at 12 o'clock to a high of 160 kN/mm (914 kip/in) at 8 o'clock. The dependence, however, is not significant. The measured stiffnesses are all within ±2.4 percent of the average, which is 156.3 kN/mm (893 kip/in).

The rotational bias of the device is most likely due to a minor misalignment of the Belleville springs relative to each other. When assembled, the Belleville springs are carefully aligned such that they are concentric and bear upon each other evenly around the entire outer diameter of the spring. After several hundred blows of the hammer, however, it is noted that the springs shift just slightly relative to each other, and are no longer concentric. The relative

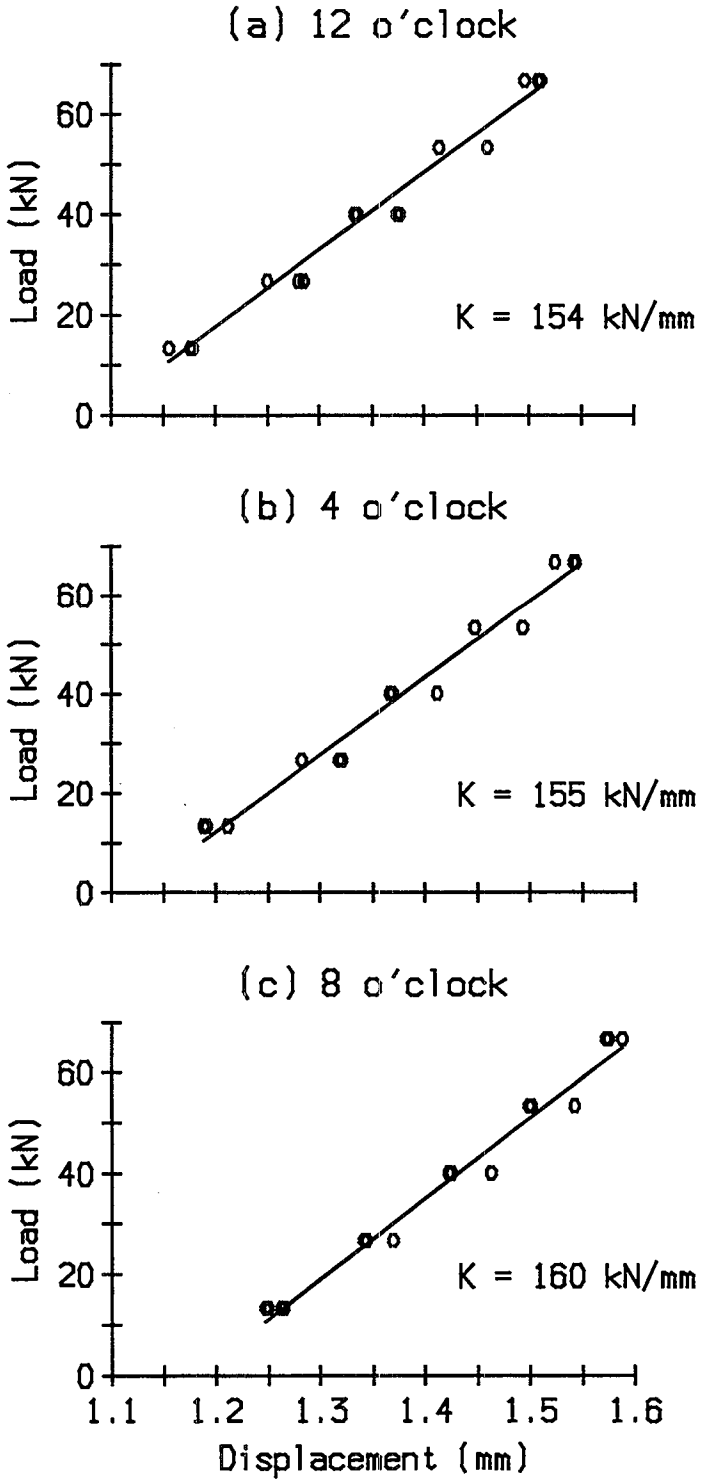

Figure 31. Stiffness of device measured in different orientations.

movement is a result of the clearance between various parts of the device, some of which is required for proper functioning of the springs. Shifting of the springs in the prototype device was probably perpetuated, to some extent, by the top plate. The threaded hole in the top plate was drilled slightly out of plum, such that when assembled, the axis of the assembly bolt is not exactly square with the bearing surface of the top plate. This has the tendency to shift the springs relative to each other during the first few blows until the springs seat themselves. This detail can be rectified with the fabrication of a new top plate. It remains to be seen, however, if this will have an effect on the rotational bias of the device.

The non-concentric springs have the effect of producing an asymmetrical stiffness when the displacement is measured at only one position on the top plate. The technique for measuring stiffness could be modified to overcome this problem by simply measuring the displacement of the top plate at three points around the parameter and using the average displacement in the calculation of stiffness. Short of that, however, the solution is to measure the stiffness in three different orientations and compute an average stiffness.

The effect of rotational bias has been incorporated in the proposed calibration procedure that is discussed in chapter 5 and is presented in appendix E. The stiffness is measured in three orientations and the average is computed. Calibration is based on the average of three sets, recorded with the device in the 4, 8, and 12 o'clock positions.

Day-to-Day Repeatability

Tests were conducted to evaluate the day-to-day repeatability of the device. The tests included 2 sets of 10 blows each with the device oriented at 3, 6, 9, and 12 o'clock. The tests were conducted in the Pine machine on consecutive days and the results were compared. Tests conducted on the first day yielded an average peak force of 66.54 kN (14.96 kip) and a coefficient of variation of 3.7 percent for the eight sets. Tests conducted on the second day yielded an average peak force of 65.70 kN (14.77 kip) and a coefficient of variation of 3.3 percent. The averages are well within the variation of the individual test results and demonstrate satisfactory repeatability.

Sensitivity to Drop Height

A set of tests were conducted to evaluate the sensitivity of the measured output to changes in drop height. Tests were conducted using the manual hammer with the device on the pedestal of the Rainhart mechanical hammer. The tests consisted of 3 sets of 50 blows each with the device oriented at 3 o'clock, and drop heights corresponding to 152, 305, 381, and 457 mm (6, 12, 15, and 18 in). The average peak force for the three sets and four drop heights are presented in table 5.

Results of the tests clearly indicate an increase in peak force with an increase in drop height, as would be expected. A 20-percent increase in drop height (energy) results in a 9.6-percent increase in average peak force, when going from a drop height of 381 mm (15 in) to a drop height of 457 mm (18 in). The results are generally consistent for the three sets at the same height.

Table 5. Variation in average peak force with drop height (manual hammer).

Drop Height mm (in)	Average Peak Force kN (kip) Set 1	Average Peak Force kN (kip) Set 2	Average Peak Force kN (kip) Set 3	Average kN (kip)
152 (6)	33.3 (7.49)	32.6 (7.33)	32.0 (7.20)	32.6 (7.34)
305 (12)	48.0 (10.8)	48.5 (10.9)	48.5 (10.9)	48.5 (10.9)
381 (15)	55.6 (12.5)	54.7 (12.3)	57.8 (13.0)	56.0 (12.6)
457 (18)	60.9 (13.7)	61.8 (13.9)	61.4 (13.8)	61.4 (13.8)

Stability of Stiffness After Repeated Blows

Calibration of the compaction hammer is to be based on the recorded force-time histories. The characteristics of the force pulse (recall) are a function of the stiffness of the spring assembly; therefore, stability of spring stiffness with prolonged use is essential.

The stability of spring stiffness was evaluated by measuring the stiffness before and after subjecting the device to 1000 continuous blows from the Pine machine. The stiffness of the device after the 1000 blows was within 4 percent of the stiffness measured before, based on measuring the stiffness in a single orientation. The difference is nearly within the range of experimental error for measuring stiffness. Furthermore, the stiffness measured after the 1000 blows was slightly higher than the stiffness before. Results of the test were felt to be satisfactory. Further observations, however, will be needed to completely characterize the stability under prolonged use.

Measured Response for Different Machines

In preparation for the laboratory evaluation program, and to get an estimate of the range of expected results, a number of tests were conducted in different machine setups. Tests were conducted in the Pine and Rainhart machines, and with the manual hammer. Different mock machine setups were developed using the two mechanical hammers to simulate varying conditions that would presumably result in variability in Marshall test data. The setups included adding additional mass to the drop weight of the hammer, placing a rubber pad between the device and pedestal, and recording data with the machine on different foundation supports. The calibration system performed satisfactorily during each of these tests. Only minor modifications were made to the system as a result of the tests, principally in modifications or enhancements to the data processing software. The most significant result to come out of these preliminary tests has to do with foundation compliance or stiffness. This is discussed in detail in the following section.

Effect of Foundation Compliance

Previous studies have maintained that the support or foundation on which the compaction machine is located has a significant effect on Marshall test results (Siddiqui, et al., 1987), and may be a major source of variability in the test data. This is based primarily on interviews with practitioners experienced in the Marshall procedure, and on limited experimental results. In planning the laboratory evaluation program, the intention was to attempt to incorporate the effect of foundation compliance by using one or two machine setups with varying non-standard foundations.

Different foundations were explored in order to find setups that would produce a measurable change in calibration data, and therefore presumably, variability in the Marshall test results. The Pine machine was used in all cases. The machine was setup on a number of different foundations, including a 2.5-mm (0.1-in) rubber pad between the pedestal and floor, resting unanchored on the concrete floor, resting unanchored on soil, and resting unanchored on a flexible wooden pallet. Results of testing with the calibration device, however, indicated *little or no change* in the calibration data, even in the extreme non-standard foundation configurations. For example, the 50-blow average peak force of the Pine machine with standard foundation (bolted to the concrete floor) was 66.3 kN (14.9 kip). The coefficient of variation in this case was 4.4 percent. The 50-blow average peak force for the Pine machine resting unanchored on a wooden pallet (the most flexible foundation) was 67.2 kN (15.1 kip), with a coefficient of variation of 3.6 percent. In summary, significant variations in foundation compliance could not be detected by the calibration device.

To further study the effect of foundation compliance, a refined analytical model of the device, compaction machine, and foundation was developed. The model is illustrated in figure 32. The system is represented by a 3 degree-of-freedom, undamped, spring-mass system. Referring to the figure, x_t, m_t, and k denote the displacement, mass, and stiffness of the calibration device (specimen); x_p, m_p and k_p denote the displacement, mass, and stiffness of the pedestal/machine; and x_s, m_s and k_s denote the displacement, mass, and stiffness of the supporting foundation. The governing equations of motion for the system are given by

$$\begin{bmatrix} m_t & 0 & 0 \\ 0 & m_p & 0 \\ 0 & 0 & m_s \end{bmatrix} \begin{Bmatrix} \ddot{x}_t \\ \ddot{x}_p \\ \ddot{x}_s \end{Bmatrix} + \begin{bmatrix} k & -k & 0 \\ -k & k+k_p & -k_p \\ 0 & -k_p & k_s+k_p \end{bmatrix} \begin{Bmatrix} x_t \\ x_p \\ x_s \end{Bmatrix} = \begin{Bmatrix} 0 \\ 0 \\ 0 \end{Bmatrix} \tag{6}$$

The response of the system was determined by numerical integration for a specified initial velocity of mass, m_t, i.e., for initial conditions

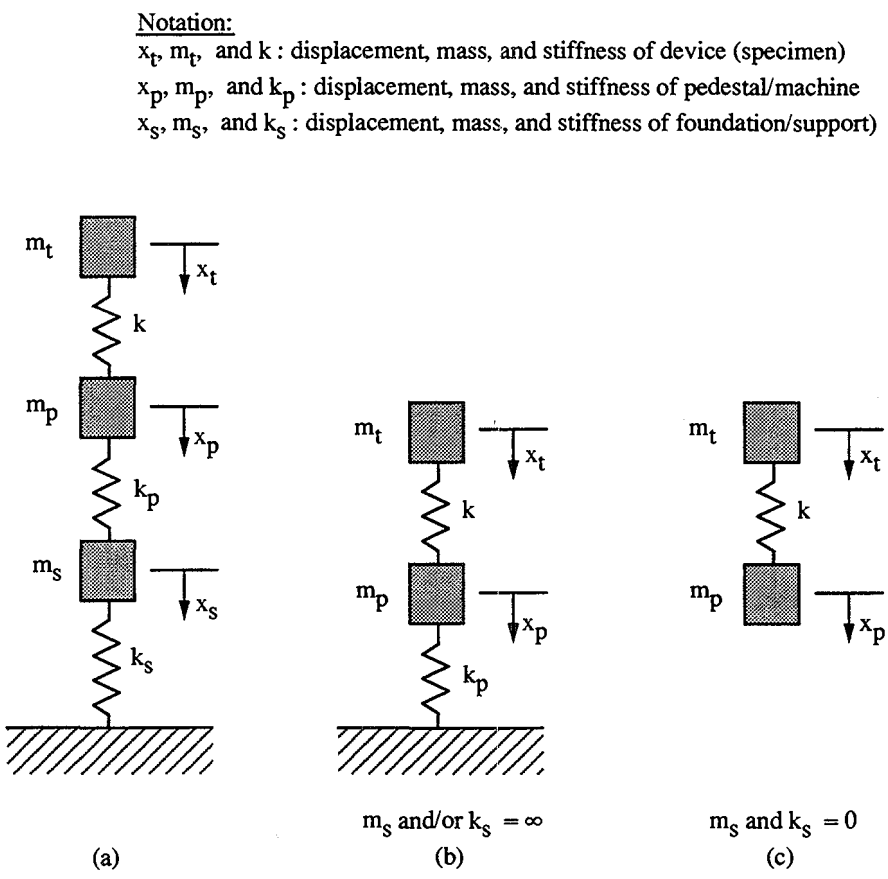

Figure 32. Refined analytical model for studying the effect of foundation compliance.

$$\left\{\begin{array}{l} x_t\ (0) = 0 \\ x_p\ (0) = 0 \\ x_s\ (0) = 0 \end{array}\right\}; \qquad \left\{\begin{array}{l} \dot{x}_t\ (0) = v' \\ \dot{x}_p\ (0) = 0 \\ \dot{x}_s\ (0) = 0 \end{array}\right\} \tag{7}$$

Comparing this model to the earlier one, the analysis begins from the time immediately following impact of the drop weight with the hammer foot. The mass of the drop weight and hammer foot are represented by the total mass (m_t) and the initial velocity (v') is given by equation 5.

To study the effect of varying foundation compliance, the peak force in the device, i.e., the force in spring k, was evaluated for varying device, pedestal/machine, and foundation properties. Pertinent results from the analysis for varying pedestal/machine and foundation properties are summarized in table 6. For the analysis, the combined mass of the pedestal and contributory mass of the machine (m_p) were determined by direct measurement, and could range from a low of 12.7 kg (28 lb) to 76.4 kg (168.5 lb), depending on the amount of machine mass that is assumed to participate. The low estimate corresponds to the actual weight of the wooden pedestal, the high estimate corresponds to the total weight of the Pine machine. The axial stiffness of the pedestal (k_p) was estimated at 1138 kN/mm (6500 kip/in), based on nominal material and section properties. The properties of the foundation (m_s, k_s) cannot be directly measured; however, there are lower and upper bounds. The upper bound corresponds to a rigid foundation, as shown in figure 32 (b), and corresponds to an infinite mass (m_s) and/or infinite stiffness (k_s). The lower bound is obtained by ignoring the foundation completely, as shown in figure 32 (c). This is modeled with the foundation mass and the foundation stiffness both being approximately equal to zero. For the results presented in table 6, mass (m_t) and initial velocity (v') was assigned nominal values of 5.89 kg (13 lb) and 2438 mm/s (96 in/s = 8 ft/s), respectively. The velocity was determined using equation 5, assuming a full-height drop and a total mass of 5.89 kg (13 lb).

The results of the refined analysis support the data obtained with the calibration system. For a wide range of foundation parameters there is *little or no change* in the estimated peak force -- the estimated force increases by less than 1 percent, in going from the assumption of no foundation (figure 32 (c)) to an infinitely rigid foundation (figure 32 (b)). On the other hand, reasonable variations in pedestal/machine mass and pedestal stiffness produce measurable variations in the peak force.

An understanding of these results is gained by examining the no-support configuration (figure 32 (c)). During a typical blow, the pedestal and machine are being accelerated by the impact of the drop weight. The mass of the pedestal and machine, however, is on the order of 2 to 15 times the mass of the drop weight, with the nominal ratio perhaps on the order of 5. The stiffness of the pedestal is also nominally on the order of 8 times the stiffness of the calibration device (specimen). The ratios are such that the pedestal tends to remain at rest and provides sufficient reaction for the impacting weight. Because of the mass and stiffness of the pedestal and machine, there is insufficient time for the foundation to participate in the

Table 6. Peak spring force for varying pedestal/machine and foundation properties.

Pedestal/Machine Mass - m_p kg (lb)	Pedestal Stiffness - k_p kN/mm (kip/in)	Foundation Mass - m_f kg (lb)	Foundation Stiffness - k_f kN/mm (kip/in)	Peak Force in Spring k kN (kip)
(a) For varying pedestal mass				
12.7 (28)	1138 (6500)			63.6 (14.3)
38.5 (85)	"	∞	∞	68.1 (15.3)
76.4 (168.5)	"			70.3 (15.8)
(b) For varying pedestal stiffness				
38.5 (85)	18 (100)			68.5 (15.4)
"	1138 (6500)	∞	∞	68.1 (15.3)
"	2800 (16,000)			71.6 (16.1)
(c) For varying foundation mass and stiffness				
38.5 (85)	1138 (6500)	1	1	67.6 (15.2)
"	"	1	500,000	68.1 (15.3)
"	"	500,000	1	68.1 (15.3)
"	"	500,000	500,000	68.1 (15.3)
"	"	∞	∞	68.1 (15.3)

dynamic event.

These results support the conclusion that foundation compliance has little effect on Marshall test results. This was further tested during the laboratory evaluation program using actual specimens. Results are discussed in chapter 6.

Summary

A test package has been developed for calibrating mechanical Marshall compaction hammers based on an elastic-spring mass device with force transducer, power supply, and data acquisition system. Initial testing has demonstrated that the system is robust, has good repeatability, and adequate sensitivity. The system is easy to use and is suitable for a laboratory or field environment.

The critical element of the calibration device is the spring assembly. The assembly consists of two Belleville springs in series that provide an effective stiffness of approximately 155

kN/mm (885 kip/in). The springs have been designed such that a peak force of approximately 67 kN (15 kip) is developed in a typical machine under a full-height drop of the hammer. The duration of the corresponding force pulse is approximately 1 ms. The fatigue life of the springs is estimated at 100,000 cycles, or approximately 500 calibration procedures. Load is measured using a piezoelectric quartz-type force transducer that has a range of 89 kN (20 kip).

Data acquisition for the prototype system is provided by a microcomputer-based system with high-speed data input card. The system is capable of sampling at a rate of 100,000 samples per second. Data is streamed to the computer hard disk during the entire calibration procedure and stored for subsequent processing. A computer program was developed to analyze individual force time histories. The peak force, peak energy, and impulse are determined for each time history. Statistics for multiple blows are computed.

The calibration system has been tested extensively to examine the repeatability, sensitivity, and overall performance of the system. The device performed satisfactorily in all tests. Output from the device, however, was found to be slightly dependent on the orientation of the device in the machine. The measurement of stiffness is also slightly dependent on the orientation of the device in the universal test machine. The rotational bias is attributed to a misalignment of the Belleville springs. Rotational bias should be examined in more detail and rectified in future designs of the device. This should further improve the repeatability and operation of the calibration system.

Results of tests conducted with the calibration device in the Pine machine on different supports indicate that foundation compliance has little effect on the loads imposed on the machine. A parametric study using a refined analytical model of the device, pedestal, and foundation supports this finding. The simple model predicts little or no change in peak force when the foundation is assumed to be infinitely rigid and when there is zero support.

CHAPTER 5. CALIBRATION PROCEDURE

Introduction

The system developed lends great flexibility to the calibration procedure because of the abundance of data collected for a set of blows from the hammer. The data includes the peak force, peak energy, and impulse for each force time history. Statistics are also computed for these measures for the set or ensemble of force time histories. This includes average, maximum, minimum, and standard deviation of peak force, peak energy, and impulse. Running totals are also computed for peak energy and impulse, as a function of blow count. These measures will be referred to as "cumulative energy" and "cumulative impulse," respectively, in the following. The data obtained from each force time history is very basic. More advanced signal processing techniques can be introduced in the future if the need arises.

There are two approaches to calibration that may be used given the available data. The first approach would require repairing, maintaining, or modifying the compaction hammer until the measured data is within a specified range. The second approach would rely on adjusting the number of blows such that an equivalent compactive effort is applied to all specimens, regardless of the machine. In the latter case, minimum requirements could also be placed on the measured results to guarantee that the blow count does not exceed some reasonable value. This would eliminate hammers from use that are clearly in need of repair. The second approach is more in line with the requirement of the current AASHTO standard for the Marshall procedure, and more in line with field practice (i.e., adjusting the number of blows to achieve a desired compaction).

The calibration procedure developed herein is based on the second approach, where compactive effort is assumed to be directly related to either cumulative impulse or cumulative energy. In developing the calibration procedure, the choice of which measureand to use - impulse or energy - remained an issue. The procedure was developed, therefore, to be applicable to either, and the scope of the laboratory evaluation program (chapter 6) was expanded to study the effect of calibrating to cumulative impulse or cumulative energy. The final recommendation of the measureand to be used in calibration would be based on the results of the evaluation program.

Outline of the Procedure

1. Determine the stiffness of the spring assembly by measurement in a universal test machine. The stiffness is required to compute cumulative energy. Stiffness only needs to be measured after the initial assembly of the device and then periodically thereafter, depending on use.

2. Calibrate the force transducer in a universal test machine and determine the calibration equations. The calibration equations are required to convert the voltage output of the device to an engineering unit (force). The transducer only needs to be calibrated after the initial assembly of the device and then periodically thereafter, depending on use.

3. Data collection:

   a. Place the calibration device in the compaction machine and secure with the specimen mold holder. Position the device in the machine such that the port hole for the transducer cable is in the 12 o'clock position, as viewed when facing the machine.

   b. Place the compaction hammer on top of the calibration device and secure it in the machine as usual during normal operation. Rest the drop weight on top of the hammer foot before starting the machine.

   c. Begin recording data and immediately start the compaction hammer.

   d. Apply 75 blows from the hammer. Be sure to record all 75-blow force-time histories.

   e. Repeat 3(a) to 3(d) with the port hole for the transducer cable in the 4 o'clock (second data set) and 8 o'clock (third data set) positions.

4. Data processing (as described in chapter 4):

   a. Analyze each recorded force time history and determine the peak force, peak energy, and impulse.

   b. For each of the three data sets, determine the average, maximum, minimum, and standard deviation of peak force, peak energy, and impulse. List the peak force, peak energy, cumulative energy, impulse, and cumulative impulse as a function of blow count (e.g., see figure 28).

   c. Compute the overall average of the results for the three data sets, i.e., overall average peak force, overall average peak energy, and overall average impulse. The compaction hammer can be calibrated provided the overall average peak force is greater than a specified minimum $[(F_{ave})_{min}]$.

   d. From the tabulated results for each data set, determine the number of blows (N_I^i), where i denotes the data set, corresponding to the standard cumulative 50-blow impulse (I_{50}). The blow count for the machine calibrated to cumulative impulse (N_I) is the average of the blow counts from the three data sets, i.e.,

$$N_I = \frac{1}{3}\sum_{1}^{3} N_I^i \tag{8}$$

   e. From the tabulated results for each data set, determine the number of blows (N_E^i), where i denotes the data set corresponding to the standard cumulative 50-

blow energy (E_{50}). The blow count for the machine calibrated to cumulative energy (N_E), is the average of the blow counts from the three data sets, i.e.,

$$N_E = \frac{1}{3}\sum_{1}^{3} N_E^i \tag{9}$$

As proposed, calibration is structured around two standard parameters: minimum overall average peak force $[(F_{ave})_{min}]$ and the standard cumulative 50-blow impulse (or energy). Values must eventually be assigned to these parameters. Values were selected for the laboratory evaluation program and are presented in the next chapter.

CHAPTER 6. LABORATORY EVALUATION

Introduction

The laboratory evaluation program was undertaken to:

- Demonstrate proof-of-concept of the calibration system, i.e., to demonstrate a reduction in variability of Marshall test results for specimens prepared in calibrated machines.
- Provide a recommendation on the best measureand to use in calibration, cumulative impulse, or cumulative energy.
- Uncover problems remaining with the device and calibration procedure.

The program involved comparing the properties of specimens prepared in uncalibrated Marshall machines to the properties of specimens prepared in the same machines, calibrated to cumulative energy (E_{50}) and calibrated to cumulative impulse (I_{50}). Multiple machine setups were used to simulate varying field conditions and to deliberately introduce scatter in the uncalibrated results.

Details of the Program

The laboratory evaluation program was designed to simulate inhouse field conditions that produce scatter in Marshall test results. Much of the scatter has been attributed to equipment-related variables, such as variation in drop weight, friction, wear, and foundation compliance. Five machine setups were developed for the program. For each machine setup, three sets of three specimens each were prepared: uncalibrated, calibrated to cumulative energy (E_{50}), and calibrated to cumulative impulse (I_{50}). Specimens were compacted and tested in accordance with AASHTO T-245, with the exception of blow count, which was varied for the calibrated series. A total of nine specimens were compacted in each machine setup. In all, 45 specimens were prepared and tested.

Two mechanical machines were available for use in the evaluation program, a Pine Instruments Marshall compaction hammer and a Rainhart Testing Equipment Marshall compaction hammer. As described previously in chapter 4, the Pine machine was new at the start of the project, the Rainhart machine was more than 20 years old and showed considerable wear. These machines provided two of the five setups for the program. Two other setups were developed, using the Pine and Rainhart machines, to deliberately produce variability in the test results: a 0.227-kg (0.5-lb) mass was added to the drop weight of the Pine machine, and a rubber pad was placed between the mold/device and the pedestal in the Rainhart machine. Although it was not in the scope of development of the calibration system (see chapter 1), a manual hammer was selected for the final machine setup. The five machine setups are summarized in table 7. For future reference, note the machine designation listed in the table.

As mentioned previously in chapter 4, the original intention was to include one or more machine setups in the laboratory evaluation program with varying foundation compliance.

Table 7. Machine setups for laboratory evaluation program.

Machine Setup	Designation	Description
Pine Standard	PS	Pine Instruments mechanical Marshall compaction machine, as previously described in chapter 4, anchored to the first-floor concrete slab on grade. The Pine machine was new at the start of the project.
Rainhart Standard	RS	Rainhart Co. Testing Equipment mechanical Marshall compaction machine, anchored to the first-floor concrete slab on grade. The machine is approximately 20 years old and shows heavy wear.
Manual Standard	M	Hogentogler & Co. manual Marshall compaction hammer, and the pedestal from the Rainhart Co. mechanical compactor with lift-column removed (i.e., free-standing pedestal typically used in manual operations). The manual hammer was new at the start of the evaluation program.
Pine with Added Weight	PW	The Pine Instruments mechanical compactor (PS) with a 0.227-kg (0.5-lb) lead collar secured to the drop weight, bringing the total drop weight to 4.76 kg (10.5 lb).
Rainhart with Rubber Pad	RP	Rainhart Co. mechanical compactor in the standard configuration (RS), with a 2.5-mm (0.1-in) rubber pad placed underneath the mold.

Results of testing with the calibration device, however, produced little or no change in the data for the Pine machine on foundations of widely varying stiffness. This was further supported by analysis using a refined analytical model. Consequently, the five machine setups in the laboratory evaluation program have the same foundation support: pedestal bolted to the concrete slab on grade, located on the first floor of the building. An element was included in the evaluation program, however, to study the effect of foundation compliance using actual specimens. This is discussed in more detail in the next section.

The mix design used for the laboratory evaluation program consisted of 115 g of 19-mm (3/4 -in) aggregate; 120 g of 13-mm (1/2-in) aggregate; 170 g of 10-mm (3/8-in) aggregate; 155 g of no. 4 aggregate; 165 g of no. 8 aggregate; 365 g of sand (passing no. 8 sieve); 25 g of mineral filler; and 65 g of asphalt cement. The mix is similar to the one used in the experimental program and yielded air voids of 4.8 percent when prepared in the Pine Instruments machine. The air void is listed here only for reference, it was not a target value for specimens prepared in the evaluation program.

The calibration parameters were assigned values as follows:

Standard cumulative impulse:	I_{50} = 1223 x 10^{-3} kN-s (275 x 10^{-3} kip-s)
Standard cumulative energy:	E_{50} = 565 kN-mm (5.0 kip-in)
Minimum average peak force:	$(F_{ave})_{min}$ = unassigned.

The parameters were selected based on the measured average peak force, 50-blow cumulative impulse, and 50-blow cumulative energy for a variety of different laboratory machine setups, including the five used in the program. Cumulative impulse and energy were selected to represent approximately the average of the measured results of all the machine setups tested. This would ensure that during the program, calibrated blow counts (N_I, N_E) would be obtained that are greater than and less than 50, and not all biased above or below 50. The criteria for minimum average peak force was not applied during the evaluation program, since that would eliminate a machine setup from the program and defeat the purpose of the program.

The laboratory evaluation was conducted as follows. Uncalibrated specimens were compacted in each of the five machine setups using a standard of 50 blows per side. All 15 uncalibrated specimens were prepared first, within a 2-day period. In turn, each machine was calibrated using the procedure described in chapter 5 and calibrated specimens were prepared. The six calibrated specimens for a given machine setup were prepared on the same day that the machine was calibrated. The three energy-calibrated specimens were prepared using N_E blows per side, based on a target cumulative energy of E_{50} = 565 kN-mm (5.0 kip-in). The three impulse-calibrated specimens were prepared using N_I blows per side, based on a target cumulative impulse of I_{50} = 1223 x 10^{-3} kN-s (275.0 x 10^{-3} kip-s). Calibrated specimens were prepared over a period of about 2 weeks. Height, bulk gravity, percentage of air void, stability, and flow were determined for all specimens. The same two operators prepared the specimens and calibrated the machines throughout the evaluation program. Two other operators assisted in subsequent testing for stability and flow.

Results

Results of Calibration

Detailed Calibration Reports are presented in appendix C for each of the machine setups; final results of calibration are summarized in table 8. Presented in the table are the number of blows required, per side, for compaction of specimens in the calibrated machine setups. For calibration to cumulative energy, the blow count ranges from a low of 38 in the Pine Standard setup, to a high of 106 in the Rainhart with Pad setup. For calibration to cumulative impulse, the spread is smaller, ranging from a low of 43 with the Manual setup, to a high of 60 with the Rainhart with Pad setup. Calibration based on energy and calibration based on impulse are fundamentally different; this is reflected to a certain extent in the results in table 8.

Overall, the calibration system functioned extremely well during the evaluation program. The calibration results are very consistent for the mechanical hammers, as indicated by the low standard deviation in peak force, peak energy, and impulse (see appendix C). Of the mechani-

Table 8. Calibrated machine blow count.

	PS	RS	M	PW	RP
Energy Calibration (N_E)	38	66	53	41	103
Impulse Calibration (N_I)	53	56	43	50	60

Notation: M - Manual Standard; PS - Pine Standard; RS - Rainhart Standard; PW - Pine with Weight; RP - Rainhart with Pad

cal hammers, the variability is the greatest in the Rainhart setups, which is indicative of the age and wear of the machine.

The calibration data for the manual hammer is not nearly as good as it is for the mechanical hammers. This can be attributed to factors that are greatly reduced or do not exist with the mechanical hammers; i.e., operator error, operator adjustments, and the integration algorithm used in processing the data. Operator error refers to the slight variations in drop height that tend to occur with each blow of a manual hammer. Operator adjustment refers to the slight misalignment of the hammer shaft during operation, i.e., that which produces a kneading action when compacting an asphalt specimen. The third factor refers to the algorithm for evaluating impulse. The algorithm is designed to integrate only the primary blow and exclude the subsequent "ring-down" phase of the force time history. Consequently, the upper limit of integration is the first zero crossing in the force time history following the peak force. In the limited studies conducted to date, the approach has worked well and consistently for the mechanical hammers. Because of greater variability in the shape of the force time history, however, impulses are not as consistent with the manual hammer using this algorithm. The current integration scheme, however, is very simple; a more "intelligent" algorithm should eliminate this problem. This issue will require further study if the device is to be used with manual hammers.

Uncalibrated and Calibrated Specimens

Results for the uncalibrated specimens are summarized in table 9. Results for the specimens calibrated to energy are summarized in table 10, and for the specimens calibrated to impulse in table 11. The results include the average and standard deviation for the three specimens and the five machine setups. Average is the top number in the table cell, standard deviation is the bottom. Data includes bulk specific gravity, stability, flow (in 0.25 mm), percentage of air voids, and height. The number of blows used in compacting the specimens is also listed in the table. Note that for all of these results air voids are based on a theoretical specific gravity of 2.524; consequently, bulk gravity and air voids are essentially one and the same. Both are presented here for completeness. For more detailed information, the raw data from all 45 specimens is summarized in appendix D.

Table 9. Laboratory evaluation: uncalibrated (average and standard deviation).

	M	PS	RS	PW	RP
BULK SPECIFIC GRAVITY	2.437	2.382	2.377	2.394	2.341
	0.005	0.008	0.020	0.005	0.015
STABILITY (N)	8473	5160	3928	5502	3025
	374	694	925	289	801
FLOW (0.25 mm)	8.00	7.75	6.17	6.00	6.42
	0.25	0.35	0.52	0.00	0.28
AIR VOIDS (%)	3.460	5.613	5.810	5.137	7.247
	0.200	0.307	0.775	0.197	0.583
HEIGHT (mm)	60.50	62.05	62.36	61.67	63.96
	0.25	0.15	0.91	0.51	0.69
Number of Blows	50	50	50	50	50

Notation: M - Manual Standard; PS - Pine Standard; RS - Rainhart Standard; PW - Pine with Weight; RP - Rainhart with Pad

Table 10. Laboratory evaluation: calibrated to energy (average and standard deviation).

	M	**PS**	**RS**	**PW**	**RP**
BULK SPECIFIC GRAVITY	2.427	2.374	2.398	2.381	2.404
	0.003	0.004	0.005	0.010	0.007
STABILITY (N)	8660	4928	5751	5338	6347
	903	258	472	178	547
FLOW (0.25 mm)	8.00	5.67	6.20	6.42	6.42
	0.43	0.29	0.57	0.29	0.38
AIR VOIDS (%)	3.840	5.927	5.003	5.680	4.767
	0.120	0.167	0.199	0.399	0.261
HEIGHT (mm)	60.45	62.08	61.62	62.15	61.26
	0.13	0.33	0.13	0.58	0.15
Number of Blows	53	38	66	41	103

Notation: M - Manual Standard; PS - Pine Standard; RS - Rainhart Standard; PW - Pine with Weight; RP - Rainhart with Pad

Table 11. Laboratory evaluation: calibrated to impulse (average and standard deviation).

	M	PS	RS	PW	RP
BULK SPECIFIC GRAVITY	2.426	2.397	2.406	2.405	2.389
	0.007	0.003	0.018	0.007	0.012
STABILITY (N)	7206	6080	5671	6036	4982
	463	560	694	623	814
FLOW (0.25 mm)	7.58	6.33	6.50	6.17	7.25
	0.58	0.29	0.43	0.38	0.35
AIR VOIDS (%)	3.897	5.030	4.673	4.713	5.333
	0.261	0.106	0.696	0.275	0.438
HEIGHT (mm)	60.81	61.72	61.72	61.72	61.77
	0.23	0.10	0.08	0.25	0.23
Number of Blows	43	53	56	50	60

Notation: M - Manual; PS - Pine Standard; RS - Rainhart Standard; PW - Pine with Weight; RP - Rainhart with Pad

There is considerable scatter in the results for the uncalibrated specimens (table 9) for nearly all measures. It is most noticeable in stability, air voids, and height. Stability averages range from a low of 3025 N to a high of 8473 N; air void averages range from a low of 3.460 to a high of 7.247; height averages range from a low of 60.50 mm to a high of 63.96 mm. The standard deviation, although only based on three data points, gives some indication of the variability of each machine. Variability is clearly the greatest in the Rainhart machine setups (RS and RP), and lowest in the Pine (PS and PW) and manual setups (M). The age and wear of the Rainhart machine is obvious from these results. The machine setups developed for the program clearly had the desired effect - to introduce variability into the test results. It is interesting to note that the variability in test results from the machine setups that are in compliance with the AASHTO standard (PS, RS, and M) is also considerable.

Several trends in the uncalibrated data are evident and are consistent with what would be expected for the different machine setups. For example, the added drop weight in the PW setup caused a reduction in both air voids and height relative to the Pine standard (PS) setup. The addition of the rubber pad underneath the mold in the RP setup caused an increase in air voids and height, relative to the Rainhart standard (RS) setup. Note also, the maximum or minimum average for all measures is obtained with the manual hammer. This is attributed, in part, to the natural kneading action that occurs when using the manual hammer.

Referring to table 10 and table 11, the effect of varied blow count on the results for the calibrated specimens is quite pronounced. Overall, *the scatter in the data for calibrated specimens is reduced significantly*, more so for the specimens calibrated to impulse than to energy. As an example, the average stability in specimens calibrated to energy ranges from a low of 4928 N to a high of 8660 N, for a range or spread of 3732 N. This is a 31 percent reduction, relative to the spread of 5448 N for the uncalibrated results. The average stability in the specimens calibrated to impulse, however, ranges from a low of 4982 N to a high of 7206 N, for a spread of 2224 N. This is a 60-percent reduction, relative to the spread in the uncalibrated results.

Calibration will in no way affect the variability or repeatability of any one machine. The standard deviations for the calibrated results are of the same order as the deviations for the uncalibrated results. Keep in mind that the standard deviations are based on only three samples.

To further quantify the effect of calibration, data were analyzed as described in the following. Statistics were computed for the sample sets that included all uncalibrated specimens, all specimens calibrated to energy, and all specimens calibrated to impulse, i.e., 3 sample sets of 15 data points each. This is more realistic for an interlaboratory evaluation and there is greater confidence in the statistics because of the larger sample size. Results are presented in table 12 and include average, standard deviation and spread (maximum minus minimum) of bulk gravity, stability, flow, air voids, and height. Average values are presented for reference, but are not intended to agree necessarily. Also presented for the energy- and impulse-calibrated data sets are the percent reduction in standard deviation and spread of each measure, relative to the uncalibrated results. The percent reduction is computed as 1 minus the ratio of calibrated result divided by uncalibrated result, times 100.

Table 12. Laboratory evaluation: summary of results.

	BULK GRAVITY		STABILITY (N)		FLOW (0.25 mm)		AIR VOIDS (%)		HEIGHT (mm)	
	Measure	%R[1]	Measure	%R	Measure	%R	Measure	%R	Measure	%R
(a) Uncalibrated										
Average	2.386	-	5222	-	6.8	-	5.453	-	62.10	-
Std Dev.	0.033	-	2055	-	0.9	-	1.325	-	1.24	-
Spread[2]	0.117	-	6716	-	2.5	-	4.630	-	4.24	-
(b) Energy Calibrated										
Average	2.397	-	6205	-	6.5	-	5.443	-	61.52	-
Std Dev.	0.020	39	1432	30	0.9	0	0.791	40	0.69	44
Spread	0.061	48	4915	27	2.8	-12	2.420	48	2.49	41
(c) Impulse Calibrated										
Average	2.405	-	6063	-	6.7	-	4.729	-	61.54	-
Std Dev.	0.016	52	881	57	0.7	22	0.610	54	0.41	67
Spread	0.058	50	3336	50	2.5	0	2.250	51	1.37	68

[1]%R is the percent reduction, i.e., 100 times (1.0 minus Calibrated/Uncalibrated)
[2]Spread is maximum minus minimum for the sample set.

Table 13. Comparison of Marshall test results for different foundation supports.

	BULK GRAVITY	STABILITY (N)	FLOW (0.25 mm)	AIR VOIDS (%)	HEIGHT (mm)
(a) Pine machine on wood pallet					
AVG	2.385	5056	7.11	5.520	62.13
STD	0.009	243	0.0	0.337	0.41
(b) Pine machine - standard foundation					
AVG	2.382	5160	7.87	5.613	62.05
STD	0.008	692	0.36	0.307	0.14

The results presented in table 12 are significant. The scatter in the data for specimens prepared in calibrated machines is reduced significantly. In four out of five measures, the standard deviation and spread for energy-calibrated specimens are reduced by at least 30 percent, relative to the uncalibrated results. For only one parameter - flow - did the results not improve or get worse. Note, however, the test to determine flow is subject to considerable variability and interpretation.

The results for specimens prepared in machines calibrated to impulse are the most notable: excluding flow, the standard deviation and spread of every measure were reduced by at least 50 percent, relative to the uncalibrated results. The greatest reductions occurred in the standard deviation and spread of height: 67 percent and 68 percent, relative to the uncalibrated results, respectively. The latter is encouraging since the measure of height is least influenced by the variability of subsequent test procedures. In this case, even the results for flow are substantial, where a 22 percent reduction in standard deviation, relative to the uncalibrated results, is computed.

Effect of Foundation Compliance

The effect of foundation compliance was tested as part of the evaluation program using actual Marshall specimens. Three specimens were prepared in the Pine Instruments machine, with the machine resting, unanchored, on a wood pallet. The pallet measured 1.2 by 0.92 by 0.25 m (4 by 3 by 0.8 ft) and was constructed of 38-mm (1.5-in) rough cut planks with two 64- by 190-mm (2.5- by 7.5-in) rails. Specimens were prepared using a standard 50 blows per side, to be compared with the results of the specimens prepared in the Pine machine standard foundation. The pallet foundation proved to be extremely flexible. During operation, the machine bounced considerably and "walked" a few centimeters across the pallet.

Test results from the three specimens are summarized in table 13. Also presented in the table for comparison are the results for specimens prepared in the Pine machine, standard setup.

Comparing the results in table 13, the differences are insignificant. The average bulk gravity, stability, air voids, and height of the specimens prepared in the machine on the wood pallet are all within 2 percent of the corresponding average for the specimens prepared on the standard foundation. The largest difference occurs in flow, but it is still less than 10 percent. Compared to the scatter in results for all the uncalibrated specimens (table 9), the results for the flexible foundation are very consistent with the results for the Pine standard setup. Although the extent of this study was limited, these results further support the finding that foundation compliance has little or no effect on Marshall test results.

Summary

The laboratory evaluation program, although limited in scope, clearly demonstrated proof-of-concept of the calibration system. Scatter in the Marshall test results for the calibrated specimens was reduced significantly, relative to the uncalibrated results, by as much as 60 percent. The program also clearly demonstrated that calibration to cumulative impulse is superior to calibration to energy as currently implemented. This is perhaps not surprising since calibration to impulse makes use of all available force time history data, whereas calibration to energy is based only on a single point, the recorded peak force.

Using actual specimens prepared in the same machine on very different foundations, results revealed that foundation compliance has little or no effect on the Marshall test results. This is contrary to the belief by many that foundation stiffness does have a significant effect on the test results.

The early results from the laboratory evaluation program are encouraging. Further study, however, should be undertaken to establish the effect of calibration using actual field machine setups.

CHAPTER 7. CONCLUSIONS AND RECOMMENDATIONS

Conclusions

The Marshall method of hot-mix asphalt design has been used for years by State and local highway agencies. Although the procedure is specified by several industry standards, Marshall test results are known to vary widely. This has been demonstrated repeatedly in round-robin mix exchange programs. Much of the variability is attributed to the compaction process and the Marshall compaction hammer. Equipment-related variables that may affect the test results include variation in the drop weight, drop height, friction, hammer alignment, pedestal support, and foundation. With the objective of reducing the variability of Marshall test results, a robust and easy-to-use testing apparatus has been developed for the calibration of mechanical Marshall compaction hammers.

The calibration test package consists of an elastic spring-mass system with force transducer, power supply, and portable data acquisition system. The calibration device has been designed such that the forces imposed on the machine due to the hammer drop are comparable to those imposed during the normal compaction process. Variations in a particular machine (e.g., drop weight or pedestal support) are manifested in the characteristics of the force pulse from the device. From a set of recorded hammer blows, the system computes the average peak force, average peak energy, average impulse, cumulative energy, and cumulative impulse for the machine.

Extensive tests under controlled conditions have demonstrated adequate system repeatability and sensitivity. The calibration device, however, is known to have a slight rotational bias, i.e., the results are dependent on the orientation of the device in the machine. This is easily compensated for in the calibration procedure by recording blows with the device in three different orientations and averaging the results.

Based on the kinetic data obtained with the system, a procedure for calibration has been developed. The approach requires adjusting the number of hammer blows to achieve a standard compactive effort. Two alternatives were considered and studied in the laboratory evaluation program: calibration based on cumulative impulse and calibration based on cumulative energy.

A limited laboratory evaluation program was undertaken for the purpose of demonstrating proof-of-concept of the system. Five mock machine setups were developed in the laboratory that would produce variability in the Marshall test results. In each of the 5 machine setups, 9 asphalt specimens were prepared: 3 uncalibrated (standard 50 blows), 3 with the machine calibrated to cumulative impulse, and 3 with the machine calibrated to cumulative energy. Marshall test results from the specimens prepared using the standard 50- blow procedure were compared to the results of specimens prepared in the calibrated machines. A number of conclusions are drawn from the evaluation program:

- The laboratory evaluation program clearly demonstrated proof-of-concept of the calibration system; scatter in the test results for the calibrated specimens was greatly

reduced, relative to the uncalibrated results. The standard deviation and range of test results for the calibrated specimens was reduced by as much as 60%, relative to the uncalibrated results.

- Calibration based on cumulative impulse is clearly superior to calibration based on cumulative energy (as presently implemented).

Based on the outcome of the laboratory evaluation program, a draft calibration standard has been developed and formatted according to AASHTO guidelines. The draft standard is presented in appendix E. The calibration procedure is based on cumulative impulse. As a preliminary requirement to calibration, the compaction hammer must satisfy a requirement of minimum average peak force. In the draft standard, calibration is related to the standard 50-blow test, or to a 75-blow test, which is also being used in the field today. If the calibration procedure is widely adopted, it is plausible that the standard for the Marshall procedure would, in the future, be revised to incorporate the concept of cumulative impulse. In that case, a specimen would be prepared with a specified compactive effort (cumulative impulse), rather than with a fixed number of hammer blows. The draft standard in appendix E includes the drawings and specifications needed to fabricate and assemble a calibration system.

Results of this study indicate that the effect of foundation compliance - or stiffness - on Marshall test results is negligible. This is contrary to the stated position of other researchers (e.g., Siddiqui et al., 1987). This conclusion, however, is based on and supported by:

- Data recorded with the calibration device in machines on widely varying foundations.
- Detailed dynamic analysis of the device/machine/foundation system using a three-degree-of-freedom model.
- Comparison of Marshall test results for specimens prepared in a machine on a very stiff foundation, and on a very flexible foundation.

The estimated cost to fabricate and assemble the calibration system is between $3500 and $4000. Of that, approximately $2500 is for the data acquisition system. The actual total cost will vary depending on material and labor costs to fabricate the custom parts of the calibration device and the force transducer selected. For a user that already has a suitable data acquisition system, the total cost of the calibration system can be greatly reduced.

Recommendations

There are issues that remain to be addressed for the calibration system, some of which will impact the extent to which the system is adopted by the construction and asphalt industries. Certain enhancements can also be made to the calibration system that would be beneficial. Recommendations are as follows:

- The effectiveness of the calibration system and procedure must be established using actual field production equipment. As a first priority, a field evaluation program should be undertaken in a manner similar to the laboratory evaluation program.

- The standard calibration parameters, i.e., standard cumulative impulse and minimum average peak force, must be established before the system can be used. These should be selected based on engineering judgment and recorded data. Data collected in a field evaluation program from several sites could be used to establish the standard parameters.

- The long-term repeatability and stability of the calibration device must be established. Although this was examined in some detail here, further observations are needed to characterize the stability of the spring stiffness and calibration of the force transducer with prolonged use. This could be undertaken as one task in a field evaluation program.

- Recommended minor enhancements to the existing calibration system are listed below. The modifications are listed in order of importance (i.e., most important first):

  » Eliminate or minimize the rotational bias in the calibration device. This may be achieved by simply specifying tighter tolerances in the fabrication of various parts.

  » Design a new top collar to reduce the clearance between the hammer foot and collar. A new top collar would minimize the amount of shifting that is permitted by the hammer between blows and would likely improve the device repeatability. The existing clearance is slightly larger than the clearance that exists during the normal compaction process: during normal compaction the hammer foot is generally positioned inside the bottom collar of the cylinder mold, whereas because of the height of the device, during calibration the hammer foot is positioned inside the top collar of the cylinder mold, the latter has a diameter slightly larger than that of the bottom collar, permitting a greater range of movement of the hammer foot during calibration. This modification would be done most easily by modifying a standard cylinder mold bottom collar to serve as the top collar for the calibration device.

  » Develop a more intelligent and robust scheme for integrating the force time history to calculate impulse. The calibration of manual hammers would likely be possible with this enhancement.

- Major modifications to the system could be explored to further enhance the existing system and expand the scope of machines to be calibrated. These include:

  » Modification of the device to permit calibration of machines that have a tapered foot.

  » Modification of the device to permit calibration of machines that have a rotating base.

» Modification of the design to incorporate a shock accelerometer in the top plate. This would provide additional data and permit the computation of the time history of energy stored in the device. With this design modification, calibration based on energy may prove to be better than calibration based on impulse (recall that the method for calibration based on energy used in the study was based only on peak energy, i.e., a single data point from the recorded force time history).

» Modification of the design to include a more robust mechanism for securing the assembly bolt to the top plate. The existing design relies solely on thread adhesive, between the assembly bolt and top plate, to ensure that the device does not vibrate loose or lose pre-load after repeated blows. Although this is inexpensive and has worked adequately thus far, more robust mechanisms for securing the assembly bolt to the top plate need to be explored to guarantee the long-term repeatability and stability of the device.

APPENDIX A. PARTS LIST AND DEVICE DRAWINGS

Presented in this appendix are the parts list, engineering drawings, and assembly instructions for the calibration device.

The parts list for the calibration device is presented in table 14; the list for the data acquisition system (optional) is presented in table 15. Parts are referenced by part number and part name. Specifications for each part are listed in the table along with the supplier of the part for the prototype device. Note, this should not be construed as an endorsement of a particular manufacturer or supplier. The suppliers are listed only so that the interested reader can obtain more detailed specifications if they so desire, which should aid in the selection of the part.

Engineering drawings are presented in figures 33 through 37 for all parts that require custom fabrication or are modified from an "off-the-shelf" item. Engineering drawings are not included for stock parts that are used as purchased (e.g., washer, Belleville spring, etc.). An assembly drawing is presented in figure 38 and a drawing of the complete device is presented in figure 39.

> *Note* - Particular attention should be paid to the details of the cable connection of the force transducer since there is limited clearance between the transducer and bottom collar, and transducer and Belleville springs. The bottom collar should slide freely on and off without having to disassemble the device.

Assembly Instructions:

1. Apply a small amount of general purpose or high-strength thread adhesive/bonding agent (e.g, LockTite™ or equivalent) to the inside threads of the top plate.

2. Secure the top plate upside-down in a bench vise. Use small blocks of wood if necessary to prevent damage to the plate.

3. Apply a lubricant to the contact surfaces of the force transducer, sleeve, and base as recommended by the transducer manufacturer (a molybdenum-based lubricant was used in the prototype device). Apply a small amount of the same lubricant to the outer diameter edges of the Belleville springs where the two springs come in contact.

4. Place the elastic band around the hub of the sleeve and hub of the top plate (the elastic band reduces the clearance between the spring and sleeve (top plate) hub, while permiting radial displacement of the spring relative to the hub).

5. Position the Belleville springs, sleeve, force transducer, base, and washer on top of the top plate in the order shown in figure 38.

6. Apply a small amount of adhesive/bonding agent to the threads of the assembly bolt.

6. Slide the assembly bolt down through the device parts and tighten the assembly by hand until snug.

7. Center and align all the parts relative to one another. Rotate the force transducer relative to the base so that the transducer cable is positioned properly to allow for installation and removal of the bottom collar.

8. Tighten the assembly using a torque wrench to 41 N-m (30 ft-lb).

9. Remove the device from the vise. Place the device upside down on a table and allow the thread adhesive to fully cure, as recommended by the adhesive manufacturer.

> *Warning* - Do not use an excessive amount of thread adhesive on the top plate and assembly bolt. Also, do not turn the device right-side up until the adhesive is fully cured. Excess adhesive may backup or drain down the shaft of the assembly bolt and obstruct the smooth operation of the device.

Table 14. Parts list - calibration device.

Part #	Name	Specification	Prototype Device Supplier
1	Assembly Bolt	25-mm (1") #14 fine thread, 152-mm (6") hex-head medium-strength cap screw, modified as shown in fabrication drawing	McMaster-Carr, Brunswick, NJ; Part # 91248A927
2	Washer	25 mm (1") SAE flat washer	McMaster-Carr, Brunswick, NJ; Part # 91083A038
3	Base	Mild steel, see fabrication drawing	Local
4	Force Ring	Piezoelectric force transducer, compression type, maximum force of 20-30 kip, nominal inner diameter - 25 mm (1"), nominal outer diameter - 51 mm (2"), nominal height less than 15 mm (0.6"), size and configuration of connection that fits the space constraint of device	PCB Piezotronics, Inc., Depew, New York; Model 216A Force Ring with M05 built-in option (1.5 m (5') low noise integral cable)
5	Sleeve	Mild steel, see fabrication drawing	Local
6	Elastic band	1-mm thick elastic band; diameter to permit snug fit around hub of sleeve and top plate	Local; standard office supply
7	Bottom Belleville Spring	High-carbon steel Belleville spring/washer	Key Belleville, Inc., Leechburg, PA; Part M3250-P-420
8	Top Belleville Spring	High-carbon steel Belleville spring/washer	Key Belleville, Inc., Leechburg, PA; Part M3250-P-420
9	Top Plate	Mild steel, see fabrication drawing	Local
10	Bottom Collar	Bottom collar, modified from a standard 102 mm (4") diameter Marshall cylinder mold as shown in the fabrication drawing	Rainhart Co., Austin, TX; Model 110CM4 Compaction Mold Assembly
11	Top Collar	Top collar, from a standard 102 mm (4") diameter Marshall cylinder mold	Rainhart Co., Austin, TX; Model 110CM4 Compaction Mold Assembly

Table 14. Parts list - calibration device (continued).

Part #	Name	Specification	Prototype Device Supplier
12	In-Line Charge Converter	In-line charge converter (amplifier) converts high-impedance charge output of a piezo-electric sensor into low-impedance voltage signal	PCB Piezotronics, Inc., Depew, New York; Model 402A In-Line Charge Converter with M144 built-in option
13	AC Power Supply	AC power supply for low-impedance piezoelectric transducers with built-in or attached amplifiers	PCB Piezotronics, Inc., Depew, New York; Model 482A06, Single-Channel Line Power Supply with BNC input/output

Table 15. Parts list - data acquisition system.

Part	Name	Specification	Prototype Device Supplier
1	Portable Computer	Portable "lunch box" 386 DX/33 or comparable, 80-MB hard disk minimum, one 1.44-MB floppy disk drive and 4-MB memory. *Note* - computer must be hardware-compatible with the selected data acquisition board.	Local
2	Data Acquisition Board	12-bit A/D converter, minimum throughput of 100,000 samples/s for a single channel, software or switch selectable gains, software drivers needed to operate the board.	Keithley/Metrabyte Taunton, MA; Model DAS-1402 high-speed analog and digital interface board
3	Stream-to-Disk Software	Software that enables direct storage (streaming) of data from the A/D board to a hard disk, at the desired sample rate for a prolonged period of time and without interruption.	Keithley/Metrabyte Taunton, MA; STREAMER version 3.3, compatible with DAS-1402

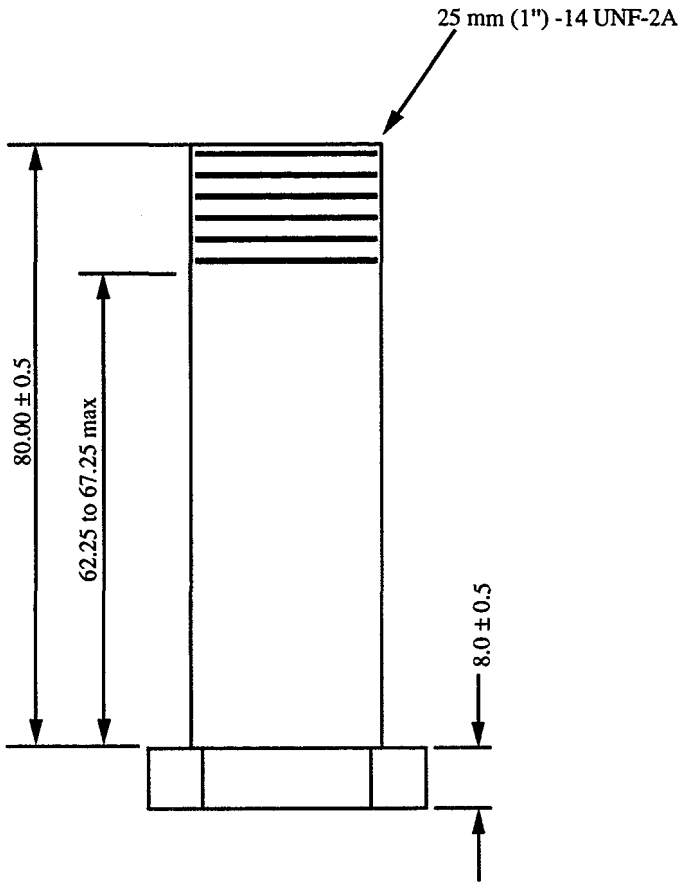

Note:
Part fabricated from a 25 mm (1") -14 fine thread, 152 mm (6") long (threaded length 64 m (2.5")) hex-head medium-strength cap screw . Thread shaft to indicated length, turn bolt head, and cut bolt to length.

PART NAME: Assembly Bolt
PART NUMBER: 1
MATERIAL: Steel
UNITS: Millimeters unless otherwise specified

Figure 33. Assembly bolt.

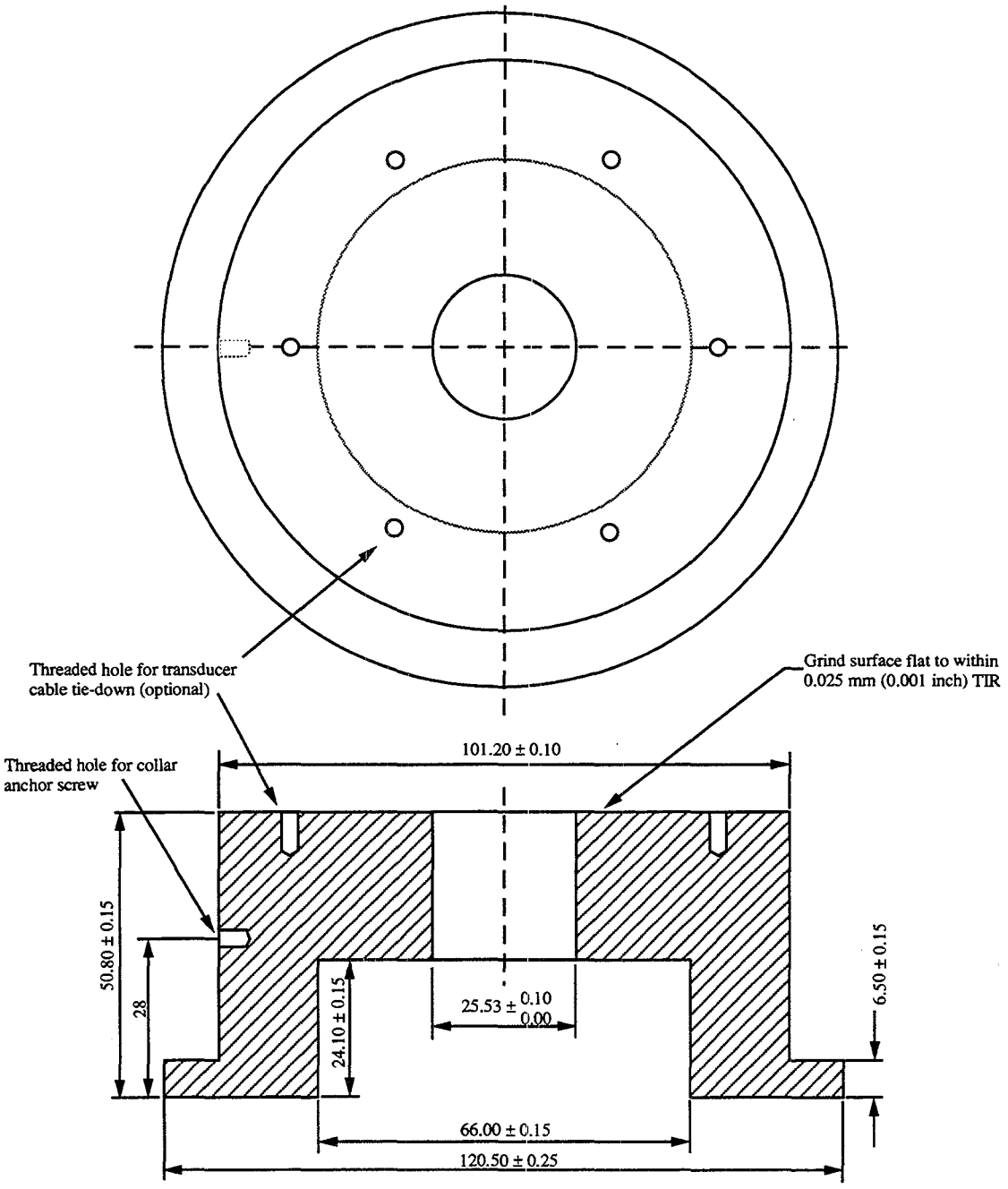

Figure 34. Base.

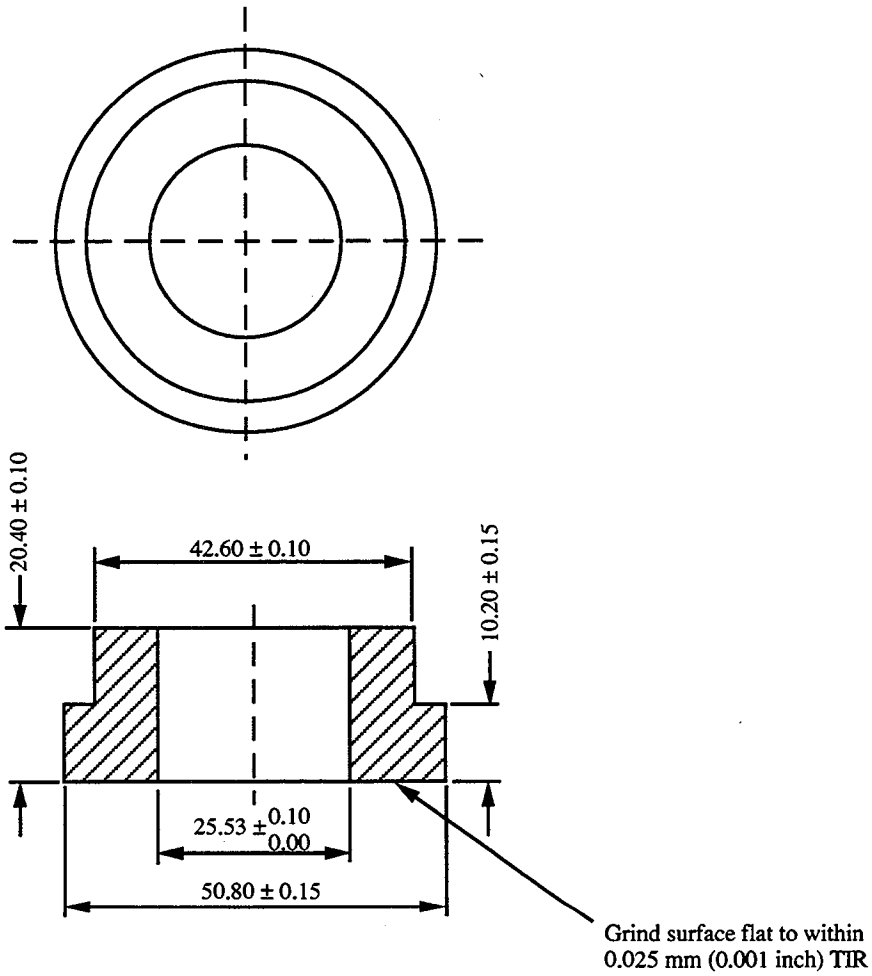

PART NAME: Sleeve
PART NUMBER: 5
MATERIAL: Mild Steel
UNITS: Millimeters unless otherwise specified

Figure 35. Sleeve.

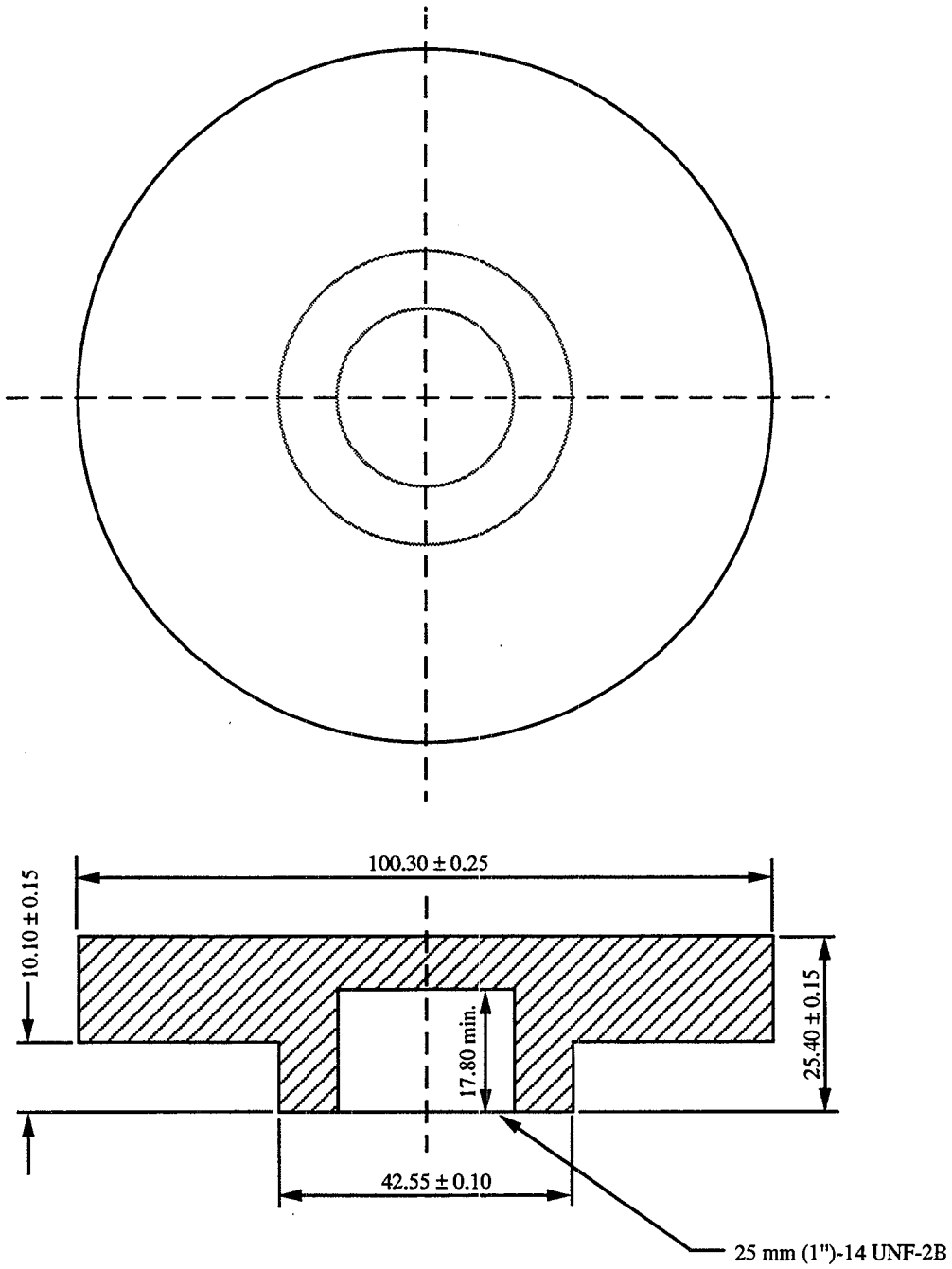

Notes:
1. Harden to minimum RC-55 after fabrication.
2. Chamfer corners as needed to prevent cracking during hardening.

PART NAME: Top Plate
PART NUMBER: 9
MATERIAL: Mild Steel
UNITS: Millimeters unless otherwise specified

Figure 36. Top plate.

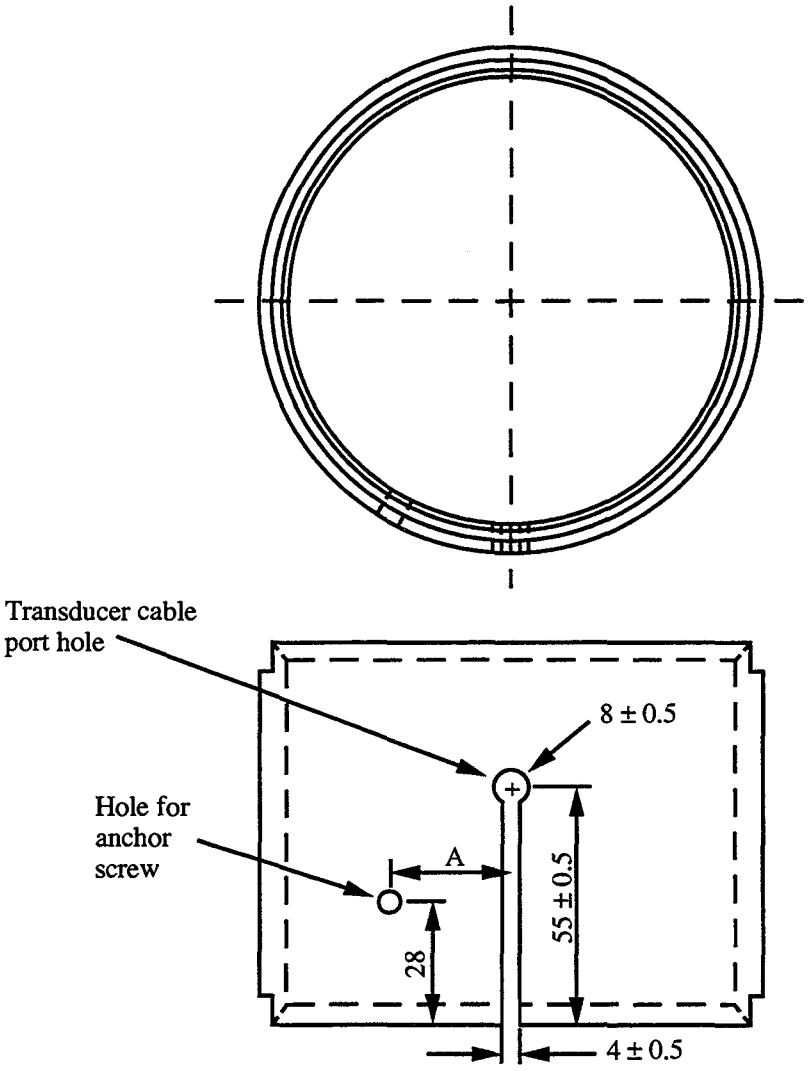

Notes:
Part fabricated from bottom collar of a standard 102 mm (4") diameter Marshall cylinder mold. Modifications include milling slot and drilling hole for transducer cable, and drilling hole for anchor screw. Slot and hole must be tailored to be compatible with transducer connection details. Measure "A" and the diameter of the anchor hole are arbitrary but must be compatible with connection detail and tapped hole in base.

PART NAME: Bottom Collar
PART NUMBER: 10
MATERIAL: Steel
UNITS: Millimeters unless otherwise specified
SCALE: 1/2

Figure 37. Bottom collar.

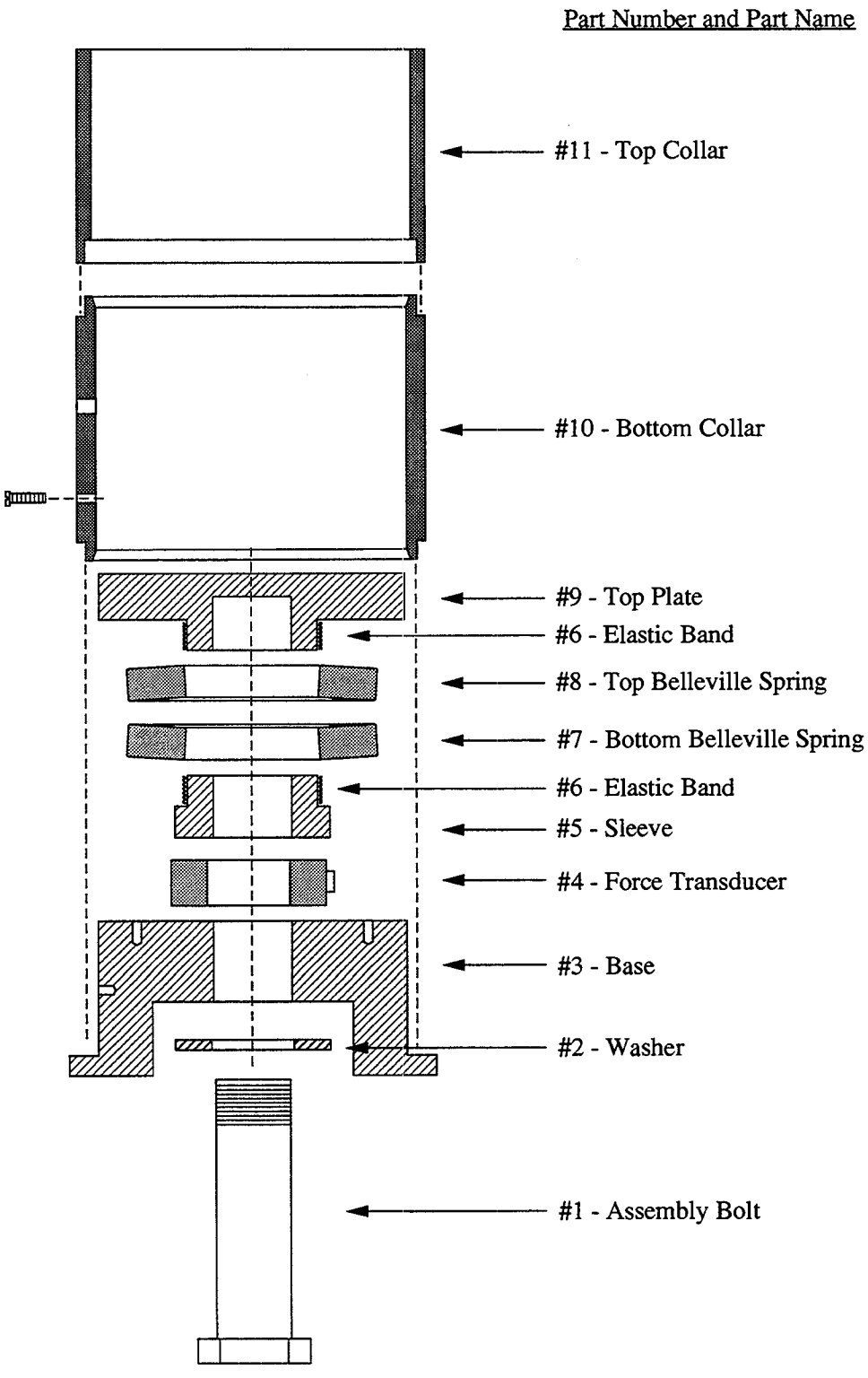

Figure 38. Assembly drawing.

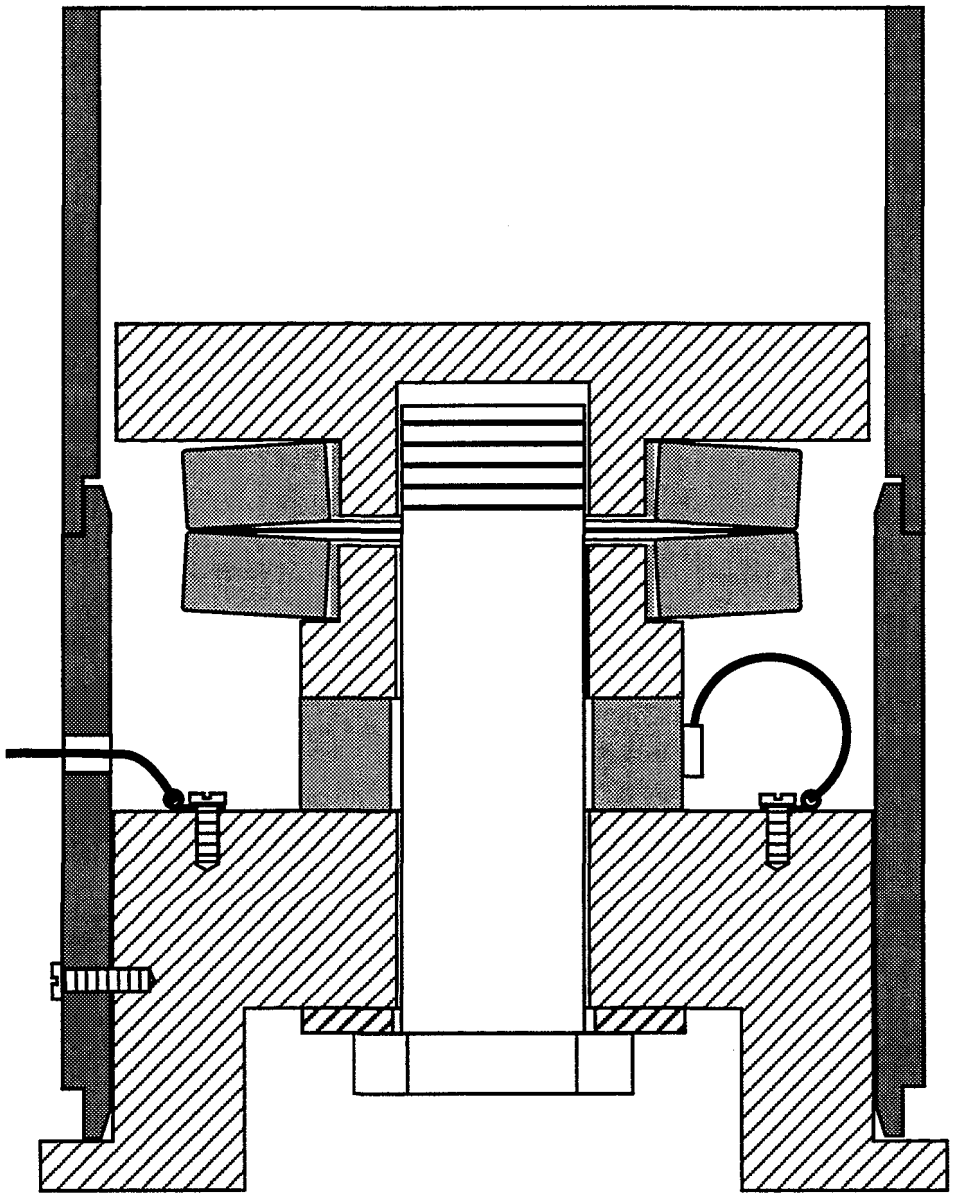

Figure 39. Completed device.

APPENDIX B. DATA PROCESSING SOFTWARE

Presented in this appendix is the custom software developed to process the data for a calibration run. A calibration run is executed from the DOS prompt (**C:**) as follows:

C: phase1
C: phase2 C:\strmtest.001 data.dat
C: phase3 data.dat data.out

in which:

PHASE1 is a DOS batch file that starts the STREAMER software and configures the data acquisition board. The system is configured to record data from channel 0 at 100,000 samples/s and store it in the bulk data file C:\STRMTEST.001. The data acquisition event is logged in the ASCII file C:\streamer.log.

PHASE2 is a "C" program that reads the bulk data file C:\STRMTEST.001 and extracts the blow force time histories, using specified trigger values and sample duration. The program reads the configuration file PHASE2.CFG for all the input parameters. The force time histories are written to another ASCII file that is specified on the command line (in this example, data.dat).

PHASE3 is a "C" program that reads the force time histories from the output file produced in **PHASE2** (data.dat) and determines the necessary statistics: peak force, impulse, and energy for each blow; average and standard deviation of all of the above; and the cumulative impulse and energy for the n blows of the data set. The average and standard deviation results are displayed on the screen. Results are printed to an output file (in this example, data.out). The program reads the configuration file PHASE3.CFG for all input data.

Listings of the three programs and two sample configuration files are presented in the following.

```
rem ***************************************************************
rem
rem Program: Phase1.bat
rem
rem Compiler: DOS 5.0 Batch File
rem
rem Developed by:       Dr. Harry Shenton
rem                             Research Structural Engineer
rem                             Building and Fire Research Laboratory
rem                             National Institute of Standards and Technology
rem
rem This batch file is set up to start STREAMER, the high-speed streaming-to-disk software
rem developed by Keithley-Metrabyte for use with their data acquisition boards. The file sets
rem up various board parameters, including the sample rem rate to 100 kHz ("r=100" on
rem command line), sets the data buffer file to c:\strmtest.001, and the log file to
rem c:\streamer.log. Once up and running, the system is ready to record data by simply
rem pressing the F2 function rem key.
rem
rem /************************************************************************
rem
rem Set-up the video to run STREAMER
rem
eagle ega mono
rem Start the STEAMER software
rem
streamer das-1602 dl=3 ba=320 r=100 df=strmtest.001 lf=c:\streamer.log
```

```
/*****************************************************************************
```

Program: **PHASE2.C**

Compiler: Microsoft C5.1 Optimizing Compiler

Developed by: Dr. Harry Shenton
Research Structural Engineer
Building and Fire Research Laboratory
National Institute of Standards and Technology

Date: April 1993

This program was developed to be used with the Marshall hammer calibration device. The program reads a binary data file that contains the raw data recorded curing the calibration run and locates the impact pulses. The data was recorded and stored using STREAMER, the high-speed streaming-to-disk software developed by Keithley-Metrabyte for use with their data acquisition boards. The program CONVERT.C, which is supplied with STREAMER, was used as the foundation for this program.

5/6/93 - Modified to incorporate a bilinear calibration curve
5/19/93 - Modified to read input from command line and configuration file

```
*****************************************************************************/
#include <stdio.h>
#include <dos.h>
#include <ctype.h>
#include <stdlib.h>

unsigned int out[8192] ;          /* Data Holding Tanks For */
unsigned int in[8192] ;           /* Buffered File Reads    */
unsigned int in1[8192] ;          /* Buffered File Reads    */

FILE *fp1 ;                       /* Input File Handle      */
FILE *fp3 ;                       /* Output File Handle     */
FILE *fp2 ;                       /* Pulse time file        */
FILE *fp4 ;                       /* Configuration file     */

char infile[80] ;                 /* Eighty Character File Names */
char outfile[80] = "output";
char pulse_file[80] = "pulse.tim";
char config_file[80] = "phase2.cfg";
char ch;

int Key ;                         /* Key from keyboard */
int OutOfData = 0 ;               /* Signal To Read Single Ints */
int Available = 0 ;               /* No. Of Extra Bytes At End Of Input */
int threshold = 1500;             /* The trigger threshold, default in */
int threshold_max = 1505;         /*   A/D counts, likewise, the threshold max */
int slope_inc = 20;               /* Data points over which to check the slope */
int pretrigger = 10;              /* Number of pretrigger data points */
int posttrigger = 6000;           /* Number of posttrigger data points */
int nsample = 0;                  /* nsample = pretrigger + posttrigger - 1 */
int inc_change;
```

```
int dloop;
int ndata = 0;
int n1 = 0;
int n2 = 0;
int result = 0;

long Count = 0 ;                    /* Display Number Of Conversions */
long nlast = 0;
long npos = -1;
long nstart = 0;
long nstop = 0;
long locations[500];

float pulse_times[500];       /* array to store time of pulses located */
float sample_rate = 100000.0; /* sample rate - default */
float Del_t = 0.0;
float Cal_factor = 0.0;       /* Calibration factor, Volts to eng. units */
float p_threshold = 0.0;      /* trigger threshold in engineering units */
float p_threshold_max = 0.0;  /*     likewise, threshold_max in eng. units */
float out_data = 0;
float Scale_factor = 0.0;     /* Conversion factor, A/D counts to Volts */
float m1 = 0.0;               /* Initial slope of calibration curve */
float m2 = 0.0;               /* final slope of calibration curve */
float b2 = 0.0;               /* Y intercept of second slope equation */
                                  /* V = m1*F, m2*F - b2 are the 2 equations */
float Fi = 0.0;               /* Force at the break point in the cal. curve */
float Vi = 0.0;               /* Voltage at the break point in the cal. curve */
float V  = 0.0;
float F  = 0.0;

void Cursor( int, int ) ;
void ClearScreen( int ) ;
float get_volts(float F,float m1,float m2,float b2,float Fi);
float get_force(float V,float m1,float m2,float b2,float Vi);

union REGS regs ;                   /* For Using DOS.H Pseudo 80x86 Regs */

int     main(argc,argv)

int     argc;                 /* command line argument count  */
char    **argv;               /* command line argument vector */

{
  register int loop = 0 ;
  if (argc != 3)
  {
  puts("\n") ;
  puts("    PHASE2 -- Usage: PHASE2 <input file> <output file>\n");
  puts("    Where: <input file>  - buffer file used by STREAMER");
  puts("           <output file> - condensed data file containing only the");
  puts("             pulse data that is subsequently used in PHASE3 processing\n\n");
  exit(1) ;
  }
```

```
  Cursor(0,0) ;

  sscanf(argv[1],"%s",infile) ;
  sscanf(argv[2],"%s",outfile) ;

  Cursor(0,0) ;
  for (loop=1; loop <= 25; loop++) puts("\n");

/*****************************************************************************

  Read the input data

*****************************************************************************/

  fp4 = fopen(config_file,"r"); rewind(fp4);

  Cursor(2,0);
  printf("Input Data File          : "); /*result=fscanf(fp4,"%s",infile);*/
  Cursor(35,0); printf("%20s",infile);
  fp1 = fopen(infile,"rb"); rewind(fp1);

  Cursor(2,1);
  printf("Output Data File         : "); /*result=fscanf(fp4,"%s",outfile);*/
  Cursor(35,1); printf("%20s",outfile);
  fp3 = fopen(outfile,"w"); rewind(fp3);

  Cursor(2,2);
  printf("Pretrigger               : "); result=fscanf(fp4,"%d",&pretrigger);
  Cursor(35,2); printf("%20d",pretrigger);

  Cursor(2,3);
  printf("Data Set Size            : "); result=fscanf(fp4,"%d",&nsample);
  Cursor(35,3); printf("%20d",nsample);
  posttrigger = nsample - pretrigger - 1;

  Cursor(2,4);
  printf("Minimum Threshold        : "); result=fscanf(fp4,"%f",&p_threshold);
  Cursor(35,4); printf("%20f",p_threshold);

  Cursor(2,5);
  printf("Maximum Threshold        : "); result=fscanf(fp4,"%f",&p_threshold_max);
  Cursor(35,5); printf("%20f",p_threshold_max);

  Cursor(2,6);
  printf("Slope_increment          : "); result=fscanf(fp4,"%d",&slope_inc);
  Cursor(35,6); printf("%20d",slope_inc);

  Cursor(2,7);
  printf("Sample Rate              : "); result=fscanf(fp4,"%f",&sample_rate);
  Cursor(35,7); printf("%20f",sample_rate);

  Cursor(2,8);
  printf("Calibration Factors      m1: "); result=fscanf(fp4,"%f",&m1);
```

```
  Cursor(35,8); printf("%20f",m1);

  Cursor(2,9);
  printf("                    m2: "); result=fscanf(fp4,"%f",&m2);
  Cursor(35,9); printf("%20f",m2);

  Cursor(2,10);
  printf("                    b2: "); result=fscanf(fp4,"%f",&b2);
  Cursor(35,10); printf("%20f",b2);

/*****************************************************************************

  Convert the trigger threshold values from engineering units
   (e.g., kips, kN, etc) to a A/D count (0 - 4095)

*****************************************************************************/

  Fi          = b2/(m2 - m1);   /* Compute the force at break point */
  /* Cursor(70,9); printf(" %8f",Fi);*/
  Vi          = Fi*m1;          /* Compute the Voltage at break point */
  /* Cursor(70,10); printf(" %8f",Vi);*/
  threshold     = get_volts(p_threshold,m1,m2,b2,Fi)*4096/20.0 + 2048;
  Cursor(60,4); printf("%5d (A/D Count)",threshold);
  threshold_max = get_volts(p_threshold_max,m1,m2,b2,Fi)*4096/20.0 + 2048;
  Cursor(60,5); printf("%5d (A/D Count)",threshold_max);
  Scale_factor  = 20.0/4096.0;

/*****************************************************************************

  First locate all the pulses within the large data file

*****************************************************************************/

for ( ; ; )                          /* Go Until A Break Command */
  {
    if (feof(fp1)) break ;

    Cursor(2,12) ;
    printf("Samples Complete          : %23ld", Count) ;
    Cursor(2,13) ;
    printf("Pulses Located            : %23d", ndata) ;

     /* Read An 8K Chunk */

    if ((Available = fread(in, sizeof(int), 8192, fp1)) < 8192)
    {                                  /* If Not Full Chunk */
    Count = Count + Available ;
    OutOfData = 1 ;
    for (loop = 0 ; loop < Available ; loop ++)    /* Near End Of File */
        {                                  /* Do Last Bytes 1 By 1 */
         out[loop] = in[loop] >> 4 ;             /* Shift out channel */
         npos = npos + 1;
         if(out[loop] >= threshold && out[loop] <= threshold_max)
```

```
          {                                   /* If within threshold window */
           inc_change = out[loop]-out[loop-slope_inc];
           if(inc_change > 0)                  /* and if the slope is positive */
           {
            if(npos > nlast+posttrigger)       /* and if trigger is outside of the */
            {                                  /*  last data set recorded */
             ndata = ndata + 1;                /* then store this position for later processing */
             locations[ndata] = npos;
             pulse_times[ndata] = npos/sample_rate; /* compute the time of the pulse*/
             nlast = npos;                     /* update the position of the most recent pulse */
             Cursor(2,13) ;
             printf("Pulses Located            : %10d", ndata) ;
            }
           }
          }
        }
      }

    if (OutOfData) break ;                     /* No More, Exit Loop */

    Count += 8192 ;

    for (loop = 0 ; loop < 8192 ; loop++)      /* If A Whole 8K Chunk */
    {
          out[loop] = in[loop] >> 4 ;          /* Shift Out Channels */
          npos = npos + 1;
          if(out[loop] >= threshold && out[loop] <= threshold_max)
           {
            inc_change = out[loop]-out[loop-slope_inc];
            if(inc_change > 0)
            {
             if(npos > nlast+posttrigger)
             {
              ndata = ndata + 1;
              locations[ndata] = npos;
              pulse_times[ndata] = npos/sample_rate;
              nlast = npos;
              Cursor(2,13) ;
              printf("Pulses Located            : %23d", ndata) ;
             }
            }
           }
      }
    }

    Cursor(2,12) ;
    printf("Samples Complete          : %23ld", Count) ;

/*****************************************************************************

    Write a summary of the pulses located and their corresponding
    times to a file
```

```
*************************************************************************/

  fp2 = fopen(pulse_file,"w"); rewind(fp2);
  fprintf(fp2," Summary of Pulses Located: \n");
  fprintf(fp2,"    #          Time         Del_Time \n");
  for(loop=1; loop <= ndata; loop++)
   if(loop > 1 )
   {
    Del_t = pulse_times[loop]-pulse_times[loop-1];
    fprintf(fp2,"%5d    %10.5f       %10.7f \n",loop,pulse_times[loop],Del_t);
   }
   else
    fprintf(fp2,"%5d    %10.5f \n",loop,pulse_times[loop]);

  fclose(fp2);

/*************************************************************************

  Now go back and re-read the input file, extract out the pulses and
  write them to a new file in ASCII format, in a single vector format, one
  after another

*************************************************************************/

    rewind(fp1) ; rewind(fp3);          /* goto beginning of files */

    fprintf(fp3,"%d %d \n",ndata,nsample);
    Available = fread(in, sizeof(int), 8192, fp1);  /* read in first buffer of data */
    Count = 0;
    Count = Count + Available ;

for (loop=1; loop <= ndata; loop++)
{
    Cursor(2,15);
    printf("Processing pulse            : %23d ",loop);
    npos   = locations[loop];        /* trigger position of pulse in large file */
    nstart = npos - pretrigger;      /* start position in large data set */
    nstop  = npos + posttrigger;     /* stop position in large data set */
    n1 = nstart;                    /* local start position in 8k buffer */
    n2 = nstop;                      /* local stop position in 8k buffer */
    while(nstart > Count)            /* continue to read buffers until you */
    {                               /*  find the start of the next data set */
     Available = fread(in, sizeof(int), 8192, fp1);
     Count = Count + Available ;
     n1 = 8192 - (Count - nstart);  /* adjust start and stop  */
     n2 = 8192 - (Count - nstop);   /*    positions in buffer  */
    }
    if(Count < nstop)                /* read another buffer in if the data set */
     {                              /*  is split over 2 buffers */
     Available = fread(in1, sizeof(int), 8192, fp1);
     Count = Count + Available;
     }
    if(n2 > 8192)                    /* if the data set is split over 2 buffers */
```

```
    {
     n2 = n2 - 8192;
     for(dloop=n1; dloop < 8192; dloop++)   /* write part in first buffer */
      {
         out[dloop] = in[dloop] >> 4;
         out_data = out[dloop];                    /* Data in A/D counts */
         out_data = (out_data-2047.5)*Scale_factor;  /* Data in Volts */
         F        = get_force(out_data,m1,m2,b2,Vi); /* Data in Eng. units */
         fprintf(fp3,"%10.5f \n",F);
      }
     for(dloop=0; dloop <= n2; dloop++)    /* write part in second buffer */
      {
         out[dloop] = in1[dloop] >> 4;
         out_data = out[dloop];                    /* Data in A/D counts */
         out_data = (out_data-2047.5)*Scale_factor;  /* Data in Volts */
         F        = get_force(out_data,m1,m2,b2,Vi); /* Data in Eng. units */
         fprintf(fp3,"%10.5f \n",F);
      }
     for(dloop=0; dloop < 8192; dloop++)   /* when complete make second  */
      {                                    /*  buffer equal to the first */
         in[dloop] = in1[dloop];
      }
    }
     else
    {
     for(dloop=n1; dloop <= n2; dloop++)   /* if the data set is contained in only 1 buffer */
      {
         out[dloop] = in[dloop] >> 4;
         out_data = out[dloop];                    /* Data in A/D counts */
         out_data = (out_data-2047.5)*Scale_factor;  /* Data in Volts */
         F        = get_force(out_data,m1,m2,b2,Vi); /* Data in Eng units */
         fprintf(fp3,"%10.5f \n",F);
      }
    }
}


  fclose(fp1) ;
  fclose(fp3) ;
}
void Cursor(x,y)
int x,y;
{
 regs.h.ah = 2;
 regs.h.bh = 0;
 regs.x.dx = (y << 8) | x;
 int86(0x10,&regs,&regs);
}

float get_volts(float F,float m1,float m2,float b2,float Fi)
{
 if (F > Fi)
  {
```

```
    return(m2*F - b2);
   }
  else
   {
    return(m1*F);
   }
}


float get_force(float V,float m1,float m2,float b2,float Vi)
{
 if (V > Vi)
   {
    return((V + b2)/m2);
   }
  else
   {
    return(V/m1);
   }
}
```

```
/*****************************************************

SAMPLE CONFIGURATION FILE FOR PHASE2

/*****************************************************
50        /* pre-trigger (sec)
1000      /* sample duration (sec)
7.0       /* minimum trigger level (kips)
10.0      /* maximum trigger level (kips)
2         /*  slope increment
100000    /* sample rate (sec)
.20       /* calibration factor m1
.41       /* calibration factor m2
.45       /* calibration factor b1
```

```
/*************************************************************************
```

Program: **PHASE3.C**

Compiler: Microsoft C5.1 Optimizing Compiler

Developed by: Dr. Harry Shenton
Research Structural Engineer
Building and Fire Research Laboratory
National Institute of Standards and Technology

Date: April 1993

This program was developed to be used with the Marshall hammer calibration device. The program reads the ASCII file created by the program PHASEI and computes statistics for the calibration run from the recorded pulse time histories. From each pulse we determine and store the peak force, peak energy, and the total impulse. We then determine the average, standard deviation, maximum, and minimum for each of the quantities over the n blows of the test. We also compute the running total of energy and impulse for the n blows of the test.

The required input includes:

Input file	: Was created using PHASE2
Output file	: To write results for later viewing or printing
Spring stiffness	: Stiffness of device springs assembly
Sample rate	: Rate at which data was sampled during calibration run

The user is responsible for suppling consistent units, and those that agree with the PHASE2 output data (force time histories)
i.e. - units of stiffness are force(F)/length(L)
- units of sample rate are 1/Time(T)
then
- peak force has units of F
- peak energy has units of F-L (force-length)
- impulse has units of F-T (force-time), however on output impulse is scaled (multiplied) by 1000.

5/13/93 Made a change to subtract out the mean of the first 10 data points from the time history before integrating to get the impulse.
5/19/93 Modified to read input from command line and the configuration file

```
*************************************************************************/
#include <stdio.h>
#include <dos.h>
#include <ctype.h>
#include <stdlib.h>
#include <math.h>

float in[5000] ;          /* Data buffer          */

FILE *fp1 ;               /* Input File Handle    */
FILE *fp2 ;               /* Output File Handle   */
FILE *fp3 ;

char infile[80];          /* Eighty Character File Names */
```

```
char outfile[80];
char temp_char[80];
char config_file[80]="phase3.cfg";
char ch;

int nsample = 0;          /* Number data points per pulse */
int ndata = 0;            /* Number of pulse time histories */
int ntotal = 0;           /* Total # of data points in PHASEI file */
int dloop  = 0;           /* Basic counters */
int ncount = 0;           /*  "             */
int cloop = 0;            /*  "             */
int dloop_max = 0;
int result = 0;

float p = 0;              /* force  */
float e = 0;              /* energy */
float p_max[100];         /* storage array for maximum forces */
float e_max[100];         /* storage array for maximum energies */
float e_sum = 0;          /* variable for summing energies */
float i_sum = 0;          /* variable for summing inpulses */
float Sample_rate = 0;    /* sample rate */
float Del_t = 0.0;        /* sample time interval = 1/sample rate */
float k = 0.0;            /* spring stiffness */
float impulse[100];       /* storage array for impulses */
float sum  = 0.0;         /* various variables for statistics calcs */
float sum2 = 0.0;         /*  "             */
float max_val = -1.0e10;  /*  "             */
float min_val =  1.0e10;  /*  "             */
float ave_val = 0.0;      /*  "             */
float std_dev = 0.0;      /*  "             */
float x[100];             /*  "             */
float stats[4][3];        /* storage array for final statistics */
float init_mean = 0.0;

int result;

void Cursor( int, int ) ;

union REGS regs ;         /* For Using DOS.H Pseudo 80x86 Regs */

int     main(argc,argv)

int     argc;             /* command line argument count  */
char    **argv;           /* command line argument vector */
{
  register int loop = 0 ;
  if (argc != 3)
  {
  puts("\n") ;
  puts("    PHASE3 -- Usage: PHASE3 <input file> <output file>\n");
  puts("    Where: <input file>  - data file created in PHASE2 processing");
  puts("           <output file> - file containing summary of results");
  exit(1) ;
```

```
  }

  Cursor(0,0) ;

  sscanf(argv[1],"%s",infile) ;
  sscanf(argv[2],"%s",outfile) ;

  Cursor(0,0) ;

  for (loop=1; loop <= 25; loop++) puts("\n");    /* A brutt force clear screen */

/*****************************************************************************

 Read the input data

*****************************************************************************/

  fp3 = fopen(config_file,"r"); rewind(fp3);

  Cursor(2,0);
  printf("Input Data File            : ");
  Cursor(35,0); printf("%20s",infile);
  fp1 = fopen(infile,"r"); rewind(fp1);

  Cursor(2,1);
  printf("Output Data File           : ");
  Cursor(35,1); printf("%20s",outfile);
  fp2 = fopen(outfile,"w"); rewind(fp2);

  Cursor(2,2);
  printf("Spring Stiffness           : "); result=fscanf(fp3,"%f",&k);
  Cursor(35,2); printf("%20f",k);

  Cursor(2,3);
  printf("Sample Rate                : "); result=fscanf(fp3,"%f",&Sample_rate);
  Cursor(35,3); printf("%20f",Sample_rate);
  Del_t = 1.0/Sample_rate;

  result = fscanf(fp1,"%d %d",&ndata,&nsample);
  ntotal = ndata*nsample;

  Cursor(1,4);
  puts("_____________________________________________________________________________");

/*****************************************************************************

 Read and process each pulse: find the maximum force, maximum energy and
  integrate to get the impulse, store each of these in an array.

*****************************************************************************/

  Cursor(1,6);
  printf(" Summary of Results:");
```

```
 Cursor(50,6);
 printf(" Number of blows: ");
 for(loop=0; loop < ndata; loop++)              /* Process each pulse */
  {
   Cursor(68,6);
   printf("%d",loop+1);
   for(dloop=0; dloop < nsample; dloop++)
    result = fscanf(fp1,"%f",&in[dloop]);       /* Read in the next pulse */
    p_max[loop] = in[0];                        /* Initialize values for finding */
    impulse[loop] = 0.0;                        /*   maximum and integrating */
    init_mean = 0.0;
   for(dloop=0; dloop < 10; dloop++)
    init_mean = init_mean + in[dloop];
    init_mean = init_mean/10.0;
   for(dloop=1; dloop < nsample; dloop++)
   {
    p = in[dloop];
    if(p > p_max[loop])
     {
      p_max[loop] = p;        /* Search for maximum */
      dloop_max = dloop;
      }
   }
   for(dloop=1; dloop < nsample; dloop++)
   {
    if(dloop > dloop_max && in[dloop] < 0.0) break;
    impulse[loop] = impulse[loop] + ((in[dloop-1]-init_mean) + (in[dloop]-init_mean))*0.5*Del_t; /*Integrate */
   }
  e_max[loop] = p_max[loop]*p_max[loop]*0.5/k;  /* Max. energy from max force */
  impulse[loop] = impulse[loop]*1000.0;         /* Scale the impulse for easy display */
 }
/*************************************************************************

  Compute statistics for various parameters (ave, std dev, max and min)

*************************************************************************/
 for(dloop=0; dloop < 3; dloop++)
 {

 if(dloop == 0)
   for(loop=0; loop < ndata; loop++) x[loop] = p_max[loop]; /*Stats for force */
 else if (dloop == 1)
   for(loop=0; loop < ndata; loop++) x[loop] = e_max[loop]; /*Stats for energy */
 else
   for(loop=0; loop < ndata; loop++) x[loop] = impulse[loop]; /* Stats for impulse */
 sum  = 0.0;
 sum2 = 0.0;
 max_val = -1.0e10;
 min_val =  1.0e10;
 ave_val = 0.0;
 std_dev = 0.0;
 for(loop=0; loop < ndata; loop++)   /* Generic statistic routine - nothing special */
 {
```

```
 if(x[loop] > max_val)max_val = x[loop];
 if(x[loop] < min_val)min_val = x[loop];
 sum = sum + x[loop];
 sum2 = sum2 + x[loop]*x[loop];
}
ave_val = sum/ndata;
std_dev = sqrt((sum2 - ndata*ave_val*ave_val)/(ndata-1));
stats[0][dloop] = ave_val;
stats[1][dloop] = std_dev;
stats[2][dloop] = max_val;
stats[3][dloop] = min_val;
}
Cursor(1,6);
printf(" Summary of Results:");
Cursor(50,6);
printf(" Number of blows: %d",ndata);
printf("\n\n\n                    Peak          Peak          Impulse");
printf("\n                  Force         Energy        x1000    \n");
printf("\n Average          :  %5.2f      %12f    %12f ",stats[0][0],stats[0][1],stats[0][2]);
printf("\n Standard Deviation :  %5.2f      %12f    %12f ",stats[1][0],stats[1][1],stats[1][2]);
printf("\n Maximum          :  %5.2f      %12f    %12f ",stats[2][0],stats[2][1],stats[2][2]);
printf("\n Minimum          :  %5.2f      %12f    %12f ",stats[3][0],stats[3][1],stats[3][2]);

/*************************************************************************

 Print out the values for each blow, and the sum for energy
  and impulse.

*************************************************************************/

 Cursor(1,20);
 printf("Print results to the output file (y/n) ? ");
 gets(temp_char); sscanf(temp_char,"%1s",&ch);

 if(ch == 'y'|| ch == 'Y')
 {
  printf(" Enter a single line of header text for the output file - \n");
  gets(temp_char);
  fprintf(fp2,"%-80s\n\n",temp_char);
  fprintf(fp2,"Summary of Results:                    Number of blows: %d", ndata);
  fprintf(fp2,"\n\n\n                    Peak          Peak          Impulse");
  fprintf(fp2,"\n                  Force         Energy    \n");
  fprintf(fp2,"\nAverage          :  %5.2f      %12f    %12f ",stats[0][0],stats[0][1],stats[0][2]);
  fprintf(fp2,"\nStandard Deviation :  %5.2f      %12f    %12f ",stats[1][0],stats[1][1],stats[1][2]);
  fprintf(fp2,"\nMaximum          :  %5.2f      %12f    %12f ",stats[2][0],stats[2][1],stats[2][2]);
  fprintf(fp2,"\nMinimum          :  %5.2f      %12f    %12f ",stats[3][0],stats[3][1],stats[3][2]);

  e_sum = 0.0;
  i_sum = 0.0;

  fprintf(fp2,"\n\n\nSummary of Per Blow Results:\n\n");
  fprintf(fp2,"Blow        P_max        E_max        E_sum        I_max        I_sum\n");
  for(loop = 0; loop < ndata; loop++)
```

```
   {
    e_sum = e_sum + e_max[loop];
    i_sum = i_sum + impulse[loop];

fprintf(fp2,"%4d%15.4f%15.4f%15.4f%15.4f%15.4f\n",loop+1,p_max[loop],e_max[loop],e_sum,impulse[loop],i_s-
um);
   }
  }
  fclose(fp1) ;
  fclose(fp2) ;
}
void Cursor(x,y)
int x,y;
{
  regs.h.ah = 2;
  regs.h.bh = 0;
  regs.x.dx = (y << 8) | x;
  int86(0x10,&regs,&regs);
}
```

```
/*****************************************************

SAMPLE CONFIGURATION FILE FOR PHASE3

/*****************************************************

890      /* spring stiffness (kip/in)
100000   /* sample rate (sec)
```

APPENDIX C. CALIBRATION REPORTS

Presented in this appendix are the calibration reports from the laboratory evaluation program. A report is included for each of the five machine setups used in the study. The machine setups, described in detail in table 7, are referred to as: Pine Standard, Rainhart Standard, Manual Standard, Pine with Weight, and Rainhart with Pad.

Calibration was conducted in accordance with the procedure outlined in chapter 5. Sets of 75 blows each were recorded with the device oriented at 4, 8, and 12 o'clock in the machine. Presented in the report are the average and standard deviation of peak force, peak energy, and impulse for each orientation. Also presented is the number of blows needed to achieve the target cumulative energy of 565 kN-mm, and the number of blows needed to achieve the target cumulative impulse of 1223 x 10^{-3} kN-s, for each of the three orientations. The average and standard deviation over the three sets is presented for all the measured quantities. The calibrated blow counts for energy and impulse are shown in the heavy boxes at the lower right-hand corner of the report.

CALIBRATION REPORT

Date: June 16, 1993

Machine: Pine

Setup: Standard

	Orientation			Avg	Standard Deviation
	12 O'Clock	4 O'Clock	8 O'Clock		
Average Peak Force (kN)	71.88	69.39	66.14	69.14	2.88
Standard Deviation	1.60	1.56	3.07	———	———
Average Peak Energy (kN-mm)	16.61	15.48	140.1	15.37	1.30
Standard Deviation	0.68	0.68	1.36	———	———
Average Impulse (x 10^{-3} kN-s)	22.89	23.73	23.09	23.24	0.44
Standard Deviation	0.20	0.14	0.19	———	———
N_E Blow Count[1]	34	37	42	**38**	4.0
N_I Blow Count[2]	53	52	53	**53**	0.6

[1]based on E_{50} = 565 kN-mm
[2]based on I_{50} = 1223 x 10^{-3} kN-s

CALIBRATION REPORT

Date: June 23, 1993

Machine: Rainhart

Setup: Standard

	Orientation			Avg	Standard Deviation
	12 O'Clock	4 O'Clock	8 O'Clock		
Average Peak Force (kN)	56.76	49.46	49.91	52.04	4.09
Standard Deviation	2.94	1.56	1.56	———	———
Average Peak Energy (kN-mm)	10.39	7.80	8.02	8.74	1.44
Standard Deviation	0.04	0.02	0.02	———	———
Average Impulse (x 10^{-3} kN-s)	22.44	21.76	21.64	21.95	0.43
Standard Deviation	0.24	0.13	0.20	———	———
N_E Blow Count[1]	55	72*	71*	**66**	9.5
N_I Blow Count[2]	54	56	57	**56**	1.5

[1]based on E_{50} = 565 kN-mm
[2]based on I_{50} = 1223 x 10^{-3} kN-s
*projected $N_E = E_{50}/E_{AVG}$

CALIBRATION REPORT

Date: July 1, 1993

Machine: Manual

Setup: Standard

	Orientation			Avg	Standard Deviation
	12 O'Clock	4 O'Clock	8 O'Clock		
Average Peak Force (kN)	55.56	56.31	59.65	57.17	2.18
Standard Deviation	6.80	6.98	5.69	———	———
Average Peak Energy (kN-mm)	10.06	10.28	11.52	10.62	0.79
Standard Deviation	2.26	0.09	0.08	———	———
Average Impulse (x 10^{-3} kN-s)	32.09	27.71	26.63	28.81	2.89
Standard Deviation	8.84	5.14	4.61	———	———
N_E Blow Count[1]	57	54	49	**53**	4.0
N_I Blow Count[2]	39	45	45	**43**	3.5

[1]based on E_{50} = 565 kN-mm
[2]based on I_{50} = 1223 x 10^{-3} kN-s

CALIBRATION REPORT

Date: June 24, 1993

Machine: Pine

Setup: with Weight

	Orientation			Avg	Standard Deviation
	12 O'Clock	4 O'Clock	8 O'Clock		
Average Peak Force (kN)	65.29	68.14	64.72	66.05	1.83
Standard Deviation	3.47	1.60	3.11	———	———
Average Peak Energy (kN-mm)	13.67	14.91	13.44	14.01	0.79
Standard Deviation	1.36	0.68	1.36	———	———
Average Impulse (x 10^{-3} kN-s)	23.85	24.96	24.33	24.38	0.56
Standard Deviation	0.24	0.16	0.16	———	———
N_E Blow Count[1]	43	39	41	**41**	2.0
N_I Blow Count[2]	51	49	50	**50**	1.0

[1]based on E_{50} = 565 kN-mm
[2]based on I_{50} = 1223 x 10^{-3} kN-s

CALIBRATION REPORT

Date: June 29, 1993

Machine: Rainhart

Setup: with Pad

	Orientation			Avg	Standard Deviation
	12 O'Clock	4 O'Clock	8 O'Clock		
Average Peak Force (kN)	40.52	39.85	43.77	41.38	2.10
Standard Deviation	1.65	0.93	2.40	———	———
Average Peak Energy (kN-mm)	5.31	5.08	6.10	5.50	0.54
Standard Deviation	0.45	0.23	0.68	———	———
Average Impulse ($\times 10^{-3}$ kN-s)	20.15	20.72	20.22	20.36	0.31
Standard Deviation	0.21	0.73	0.29	———	———
N_E Blow Count[1]	107*	111*	92*	**103**	10.0
N_I Blow Count[2]	61	59	60	**60**	1.0

[1]based on E_{50} = 565 kN-mm
[2]based on $I_{50} = 1223 \times 10^{-3}$ kN-s
*projected $N_E = E_{50}/E_{AVG}$

APPENDIX D. LABORATORY EVALUATION PROGRAM: RAW DATA

Presented in this appendix is the raw data from the laboratory evaluation program described in chapter 6. A data sheet is included for each of the five machine setups. The machine setups, described in detail in table 7, are referred to as: Pine Standard, Rainhart Standard, Manual Standard, Pine with Weight, and Rainhart with Pad.

Presented are the results for three sets of specimens of three replicates each. The three sets correspond to uncalibrated (standard 50 blows), calibrated to energy, and calibrated to impulse. Calibration to energy was based on a standard cumulative energy of 565 kN-mm (5 kip-in). Calibration to impulse was based on a standard cumulative impulse of 1223 x 10^{-3} kN-s (275 x 10^{-3} kip-s). Pertinent calibration data is noted on the sheet for the specimens calibrated to energy. This includes number of blows (N_E), average peak force (APF), and average energy (AE). Similarly, the number of blows (N_I), average peak force (APF), and average impulse (AI) are noted on the data sheet for the specimens prepared with the machine calibrated to impulse.

Test results include bulk gravity, stability, flow, air voids, and height. Results are presented for individual specimens, along with the average and standard deviation for the three specimens. Properties of the test specimens were determined in accordance with the applicable AASHTO standard:

Property	Notation	AASHTO Test Method
Maximum Theoretical Specific Gravity		T209
Bulk Specific Gravity	BULK GRAV	T166
Stability	STAB	T245
Flow Value	FLOW	T245
Percent Air Voids	AIR VOIDS	T269
Specimen Height	HGT	

MARSHALL LABORATORY EVALUATION

MAXIMUM THEORETICAL SPECIFIC GRAVITY : 2.524

MACHINE CONFIGURATION: Pine - Standard

UNCALIBRATED

SAMPLE ID	AIR MASS (g)	H_2O MASS (g)	SSD MASS (g)	BULK GRAV	STAB (N)	FLOW (0.25 mm)	AIR VOIDS (%)	HGT (mm)
PSU1	1174.32	682.57	1176.73	2.376	---	---	5.860	62.20
PSU2	1172.06	681.53	1174.05	2.380	5649	8.13	5.710	62.03
PSU3	1176.96	687.03	1179.20	2.391	4670	7.62	5.270	61.93
AVG				2.382	5160	7.87	5.613	62.05
STD				0.008	692	0.36	0.307	0.14

CALIBRATED TO ENERGY: N_E = 38 APF 69.1 kN AE 15.4 kN-mm

SAMPLE ID	AIR MASS (g)	H_2O MASS (g)	SSD MASS (g)	BULK GRAV	STAB (N)	FLOW (0.25 mm)	AIR VOIDS (%)	HGT (mm)
PSE2	1171.34	679.22	1173.33	2.371	5226	6.10	6.060	62.30
PSE3	1165.44	675.92	1167.02	2.373	4782	5.59	5.980	61.70
PSE4	1173.25	681.88	1175.15	2.379	4782	5.59	5.740	62.20
AVG				2.374	4930	5.76	5.927	62.07
STD				0.004	256	0.29	0.167	0.32

CALIBRATED TO IMPULSE: N_I = 53 APF 69.1 kN AI 23.2 x 10^{-3} kN-s

SAMPLE ID	AIR MASS (g)	H_2O MASS (g)	SSD MASS (g)	BULK GRAV	STAB (N)	FLOW (0.25 mm)	AIR VOID (%)	HGT (mm)
PSI1	1175.14	685.87	1176.36	2.396	6672	6.60	5.070	61.72
PSI2	1171.13	682.99	1171.98	2.395	6005	6.60	5.110	61.62
PSI3	1169.51	683.99	1171.32	2.400	5560	6.10	4.910	61.82
AVG				2.397	6079	6.43	5.030	61.72
STD				0.003	560	0.29	0.106	0.10

MARSHALL LABORATORY EVALUATION

MAXIMUM THEORETICAL SPECIFIC GRAVITY : 2.524

MACHINE CONFIGURATION: Rainhart - Standard

UNCALIBRATED

SAMPLE ID	AIR MASS (g)	H_2O MASS (g)	SSD MASS (g)	BULK GRAV	STAB (N)	FLOW (0.25mm)	AIR VOIDS (%)	HGT (mm)
RU4	1171.81	679.45	1173.46	2.372	3736	6.10	6.020	62.31
RU5	1174.32	685.62	1175.22	2.399	4937	5.84	4.950	61.47
RU6	1175.32	680.14	1177.89	2.361	3114	6.86	6.460	63.30
AVG				2.377	3929	6.27	5.810	62.36
STD				0.020	927	0.53	0.775	0.92

CALIBRATED TO ENERGY: N_E = 66 APF 52.0 kN AE 8.74 kN-mm

SAMPLE ID	AIR MASS (g)	H_2O MASS (g)	SSD MASS (g)	BULK GRAV	STAB (N)	FLOW (0.25 mm)	AIR VOIDS (%)	HGT (mm)
RSE1	1177.75	689.17	1179.22	2.403	6005	6.20	4.790	61.49
RSE2	1173.33	684.62	1174.92	2.393	6049	6.86	5.190	61.65
RSE3	1174.02	685.08	1174.95	2.397	5204	5.84	5.030	61.72
AVG				2.398	5756	6.30	5.003	61.62
STD				0.005	476	0.52	0.199	0.12

CALIBRATED TO IMPULSE: N_I = 56 APF 52.0 kN AI 22.0 x 10^{-3} kN-s

SAMPLE ID	AIR MASS (g)	H_2O MASS (g)	SSD MASS (g)	BULK GRAV	STAB (N)	FLOW (0.25 mm)	AIR VOIDS (%)	HGT (mm)
RSI1	1174.94	684.82	1175.84	2.393	5449	6.35	5.190	61.75
RSI2	1173.52	685.63	1174.78	2.399	6450	7.11	4.950	61.62
RSI3	1176.02	692.01	1176.83	2.426	5115	6.35	3.880	61.75
AVG				2.406	5671	6.60	4.673	61.71
STD				0.018	695	0.44	0.696	0.08

MARSHALL LABORATORY EVALUATION

MAXIMUM THEORETICAL SPECIFIC GRAVITY : 2.524

MACHINE CONFIGURATION: Manual - Standard

UNCALIBRATED

SAMPLE ID	AIR MASS (g)	H_2O MASS (g)	SSD MASS (g)	BULK GRAV	STAB (N)	FLOW (0.25 mm)	AIR VOIDS (%)	HGT (mm)
HU4	1174.13	693.62	1174.59	2.441	8184	8.13	3.290	60.25
HU5	1171.66	691.56	1172.21	2.438	8896	8.38	3.410	60.48
HU6	1174.20	691.78	1174.88	2.431	8340	7.87	3.680	60.76
AVG				2.437	8473	8.13	3.460	60.50
STD				0.005	374	0.26	0.200	0.26

CALIBRATED TO ENERGY: N_E = 53 APF 57.2 kN AE 10.6 kN-mm

SAMPLE ID	AIR MASS (g)	H_2O MASS (g)	SSD MASS (g)	BULK GRAV	STAB (N)	FLOW (0.25 mm)	AIR VOIDS (%)	HGT (mm)
HE1	1169.59	688.12	1170.55	2.424	8229	7.62	3.960	60.45
HE2	1170.02	688.73	1170.85	2.427	8051	8.38	3.840	60.58
HE3	1171.06	689.74	1171.58	2.430	9697	8.38	3.720	60.35
AVG				2.427	8659	8.13	3.840	60.46
STD				0.003	903	0.44	0.12	0.12

CALIBRATED TO IMPULSE: N_I = 43 APF 57.2 kN AI 28.8 x 10^{-3} kN-s

SAMPLE ID	AIR MASS (g)	H_2O MASS (g)	SSD MASS (g)	BULK GRAV	STAB (N)	FLOW (0.25 mm)	AIR VOIDS (%)	HGT (mm)
HI1	1176.70	691.47	1177.69	2.420	6983	7.37	4.120	61.06
HI2	1178.46	694.64	1179.05	2.433	7740	8.38	3.610	60.66
HI3	1172.01	689.06	1172.60	2.424	6894	7.37	3.960	60.73
AVG				2.426	7206	7.71	3.897	60.82
STD				0.007	465	0.58	0.261	0.21

MARSHALL LABORATORY EVALUATION

MAXIMUM THEORETICAL SPECIFIC GRAVITY : 2.524

MACHINE CONFIGURATION: Pine with Weight

UNCALIBRATED

SAMPLE ID	AIR MASS (g)	H_2O MASS (g)	SSD MASS (g)	BULK GRAV	STAB (N)	FLOW (0.25 mm)	AIR VOIDS (%)	HGT (mm)
PWU1	1176.35	686.64	1178.67	2.391	5782	6.10	5.270	62.05
PWU2	1174.80	686.21	1177.43	2.392	5204	6.10	5.230	61.87
PWU3	1163.23	680.26	1165.05	2.400	5516	6.10	4.910	61.11
AVG				2.394	5501	6.10	5.137	61.68
STD				0.005	289	0.00	0.197	0.50

CALIBRATED TO ENERGY: N_E = 41 APF 66.1 kN AE 14.0 kN-mm

SAMPLE ID	AIR MASS (g)	H_2O MASS (g)	SSD MASS (g)	BULK GRAV	STAB (N)	FLOW (0.25 mm)	AIR VOIDS (%)	HGT (mm)
PWE1	1175.00	683.66	1179.56	2.369	5160	6.86	6.140	62.84
PWE2	1176.12	684.36	1177.03	2.387	5338	6.35	5.430	61.93
PWE3	1170.03	680.71	1171.14	2.386	5515	6.35	5.470	61.72
AVG				2.381	5338	6.52	5.680	62.15
STD				0.010	178	0.29	0.399	0.58

CALIBRATED TO IMPULSE: N_I = 50 APF 66.1 kN AI 24.4 x 10^{-3} kN-s

SAMPLE ID	AIR MASS (g)	H_2O MASS (g)	SSD MASS (g)	BULK GRAV	STAB (N)	FLOW (0.25 mm)	AIR VOIDS (%)	HGT (mm)
PWI1	1172.41	684.57	1173.40	2.398	6672	6.60	4.990	61.52
PWI2	1172.21	687.48	1173.46	2.412	5427	6.35	4.440	62.00
PWI3	1176.86	688.74	1178.04	2.405	6005	5.84	4.710	61.65
AVG				2.405	6035	6.26	4.713	61.72
STD				0.007	623	0.39	0.275	0.25

MARSHALL LABORATORY EVALUATION

MAXIMUM THEORETICAL SPECIFIC GRAVITY : 2.524

MACHINE CONFIGURATION: Rainhart with Pad

UNCALIBRATED

SAMPLE ID	AIR MASS (g)	H_2O MASS (g)	SSD MASS (g)	BULK GRAV	STAB (N)	FLOW (0.25 mm)	AIR VOIDS (%)	HGT (mm)
RPU1	1174.55	678.11	1178.24	2.349	3114	6.35	6.930	63.20
RPU2	1173.14	678.81	1178.08	2.350	3781	6.86	6.890	64.16
RPU3	1175.47	674.59	1180.47	2.324	2179	6.35	7.920	64.49
AVG				2.341	3025	6.52	7.247	63.96
STD				0.015	805	0.29	0.583	0.69

CALIBRATED TO ENERGY: N_E = 103 APF 41.4 kN AE 5.50 kN-mm

SAMPLE ID	AIR MASS (g)	H_2O MASS (g)	SSD MASS (g)	BULK GRAV	STAB (N)	FLOW (0.25 mm)	AIR VOIDS (%)	HGT (mm)
RPE1	1171.46	683.85	1172.34	2.398	6494	6.60	4.990	61.42
RPE2	1171.95	684.58	1172.53	2.402	6805	6.86	4.830	61.11
RPE3	1173.66	687.45	1174.32	2.411	5738	6.10	4.480	61.26
AVG				2.404	6346	6.52	4.767	61.26
STD				0.007	549	0.39	0.261	0.15

CALIBRATED TO IMPULSE: N_I = 60 APF 41.4 kN AI 20.4 x 10^{-3} kN-s

SAMPLE ID	AIR MASS (g)	H_2O MASS (g)	SSD MASS (g)	BULK GRAV	STAB (N)	FLOW (0.25 mm)	AIR VOIDS (%)	HGT (mm)
RPI1	1170.31	679.86	1172.38	2.376	--	---	5.860	62.03
RPI2	1170.27	682.08	1171.34	2.392	4403	7.62	5.230	61.70
RPI3	1171.80	684.21	1172.53	2.400	5560	7.11	4.910	61.62
AVG				2.389	4982	7.37	5.333	61.77
STD				0.012	818	0.36	0.438	0.23

APPENDIX E. PROPOSED AASHTO CALIBRATION STANDARD

Presented in this appendix is the draft standard for calibration of Marshall compaction hammers. The proposed standard has been formatted *according to AASHTO guidelines*, and does not conform to the format or numbering of the remainder of this report. To ensure that the draft standard is complete, in and of itself, there is some duplication of material from the report and other appendixes in the draft.

Proposed Standard Practice for Calibrating Mechanical Marshall Compaction Hammers[1]

1. Scope

1.1 This practice addresses the calibration of mechanical compaction hammers that are used in the test for R resistance to plastic flow of bituminous mixtures using the Marshall apparatus T245.

1.2 The practice is limited to mechanical compaction hammers capable of applying an average peak force of at least 33 kN with a flat hammer foot and a non-rotating base. The practice is intended for single-hammer machines, although it may be applicable to dual- or triple-hammer machines under certain circumstances. It is the responsibility of the user to establish the applicability of the procedure in those cases.

1.3 The values stated in SI units are to be regarded as the standard.

1.4 This standard may involve hazardous materials, operations, and equipment. This standard does not purport to address all of the safety problems associated with its use. It is the responsibility of the user of this standard to establish appropriate safety and health practices and determine the applicability of regulatory limitations prior to use.

2. Reference Documents

2.1 AASHTO Standards

T245 Method of Test for Resistance to Plastic Flow of Bituminous Mixtures Using Marshall Apparatus

3. Terminology

3.1 Symbols

3.1.1 m_1, m_2, b_2 = calibration factors ($slope_1$-mV/kN, $slope_2$-mV/kN, and $intercept_2$-mV values) for the device force transducer

3.1.2 V = device readout

3.1.3 K_s = stiffness of the device spring assembly, kN/mm

3.1.4 F = test machine applied load, kN

3.1.5 δ = displacement of the device top plate, mm

3.2 Description of Terms Specific to this Standard

3.2.1 Data Set - One of three ensembles of 75 or 100 force time histories recorded as part of the calibration procedure

---

[1]This standard is based on research described in NISTIR XXXX (reference to this report).

3.2.2 Peak Force; kN - The maximum force recorded for an individual blow

3.2.3 Average Peak Force; kN - The average of the peak forces for a data set

3.2.4 Impulse; kN-s - The integrated force time history for an individual blow

3.2.5 Cumulative Impulse; kN-s - The running sum total of the impulses as a function of blow count

3.2.6 Standard Cumulative Impulse; kN-s - The standard compactive effort, expressed in terms of cumulative impulse, required for calibration (Usually a compactive effort equivalent to a 50 or 75 blow Marshall procedure is specified.)

4. Summary of Calibration Procedure

4.1 Three data sets are recorded with the calibration device positioned in the machine at 12, 4, and 8 o'clock. Seventy-five or one hundred blows are recorded per data set. The peak force and impulse is determined for each blow of the compaction hammer.

4.2 The average peak force for each data set is obtained to determine if the mechanical hammer can be calibrated.

4.3 The cumulative impulse is computed for each data set and the number of blows required to deliver the specified standard compactive effort is established for the device.

5. Significance and Use

5.1 The procedures described in this practice are used to determine the number of blows required for a given mechanical hammer to provide a compactive effort equivalent to a standard 50- or 75-blow Marshall procedure as described in T245.

5.2 The application of the calibration procedures described in this practice can greatly reduce the variability of tests performed on Marshall test specimens prepared using different mechanical compactors.

6. Apparatus

6.1 Calibration Device - A calibration device as shown in Figure 1 and described in Annex A1.

6.2 Data Acquisition System - The data acquisition shall have, at a minimum, an 8-bit A/D converter and shall be capable of sampling a single channel at a rate of at least 100,000 samples/s. The system shall have trigger and storage capabilities such that multiple force time histories can be automatically captured and stored for subsequent processing. The system shall be capable of storing a minimum of 100 sample time histories of 500 data points each. Triggering shall be such that the start of the pulse is easily and clearly defined for any given time history. Software or switch selectable gains are a desirable option.

> Note 1 -- The prototype system described in NISTIR XXXX (reference to this report) included a portable "lunch box" 386 DX/33 with an 80 MB hard disk, one 1.44-MB floppy disk drive and 4-MB memory; a Keithley/Metrabyte, Taunton, MA, Model DAS-1402 high-speed analog input board; and Keithley/Metrabyte Taunton, MA, STREAMER software, version 3.3, compatible with DAS-1402.

6.3 Data Processing Software - The data processing software shall be capable of processing individual force time histories to determine the peak force and impulse (impulse is defined as the area under the force time history between

the start of the initial pulse and the first zero crossing). The software shall be capable of evaluating the average and standard deviation of the peak force and impulse, for a sample set of up to 100 time histories.

Note 2 -- The force time histories may be processed using custom-developed software. Appendix B of NISTIR 5338 lists two programs written in Microsoft C5.1 that were used with the prototype system.

7. Calibration and Standardization

7.1 Measure the stiffness of the device spring assembly at least once a year, or more frequently as use requires. Determine the spring stiffness as described in Annex A2. The spring stiffness K_s shall be 150 ± 10 kN/mm.

7.2 Calibrate the device force transducer whenever any component of the data acquisition system is replaced, or more frequently as use requires, but at least once a year. Determine the transducer calibration factors m_1, m_2, b_2, as described in Annex A3. These factors are needed to convert the analog output of the device to engineering units.

8. Procedure

8.1 Place the calibration device in the compaction machine and secure with the specimen mold holder. Position the device in the machine such that the port hole for the transducer cable is in the 12 o'clock position, as viewed when facing the machine.

8.2 Place the compaction hammer on top of the calibration device and secure it in the machine as usual during normal operation. Rest the drop weight on top of the hammer foot before starting the machine.

8.3 Begin recording data and immediately start the compaction hammer.

8.4 Record the force time history for each blow. Apply 75 blows when calibration for a 50-blow Marshall procedure is desired. Apply 100 blows when calibration for a 75-blow Marshall procedure is desired.

8.5 Sufficient "pre-trigger" shall be recorded for each blow to ensure that the start of the blow is captured. The duration of the recorded force time history shall be of a length such that all significant/measurable force is recorded (Figure 2). Individual force time histories shall be stored, either temporarily or permanently, for subsequent processing.

8.6 Repeat Sections 8.1 to 8.4 with the port hole for the transducer cable in the 4 o'clock (second data set) and 8 o'clock (third data set) positions.

9. Calculation and Interpretation of Results

9.1 Determine the peak force of each recorded force time history, the average peak force for each data set, and the average of the average peak forces to the nearest kN (Figure 2).

9.2 If the average of the average peak forces is less than 33 kN, calibration of the compaction device is not valid.

Note 3 -- A very low average peak force is an indication of a machine that is in need of repair or maintenance. Calibration can be carried out; however, the calibrated blow count is likely to be excessive when compared to the calibrated blow count of typical machines. In this case, the machine should be inspected and repaired as necessary and the average peak force measured again.

9.3 Determine the impulse for each recorded force time history and the average of the impulses for each data set. The impulse is defined as the area under the force time history curve from the start of the blow to the first zero crossing. (Figure 2)

9.4 Determine the cumulative impulse for each data set in kN·s. The cumulative impulse is the running total sum of the individual impulses, computed as a function of the blow count.

9.5 From the cumulative impulse data, determine the blow count for each data set that corresponds to the standard cumulative impulse specified. Use a standard cumulative impulse value of (Note 4) kN·s when calibration for a 50-blow Marshall procedure is desired, and a standard cumulative impulse value of (Note 4) kN·s when calibration for a 75-blow Marshall procedure is desired.

> Note 4 -- Standard cumulative impulse values corresponding to the 50- and 75-blow Marshall compaction effort will be developed under future research.

9.6 Average the blow count from each data set that corresponds to the standard cumulative impulse specified.

10. Report

10.1 For each data set report the following:

10.1.1 the average of the peak forces, nearest kN,

10.1.2 the average of the impulses, nearest kN·s, and

10.1.3 the blow count that corresponds to the standard cumulative impulse.

10.2 The report shall include an identification of the hammer being calibrated.

10.3 Report the average of the average peak forces for the 3 data sets, nearest kN.

10.4 Report the standard cumulative impulse used, nearest kN·s.

10.5 Report the average blow count for the three data sets as the calibrated blow count N_{50} or N_{75}.

11. Keywords - Calibration, Mechanical Compactor, Marshall Test

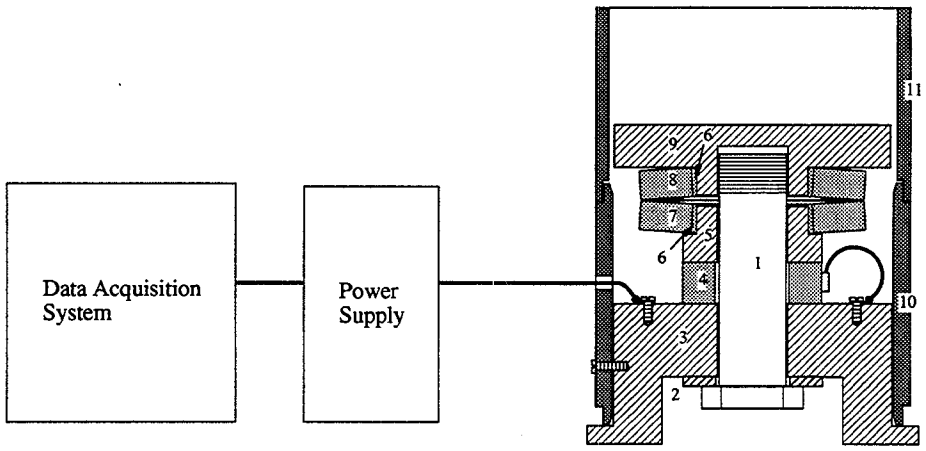

Parts:

1	Bolt	5	Sleeve	9	Top Plate
2	Washer	6	Elastic Band	10	Bottom Collar
3	Base	7	Bottom Belleville Spring	11	Top Collar
4	Force Transducer	8	Top Belleville Spring		

Figure 1: Calibration Device

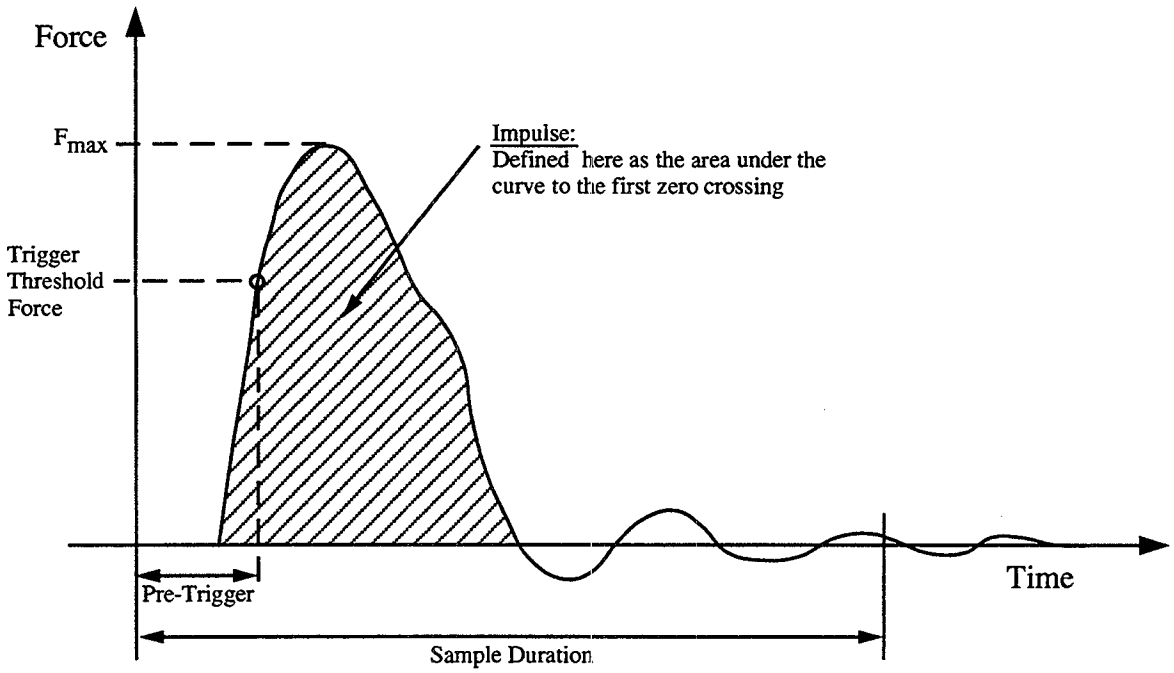

Figure 2: Typical Force Time History Showing Peak Force and Impulse

ANNEX A1 - Calibration Device Parts List and Drawings
(Mandatory Information)

A1.1 Parts List - The parts list for the calibration device is presented in Table A1.1. Parts are referenced by part number and part name. Specifications for each part are listed in the table along with the supplier of the part for the prototype device.

> Note A1.1 -- This should not be construed as an endorsement of a particular manufacturer or supplier. The suppliers are listed only so that the interested reader can obtain more detailed specifications if they so desire, which should aid in the selection of the part.

A1.2 Engineering Drawings - Engineering drawings are presented in Figures A1.1 through A1.5 for all parts that require custom fabrication, or are modified from an "off-the-shelf" item. Engineering drawings are not included for stock parts that are used as purchased (e.g., washer, Belleville spring, etc.). An assembly drawing is presented in Figure A1.6.

> Note A1.2 -- Particular attention should be paid to the details of the cable connection of the force transducer since there is limited clearance between the transducer and bottom collar, and transducer and Belleville springs. The bottom collar should slide freely on and off without having to disassemble the device.

A1.3 Assembly Instructions:

A1.3.1 Apply a small amount of general purpose or high-strength thread adhesive/bonding agent (e.g, LockTite™ or equivalent) to the inside threads of the top plate.

A1.3.2 Secure the top plate upside-down in a bench vise. Use small blocks of wood if necessary to prevent damage to the plate.

A1.3.3 Apply a lubricant to the contact surfaces of the force transducer, sleeve, and base as recommended by the transducer manufacturer (a molybdenum-based lubricant was used in the prototype device). Apply a small amount of the same lubricant to the outer diameter edges of the Belleville springs where the two springs come in contact.

A1.3.4 Place the elastic band around the hub of the sleeve and hub of the top plate (the elastic band reduces the clearance between the spring and sleeve (top plate) hub, while permiting radial displacement of the spring relative to the hub).

A1.3.5 Position the Belleville springs, sleeve, force transducer, base, and washer on top of the top plate in the order shown in figure A1.6.

A1.3.6 Apply a small amount of adhesive/bonding agent to the threads of the assembly bolt.

A1.3.7 Slide the assembly bolt down through the device parts and tighten the assembly by hand until snug.

A1.3.8 Center and align all the parts relative to one another. Rotate the force transducer relative to the base so that the transducer cable is positioned properly to allow for installation and removal of the bottom collar.

A1.3.9 Tighten the assembly using a torque wrench to 41 N-m (30 ft-lb).

A1.3.10 Remove the device from the vise. Place the device upside down on a table and allow the thread adhesive to fully cure, as recommended by the adhesive manufacturer.

Warning - Do not use an excessive amount of thread adhesive on the top plate and assembly bolt. Also, do not turn the device right-side up until the adhesive is fully cured. Excess adhesive may backup or drain down the shaft of the assembly bolt and obstruct the smooth operation of the device.

Table A1.1: Calibration Device - Parts List

Part #	Name	Specification	Prototype Device Supplier
1	Assembly Bolt	25-mm (1") #14 fine thread, 152-mm (6") hex-head medium-strength cap screw, modified as shown in fabrication drawing	McMaster-Carr, Brunswick, NJ; Part # 91248A927
2	Washer	25 mm (1") SAE flat washer	McMaster-Carr, Brunswick, NJ; Part # 91083A038
3	Base	Mild steel, see fabrication drawing	Local
4	Force Ring	Piezoelectric force transducer, compression type, maximum force of 20-30 kips, nominal inner diameter - 25 mm (1"), nominal outer diameter - 51 mm (2"), nominal height less than 15 mm (0.6"), size and configuration of connection that fits the space constraint of device	PCB Piezotronics, Inc., Depew, New York; Model 216A Force Ring with M05 built-in option (1.5 m (5') low noise integral cable)
5	Sleeve	Mild steel, see fabrication drawing	Local
6	Elastic band	1-mm thick elastic band; diameter to permit snug fit around hub of sleeve and top plate	Local; standard office supply
7	Bottom Belleville Spring	High-carbon steel Belleville spring/washer	Key Belleville, Inc., Leechburg, PA; Part M3250-P-420
8	Top Belleville Spring	High-carbon steel Belleville spring/washer	Key Belleville, Inc., Leechburg, PA; Part M3250-P-420
9	Top Plate	Mild steel, see fabrication drawing	Local
10	Bottom Collar	Bottom collar, modified from a standard 102 mm (4") diameter Marshall cylinder mold as shown in the fabrication drawing	Rainhart Co., Austin, TX; Model 110CM4 Compaction Mold Assembly
11	Top Collar	Top collar, from a standard 102 mm (4") diameter Marshall cylinder mold	Rainhart Co., Austin, TX; Model 110CM4 Compaction Mold Assembly
12	In-Line Charge Converter	In-line charge converter (amplifier) converts high-impedance charge output of a piezoelectric sensor into low-impedance voltage signal	PCB Piezotronics, Inc., Depew, New York; Model 402A In-Line Charge Converter with M144 built-in option
13	AC Power Supply	AC power supply for low-impedance piezoelectric transducers with built-in or attached amplifiers	PCB Piezotronics, Inc., Depew, New York; Model 482A06, Single-Channel Line Power Supply with BNC input/output

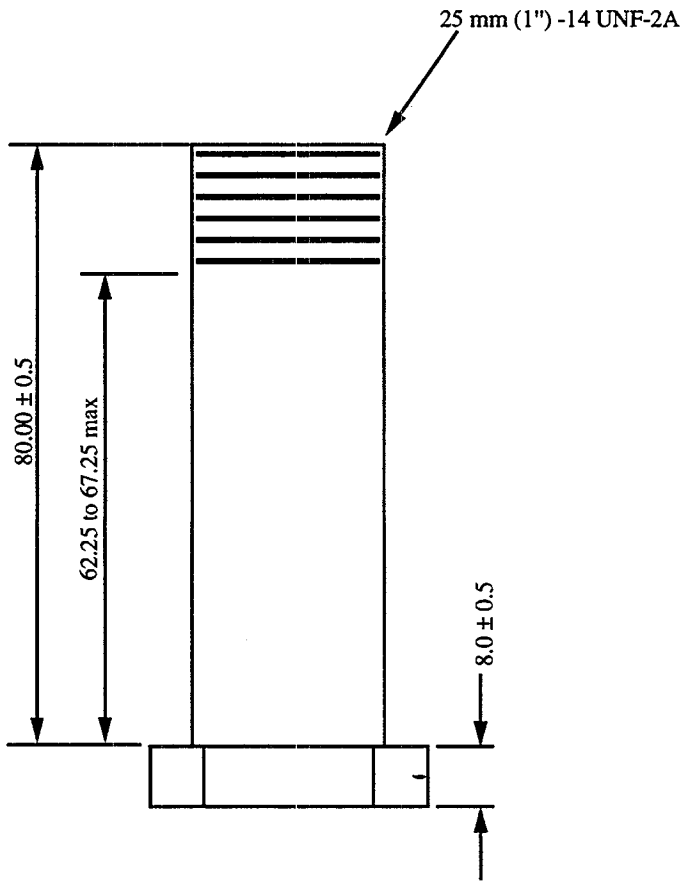

Note:
Part fabricated from a 25 mm (1") -14 fine thread, 152 mm (6") long (threaded length 64 m (2.5")) hex-head medium-strength cap screw . Thread shaft to indicated length, turn bolt head, and cut bolt to length.

PART NAME: Assembly Bolt
PART NUMBER: 1
MATERIAL: Steel
UNITS: Millimeters unless otherwise specified

Figure A1.1: Assembly Bolt

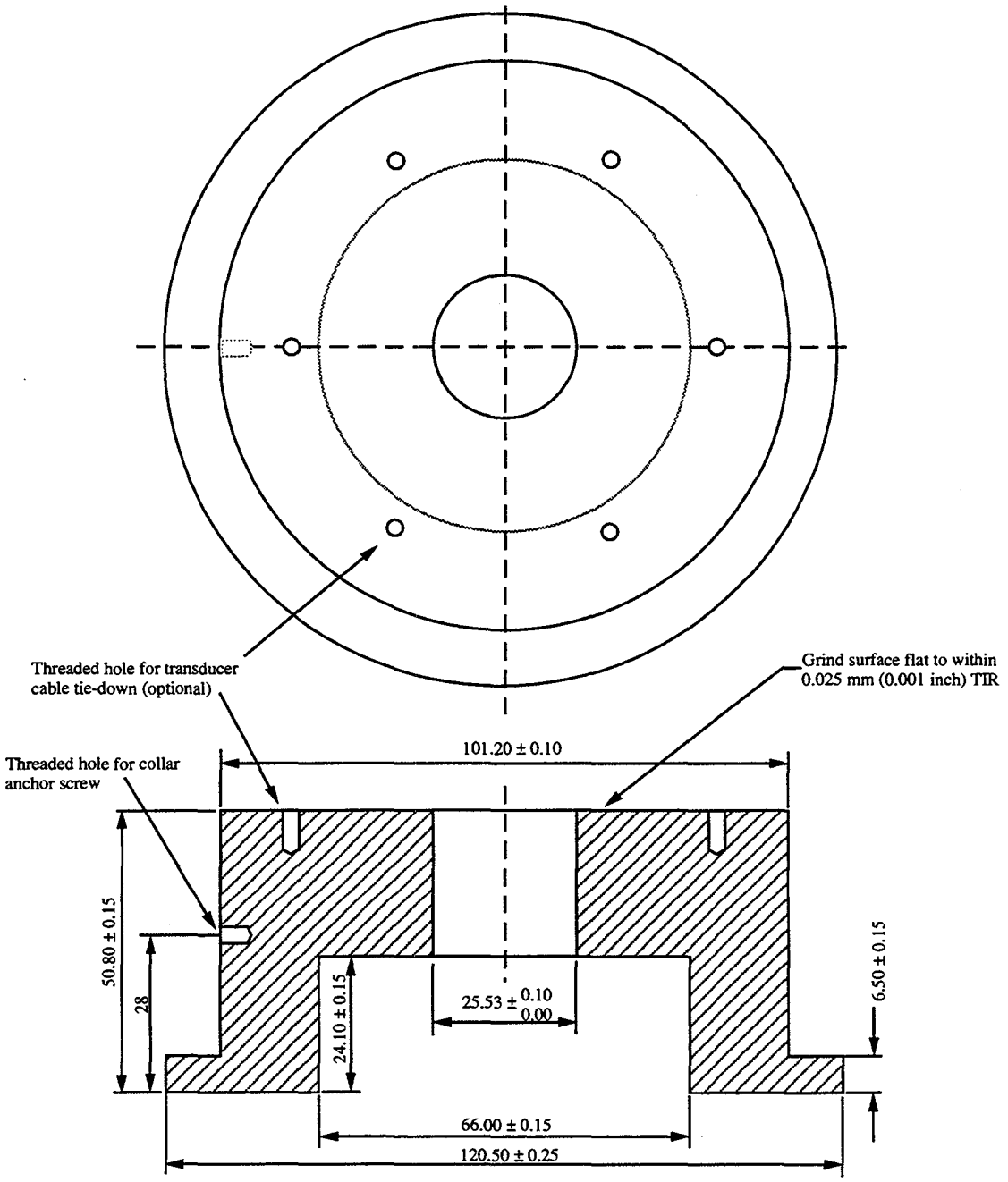

PART NAME: Base PART NUMBER: 3
MATERIAL: Mild Steel UNITS: Millimeters unless otherwise specified
Not to scale

Figure A1.2: Base

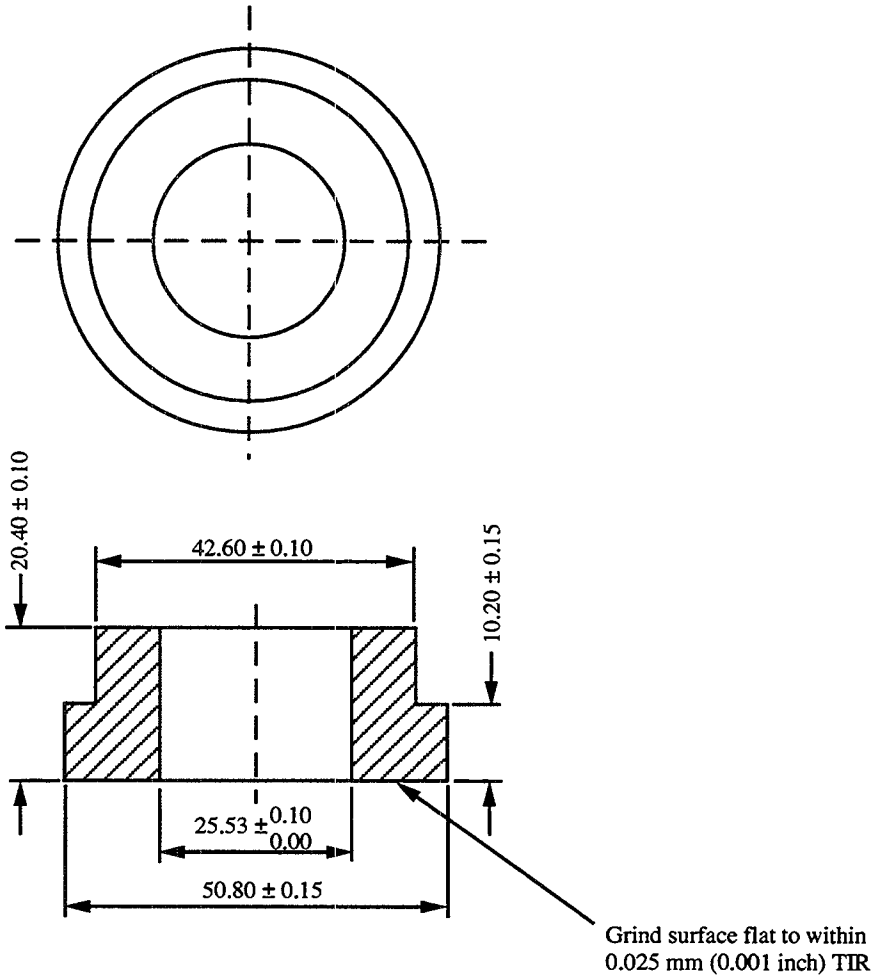

PART NAME: Sleeve
PART NUMBER: 5
MATERIAL: Mild Steel
UNITS: Millimeters unless otherwise specified

Figure A1.3: Sleeve

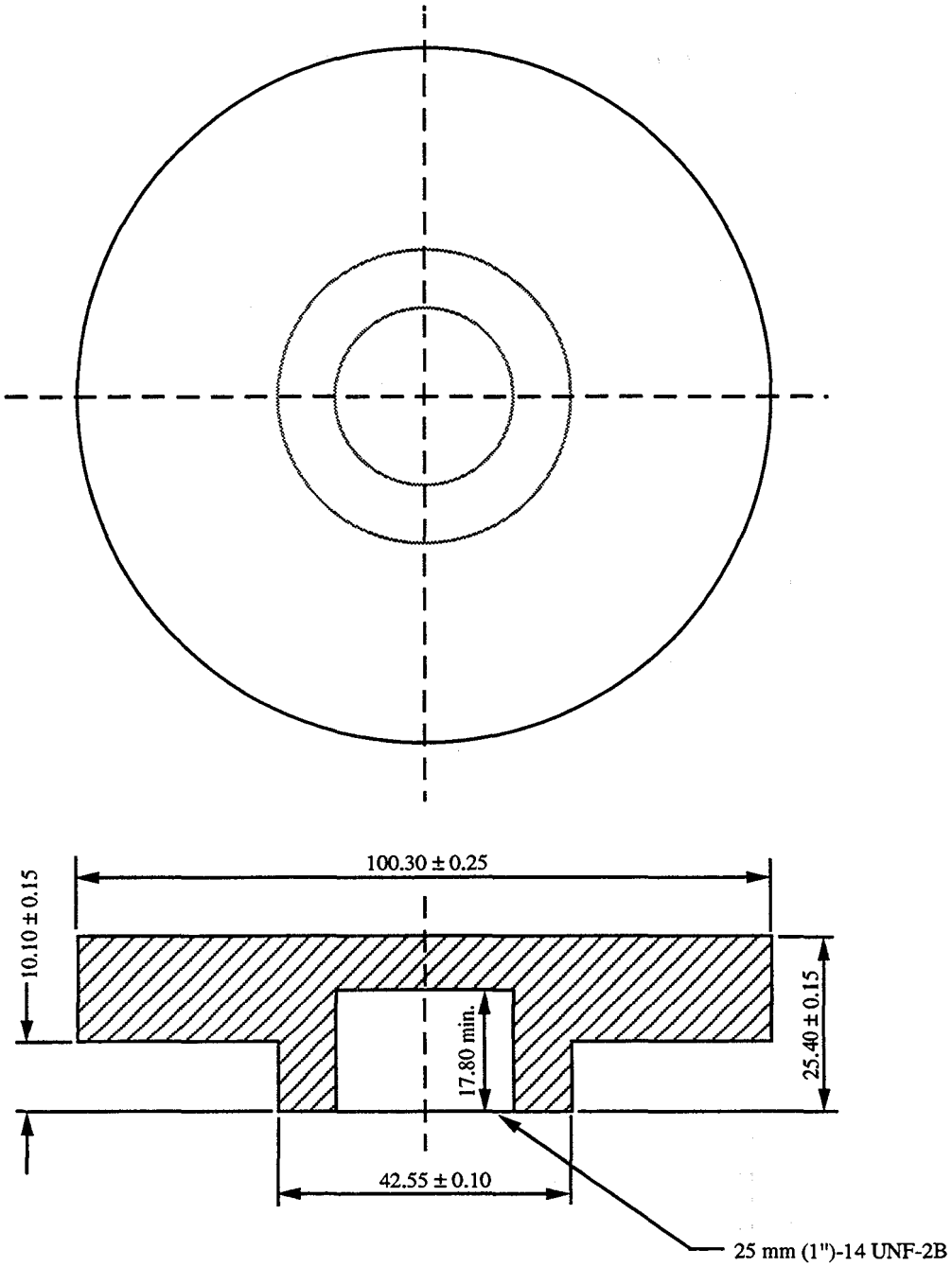

Notes:
1. Harden to minimum RC-55 after fabrication.
2. Chamfer corners as needed to prevent cracking during hardening.

PART NAME: Top Plate
PART NUMBER: 9
MATERIAL: Mild Steel
UNITS: Millimeters unless otherwise specified

Figure A1.4: Top Plate

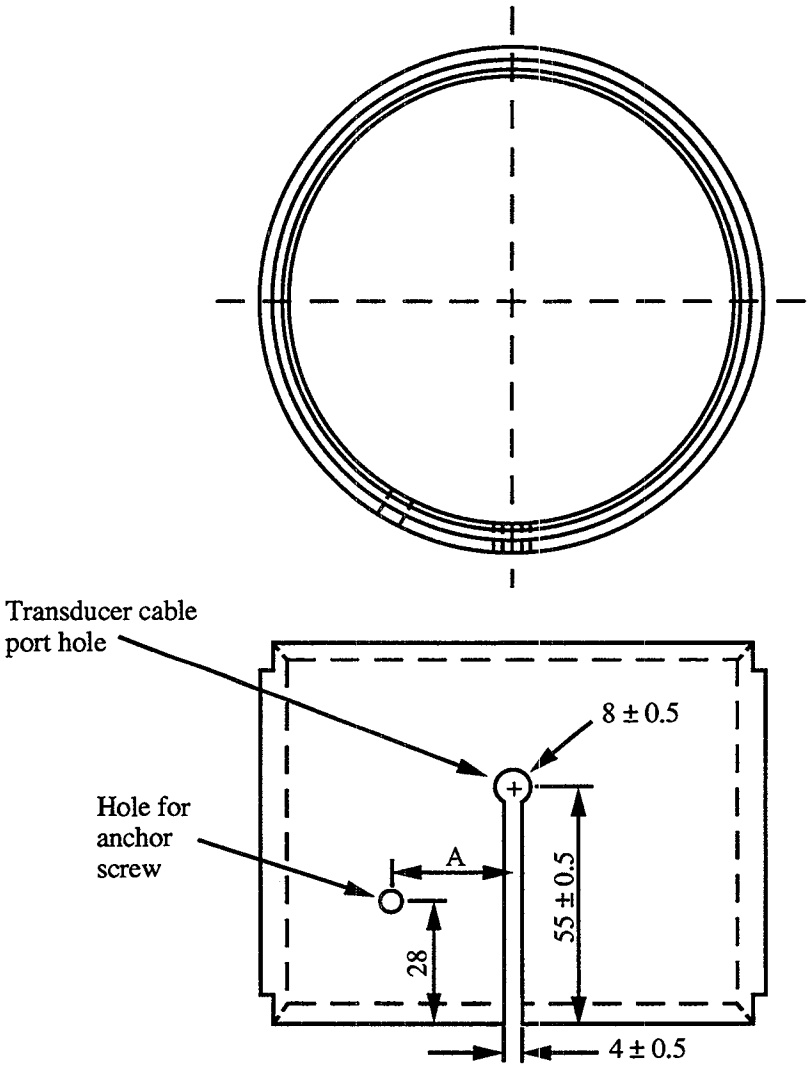

Notes:
Part fabricated from bottom collar of a standard 102 mm (4") diameter Marshall cylinder mold. Modifications include milling slot and drilling hole for transducer cable, and drilling hole for anchor screw. Slot and hole must be tailored to be compatible with transducer connection details. Measure "A" and the diameter of the anchor hole are arbitrary but must be compatible with connection detail and tapped hole in base.

PART NAME: Bottom Collar
PART NUMBER: 10
MATERIAL: Steel
UNITS: Millimeters unless otherwise specified
SCALE: 1/2

Figure A1.5: Bottom Collar

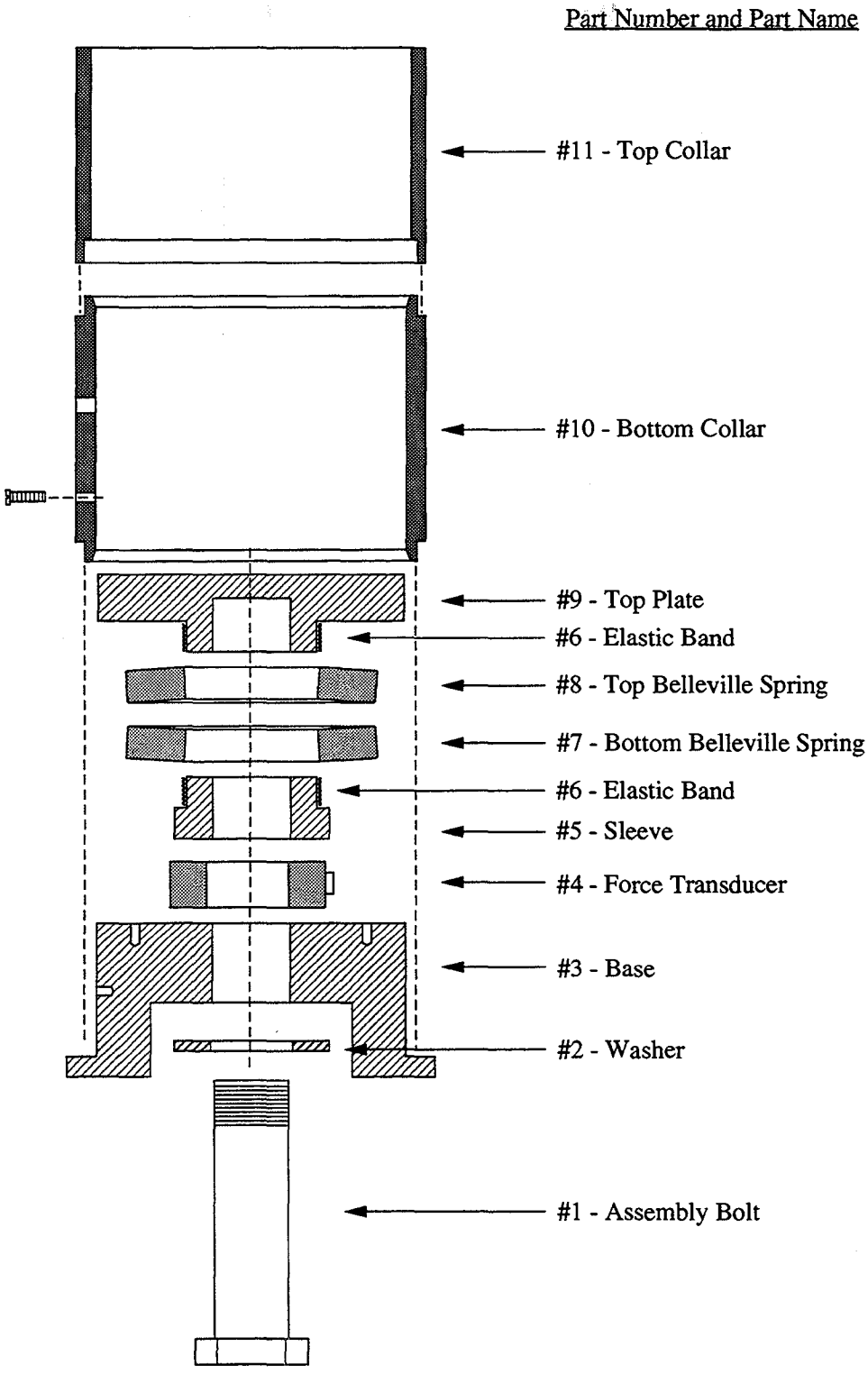

Figure A1.6: Assembly Drawing

ANNEX A2 - Spring Stiffness Determination
(Mandatory Information)

A2.1 Place the device in a universal test machine having a load range between 130 and 450 kN.

A2.2 Measure the displacement of the top plate of the calibration device with a displacement measuring device (e.g., dial gauge or LVDT) that has a resolution of at least 0.0025 mm (0.0001"). Care should be taken to ensure that the measuring device has rigid support and is securely anchored to ensure that there is no relative movement of the measuring device during testing.

A2.3 Condition the calibration device by completing 3 cycles, loading between 20 and 120 percent F_{max}.

A2.4 Complete 3 load cycles between 20 and 100 percent F_{max}. Load and unload in 5 equal increments. At each load increment record the displacement (δ) of the top plate.

A2.5 Plot load (F) versus deflection (δ).

A2.6 Determine the best fit line to the data using the method of least squares.

A2.7 The slope of the fitted curve is the calibrated stiffness K_s. The calibrated stiffness K_s shall be 150 ± 10 kN/mm.

ANNEX A3 - Load Cell Calibration
(Mandatory Information)

A3.1 Place the device in a universal test machine having a load capacity of at least 135 kN (30 kip), and a resolution of at least 0.5 kN (0.1 kip).

A3.2 Record the load during calibration using the actual data acquisition system to be used during Marshall hammer calibration; this includes power supply, cables, and recording instrument.

A3.3 Power the force transducer and allow sufficient time, as noted in the manufacturers specifications, for the instrument to thermally stabilize.

A3.4 Condition the device by completing 3 cycles between 0 and 90 kN (0 and 20 kip).

A3.5 Apply loads of 5, 10, 15, 25, 40, 50, and 70 kN (1, 2, 3, 6, 9, 12, and 15 kip), in that order. At each load increment, record the force transducer readout (V). Apply the loading sequence three times, such that three independent readings are taken at each load increment for a total of 21 data points.

A3.6 Plot readout (V) versus load (F).

> Note A3.1 -- The sensitivity of a piezoelectric force transducer varies with the pre-load on the instrument: sensitivity decreases with an increase in pre-load. As a result, the calibration curve for the instrument is likely to be bilinear, as shown by a typical example in Figure A3.1. For low loads, the transducer has a certain sensitivity because of the pre-load in the assembly bolt. Sensitivity increases, however, as the springs are compressed and the pre-load on the bolt is relieved. Accurate calibration requires determining the best fit lines to the two legs of the calibration curve.

A3.7 Determine the best fit line to the data corresponding to loads of 0, 5, and 10 kN (0, 1 and 2 kip) using the method of least squares. The equation for the fitted line shall be in the form:

$$V = m_1 F; \qquad 0 \le F \le F_i$$

in which V is the instrument readout, F is the force, m_1 is the slope of the fitted line, and F_i is determined in A3.9.

A3.8 Determine the best fit line to the data corresponding to loads of 15, 25, 40, 50, and 70 kN (3, 6, 9, 12, and 15 kip) using the method of least squares. The equation for the fitted line shall be in the form:

$$V = m_2 F + b_2; \qquad F_i < F$$

in which V is the instrument readout, F is the force, m_2 is the slope of the fitted line, b_2 is the y-intercept of the fitted line, and F_i is determined in A3.9.

A3.9 The intercept of the two calibration curves, corresponding to F_i, is given by

$$F_i = b_2 / (m_1 - m_2)$$

> Note A3.2 -- F_i is an estimate of the pre-load in the calibration device.

A3.10 Factors m_1, m_2, and b_2 define the calibration curve of the force transducer.

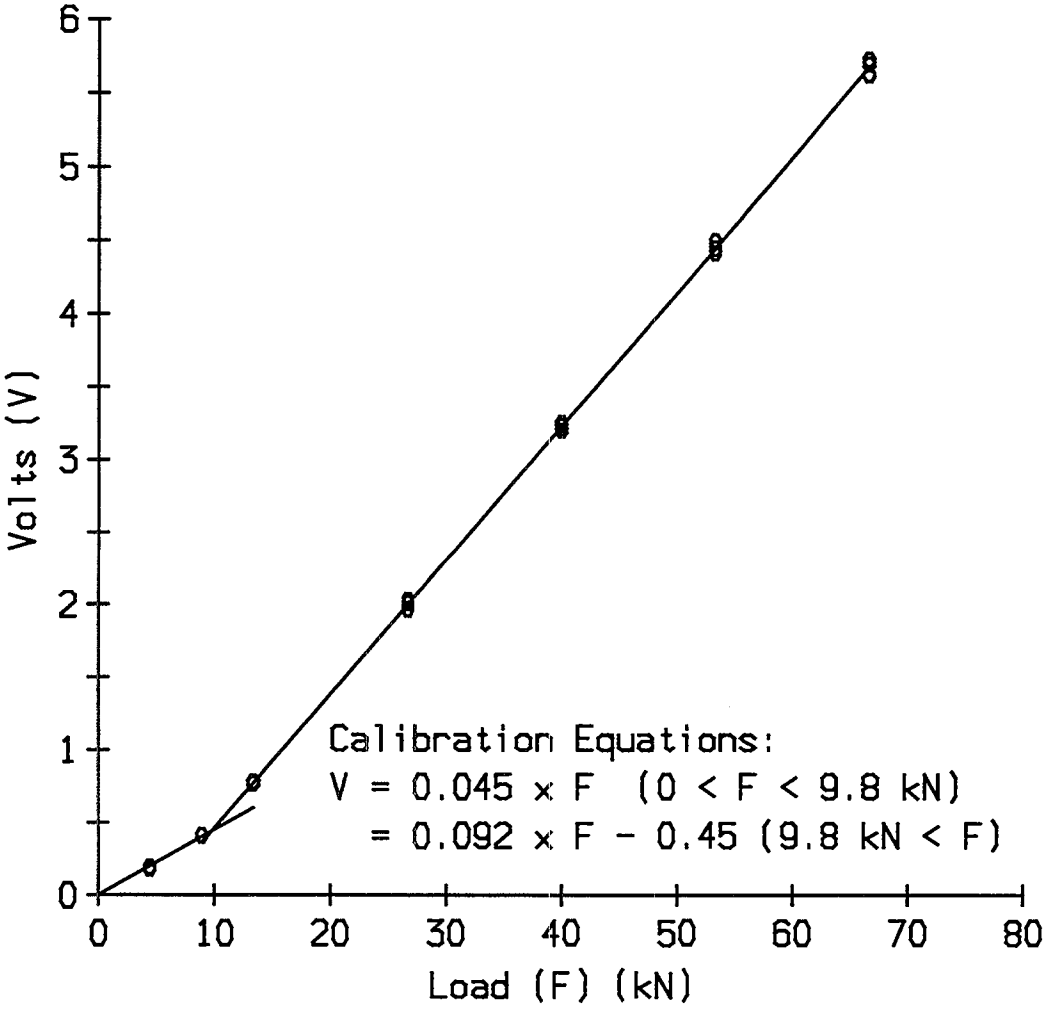

Figure A3.1: Typical Bi-Linear Calibration Curve

REFERENCES

Sy, A., and Campanella, R.G., "An Alternative Method of Measuring SPT Energy," *Proceedings*, Second International Conference on Recent Advances in Geotechnical Earthquake Engineering and Soil Dynamics, March 11-15, 1991, St. Louis, Missouri.

Siddiqui, Z., Tretheway, M.W., and Anderson, D.A., *Calibration of Marshall Hammer: State of the Art, Final Report*, Arizona Department of Transportation, Report Number FHWA-AZ87-808, June 1987.

Siddiqui, Z., Tretheway, M.W., and Anderson, D.A., "Variables Affecting Marshall Test Results," Transportation Research Record, No. 1171, pp. 139-148, 1988.

Wahl, A.M., *Mechanical Springs*, Second Edition, McGraw-Hill Book Company, New York, 1944.